



UNIL | Université de Lausanne

Unicentre

CH-1015 Lausanne

<http://serval.unil.ch>

Year : 2021

SMC and SMC-like proteins in genome folding and maintenance in *Bacillus subtilis*

Anchimiuk Anna

Anchimiuk Anna, 2021, SMC and SMC-like proteins in genome folding and maintenance
in *Bacillus subtilis*

Originally published at : Thesis, University of Lausanne

Posted at the University of Lausanne Open Archive <http://serval.unil.ch>

Document URN : urn:nbn:ch:serval-BIB_BE570D550B307

Droits d'auteur

L'Université de Lausanne attire expressément l'attention des utilisateurs sur le fait que tous les documents publiés dans l'Archive SERVAL sont protégés par le droit d'auteur, conformément à la loi fédérale sur le droit d'auteur et les droits voisins (LDA). A ce titre, il est indispensable d'obtenir le consentement préalable de l'auteur et/ou de l'éditeur avant toute utilisation d'une oeuvre ou d'une partie d'une oeuvre ne relevant pas d'une utilisation à des fins personnelles au sens de la LDA (art. 19, al. 1 lettre a). A défaut, tout contrevenant s'expose aux sanctions prévues par cette loi. Nous déclinons toute responsabilité en la matière.

Copyright

The University of Lausanne expressly draws the attention of users to the fact that all documents published in the SERVAL Archive are protected by copyright in accordance with federal law on copyright and similar rights (LDA). Accordingly it is indispensable to obtain prior consent from the author and/or publisher before any use of a work or part of a work for purposes other than personal use within the meaning of LDA (art. 19, para. 1 letter a). Failure to do so will expose offenders to the sanctions laid down by this law. We accept no liability in this respect.



UNIL | Université de Lausanne

Faculté de biologie
et de médecine

Département de Microbiologie Fondamentale

**SMC and SMC-like proteins in genome folding and
maintenance in *Bacillus subtilis***

Thèse de doctorat ès sciences de la vie (PhD)

présentée à la

Faculté de biologie et de médecine
de l'Université de Lausanne

par

Anna ANCHIMIUK

Master de l'Université de Gdansk et L'Université de médecine de Gdansk

Jury

Prof. Lluís Fajás Coll, Président
Prof. Stephan Gruber, Directeur de thèse
Prof. Marc Bramkamp, Expert
Prof. Jan-Willem Veening, Expert

Lausanne
(2021)



UNIL | Université de Lausanne

Faculté de biologie
et de médecine

Ecole Doctorale

Doctorat ès sciences de la vie

Imprimatur

Vu le rapport présenté par le jury d'examen, composé de

Président·e	Monsieur	Prof.	Lluis	Fajas Coll
Directeur·trice de thèse	Monsieur	Prof.	Stephan	Gruber
Expert·e·s	Monsieur	Prof.	Marc	Bramkamp
	Monsieur	Prof.	Jan-Willem	Veening

le Conseil de Faculté autorise l'impression de la thèse de

Madame Anna Anchimiuk

Master, Université de Gdańsk, Pologne

intitulée

**SMC and SMC-like proteins in genome folding
and maintenance in *Bacillus subtilis***

Date de l'examen : 27 août 2021

Date d'émission de l'imprimatur : Lausanne, le 14 septembre 2021

pour le Doyen
de la Faculté de biologie et de médecine

Prof. Niko GELDNER
Directeur de l'Ecole Doctorale

Table of Contents

ACKNOWLEDGEMENTS	4
ABSTRACT	5
RÉSUMÉ.....	6
LAY SUMMARY	8
RÉSUMÉ DESTINÉ À UN LARGE PUBLIC	9
LIST OF ABBREVIATIONS	11
OVERVIEW OF THE THESIS	12
CHAPTER 1: Chromosome organisation by the proteins from the SMC family	14
INTRODUCTION.....	15
General remarks on chromosome organisation by SMC complexes	15
3D genome organisation	16
Architecture of SMC complexes	20
The SMC ATPase cycle	20
Mechanistic models of chromosome folding.....	21
AIM OF THE STUDY	26
RESULTS.....	27
A low Smc flux avoids collisions and facilitates chromosome organization in <i>B. subtilis</i>	27
Specific author contributions to the paper	28
PUBLICATION	29
CHAPTER 2: Characterization of <i>BsRecN</i> and its role in DNA repair.....	30
INTRODUCTION.....	31
DNA damage and repair	31
Double Strand Breaks (DSBs) and their repair.....	31
Mitomycin C (MMC) for random DSB induction.....	34
I-SceI endonuclease for site-specific induction of DSBs	35
The role of SMC-like proteins in DNA repair	35
Architecture of SMC-like proteins	37
Focus on RecN and its role in DSB repair	37
AIM OF THE STUDY	42
RESULTS.....	43
RecN is involved in repair of Mitomycin C induced damage as previously reported	43
Studying architecture of RecN <i>in vivo</i>	44
Is there a link between the position of DSB and requirement for RecN?	55
DISCUSSION.....	59
Concerted Smc action is responsible for maintaining specific chromosomal architecture.....	59
Why do elongated chimeric Smc complexes not align the chromosome?	61
Viability of <i>B. subtilis</i> is not determined by maintaining chromosome arm juxtaposition.	61
Recombinational repair as the pathway of choice in bacteria.....	63
RecN-RecN dimers are a functional unit required for DNA repair.....	63

What is the role of RecN in DSB repair?	64
Correlation between the position of the cut-site and RecN presence.	64
How does 3D genome organisation influence DNA repair?.....	65
MATERIALS AND METHODS	67
<i>B. subtilis</i> strain construction and growth	67
Expression analysis of HaloTagged proteins.....	67
MMC Challenge.....	67
Site-specific DSB induction	68
<i>In vivo</i> cross-linking.....	68
REFERENCES	70

ACKNOWLEDGEMENTS

I dedicate this thesis to my Aunt, Halina Matejczuk, who always motivated me and supported all my decisions without judgement.

This thesis would have not been possible if Stephan did not welcome me in his lab, first in 2013 for a summer internship, and then in Autumn 2015 to start my PhD in Munich. Throughout the years, I had the opportunity to participate in several projects and learned more than I could possibly imagine. I would like to thank Stephan for supervising my work carefully and at the same time leaving a lot of space for exploring. It was a pleasure to be a part of the lab!

I am also extremely grateful to Vicky (aka Señora) who took care of me in Gif-sur-Yvette and taught me all there is to know about 3C-seq. It was intense but also very rewarding to work with her, and more importantly, inspiring on a personal level!

I would like to thank all the former and present members of the Gruber Lab for great atmosphere and always keeping the morale high. To Anita, who supervised me during the internship, for her time and commitment. That summer pushed me to another level. To Flo-berto with whom we moved to Lausanne in 2016 and swiftly set up the lab. To Flo for countless words of wisdom and hard judgement. To Roberto for engraving “Just don’t think about it.” in my brain. To Taschi for making me reconsider my complaining and procrastination events. To Young-Min (and his family) for being a friend and one-of-a-kind companion from day 1.

Moreover, I would like to thank all the smart people that went through this thesis and helped to make it better with their valuable comments and suggestions: to Maya, Taschi, Kuba and Flo.

I would also like to give special thanks to all the wonderful people I met at the DMF. To Rita for so many things I would have to write a separate chapter. To Marc for endless patience and excellent teaching skills. To Silvia for giving perspective and for NGS consulting. To Dimi for always being cool and reminding me about my rights.

To Alon, my role model and Friend, for the best partnership ever.

To my training group for lifting kettlebells together.

To my dear Friends in Poland for continuous support.

To my hiking and/or cycling Buddies for countless adventures and exploration of beautiful Switzerland allowing me to efficiently disconnect from work.

Finally, this thesis would have never seen the light of day if it was not for my wonderful chocolate suppliers: Francesco, Rita and Mathieu.

ABSTRACT

DNA metabolism across all kingdoms is managed by proteins belonging to the SMC and SMC-like protein families. Members of those families fold, compact, and preserve the structure of the chromosomes throughout the cell cycle. In this thesis, I address the roles and mechanisms of action of Smc and RecN, members of the SMC and SMC-like protein family, respectively, in the model organism *B. subtilis*.

Loop extrusion is a widely accepted model for DNA organisation mediated by SMC action. Mechanistic details of SMC transactions on the DNA remain unknown. The busy DNA translocation track raises several questions about the interplay of SMC complexes with replication and transcription machinery as well as between Smc complexes themselves. In Chapter 1, I investigate the plasticity of *B. subtilis* segregation system to maintain the characteristic, juxtaposed chromosome organisation. I identified and studied factors leading to Smc-Smc encounters. By utilizing chimeric Smc complexes with varying coiled coil length, I observed unexpected accumulation of proteins around loading sites which correlated with the loss of chromosome juxtaposition as seen in 3C-seq maps. Similar scenarios were obtained for wild-type complexes upon mild increase in protein levels or displacement of loading sites. Results presented in Chapter 1, strongly suggest that two translocating Smcs are unlikely to bypass one another and in wild-type cells Smc-Smc meetings are generally avoided. Loss of chromosome configuration upon mild increase in the amount of Smc complexes, modification of the number, and the location of the loading sites, demonstrate that aligning the chromosome arms is a finely tuned procedure. Perturbations, although not detrimental to cell viability, alter the architecture of the chromosome, possibly not without consequences for downstream processes, yet to be elucidated.

In Chapter 2, I confirm that bacterial specific RecN protein is involved in repair of double strand breaks (DSBs). Here, for the first time I give insights into RecN's architecture *in vivo*. I perform site-specific cysteine cross-linking to test published structural data for *D. radiodurans* RecN. Tools for reporting intermolecular interactions between dimerization interfaces and head domains of two monomers were established and confirmed, however, I did not find evidence for RecN playing a structural role through chain formation as proposed previously. Moreover, no DSB induced changes in cross-linking patterns could be observed, despite numerous trials. Interestingly, sensitivity to DSB seems to be correlated with location of the cut on the chromosome and RecN's presence. Single breaks close to the origin are less detrimental than *ter*-proximal.

RÉSUMÉ

Dans tous les règnes du vivant, le métabolisme de l'ADN est régi par des protéines appartenant à deux familles : les SMC et les protéines qui leur sont apparentées dénotées « SMC-like ». Les membres de ces familles protéiques se replient, se compactent et préservent la structure des chromosomes tout au long du cycle cellulaire. Dans cette thèse, j'aborde les rôles et les mécanismes d'action de Smc et de RecN, respectivement membres de la famille des protéines SMC, et «SMC-like», en me servant de l'organisme modèle *B. subtilis*.

L'extrusion de boucles d'ADN est un modèle largement admis pour l'organisation de l'ADN médiée par l'action des SMC. Les détails mécanistiques des transactions des SMC sur l'ADN restent inconnus. La piste de translocation d'ADN soulève plusieurs questions quant à l'interaction des complexes SMC avec les machineries de réplication et de transcription ainsi qu'entre les complexes Smc eux-mêmes. Dans le chapitre 1, j'examine la plasticité du système de ségrégation de *B. subtilis* pour maintenir l'organisation caractéristique des chromosomes juxtaposés. J'ai identifié et étudié les facteurs conduisant aux rencontres entre Smc (contacts Smc-Smc). En utilisant des complexes Smc chimériques ayant deux bras en super-hélice de longueur variable, j'ai observé une accumulation inattendue de protéines autour des sites de chargement, ceci étant corrélé avec la perte de juxtaposition des chromosomes analysée par cartographie des interactions chromosomiques (3C-seq). Des scénarios similaires ont été obtenus pour les complexes de type sauvage lors d'une légère augmentation des niveaux protéiques ou du déplacement des sites parS. Les résultats présentés dans le chapitre 1 suggèrent que deux Smc en translocation sont peu susceptibles de se contourner, et que dans les cellules de type sauvage, les contacts Smc-Smc sont généralement évités. La perte de configuration chromosomique lors d'une légère augmentation de la quantité de complexes Smc, la modification du nombre et de l'emplacement des sites de chargement, démontrent que l'alignement des bras chromosomiques est une procédure finement régulée. Les perturbations, bien que non préjudiciables à la viabilité des cellules, modifient l'architecture du chromosome, probablement non sans conséquences sur les processus en aval, qui eux restent à élucider.

Dans le chapitre 2, je confirme que la protéine RecN, spécifique aux bactéries, est impliquée dans la réparation des cassures double-brin (CDBs). Ici, pour la première fois, je donne un aperçu de l'architecture de RecN *in vivo*. J'effectue une technique de réticulation de protéines employant des résidus spécifiques de cystéines afin de tester les données structurelles publiées pour la protéine RecN appartenant à *D. radiodurans*. Les moyens permettant de rapporter les interactions intermoléculaires entre les interfaces de dimérisation et les domaines globulaires (dénotés têtes) de deux monomères ont été établis et confirmés. Cependant, je n'ai pas réussi à prouver que RecN joue un rôle structural par la formation de chaînes, comme proposé précédemment. De plus, aucun changement induit par les CDBs dans les modèles de

réticulation protéique n'a pu être observé, malgré plusieurs essais. Il est intéressant de noter que la sensibilité aux CDBs semble être corrélée à la localisation de la coupure sur le chromosome et à la présence de RecN. Les cassures simple-brin proches de l'origine de réplication sont moins préjudiciables que les cassures terminales.

LAY SUMMARY

Proper segregation of genetic material to the daughter cells as well as maintenance of a specific structure and continuity of the chromosome depends on the presence of the SMC and SMC-like proteins. Both protein families are conserved from bacteria to humans. In this thesis I have investigated Smc and RecN, members of SMC and SMC-like families, respectively, in the model organism *B. subtilis*.

The interior of the cells is extremely crowded. Furthermore, the DNA is not naked but decorated with a variety of proteins. In *B. subtilis*, ring-shaped Smc complexes reel in the DNA, starting from specific loading sites (entry sites), close to the origin of replication. While translocating away from the loading sites, they align the left and right arm of the chromosome. Finally, they dissociate from the chromosome close to the terminus (exit site). On the chromosome there are several entry sites and so, it is conceivable that when two Smc complexes are loaded independently onto them and start translocating, they will eventually meet. This is a relevant question as unresolved Smc-Smc encounters might perturb chromosome organisation and limit the level of DNA compaction, potentially influencing subsequent DNA segregation to daughter cells. In Chapter 1, I investigate what happens and what are the consequences of Smc-Smc meetings. I show that several strategies are employed by *B. subtilis* cells to avoid Smc-Smc encounters: a limited, small number of Smc complexes available in the cell and presence of dedicated entry and exit sites. Moreover, Smc complexes are stably associated with the DNA and do not tend to fall off before reaching the destination. Surprisingly, it seems that to some extent, the cells can tolerate perturbations in chromosome organisation.

In Chapter 2, I address RecN, a protein involved in DNA repair of a type of DNA damage called double strand breaks (DSBs). There is not much known about RecN's interactions with the DNA, nor on its specific role in the DNA repair process. Here, by using available structural information for RecN from another bacterium obtained *in vitro*, I prepare mutant strains to investigate RecN's architecture in living cells for the first time. Moreover, I assess whether the introduced mutations influence sensitivity to DNA damage. In addition, by generating DSBs at different locations along the chromosome, I study the importance of RecN's presence on DNA repair. It seems that there is a dependence between the position of the break and cell viability if RecN is present. Upon RecN deletion, survival is very limited regardless of where the cut is.

RÉSUMÉ DESTINÉ À UN LARGE PUBLIC

Les protéines SMC et SMC-like dans le repliement et le maintien du génome au sein de l'organisme modèle *Bacillus subtilis*

La ségrégation adéquate du matériel génétique vers les cellules filles ainsi que le maintien d'une structure spécifique et de la continuité du chromosome dépendent de la présence de protéines de type SMC et de protéines qui leur sont apparentées dénotées SMC-like. Ces deux familles protéiques sont conservées des bactéries à l'Homme. Dans cette thèse, j'ai étudié Smc et RecN, respectivement membres des familles SMC et SMC-like, au sein de l'organisme modèle *B. subtilis*.

L'intérieur des cellules est extrêmement encombré. De plus, l'ADN n'est pas nu, mais plutôt agrémenté par une variété de protéines. Chez *B. subtilis*, les complexes Smc en forme d'anneau s'enroulent dans l'ADN, à partir de sites de chargement spécifiques (sites d'entrée), proches de l'origine de réplication. En s'éloignant des sites de chargement par translocation, ils alignent les bras gauche et droit du chromosome. Enfin, ils se dissocient du chromosome près du terminus (site de sortie). Dans le chapitre 1, je m'intéresse à ce qui se produit et aux conséquences des rencontres entre Smc (contacts Smc-Smc). Sur le chromosome, il y a plusieurs sites d'entrée et il est donc concevable que lorsque deux complexes Smc sont chargés indépendamment sur ceux-ci et commencent à transloquer, ils finissent par se rencontrer. C'est une question pertinente car les contacts Smc-Smc non maîtrisés pourraient perturber l'organisation du chromosome et limiter le niveau de compaction de l'ADN, ce qui pourrait potentiellement influencer la ségrégation ultérieure de l'ADN dans les cellules filles. Ici, je montre que plusieurs stratégies sont employées par les cellules de *B. subtilis* pour éviter les rencontres entre Smc : un petit nombre limité de complexes Smc sont disponibles dans la cellule avec la présence de sites d'entrée et de sortie dédiés. De plus, les complexes Smc sont associés de manière stable à l'ADN et n'ont pas tendance à se détacher avant d'atteindre leur destination. De manière surprenante, il semble que, dans une certaine mesure, les cellules puissent tolérer des perturbations dans l'organisation des chromosomes.

Dans le chapitre 2, je m'intéresse à RecN, une protéine impliquée dans la réparation d'un type particulier de dommage à l'ADN désigné par cassures double-brin (CDBs). Les interactions entre RecN et l'ADN sont très peu documentées, il en est de même pour son rôle spécifique dans le processus de réparation de l'ADN. Ici, en utilisant les informations structurales disponibles pour RecN provenant d'une autre bactérie et obtenues *in vitro*, j'élabore des souches mutantes afin d'étudier l'architecture de RecN dans des cellules vivantes pour la première fois. De plus, j'évalue si les mutations introduites influencent la sensibilité aux dommages de l'ADN. Par ailleurs, en générant des CDBs à différents endroits le long du chromosome, j'étudie l'importance de la présence de RecN sur la réparation de l'ADN. Il semblerait y avoir une dépendance

entre la position de la cassure et la viabilité cellulaire en présence de RecN. Dans le cas d'une délétion de RecN, la survie cellulaire est très limitée quel que soit l'endroit de la coupure.

LIST OF ABBREVIATIONS

DNA	Deoxyribonucleic Acid
SMC	Structural Maintenance of Chromosomes
3C-seq	Chromosome Conformation Capture coupled with deep sequencing
ATP	Adenosine Triphosphate
BMOE	Bismaleimidoethane
CID	Chromosome Interaction Domain
CTCF	CCCTC-binding factor
DLS	Dynamic Light Scattering
DSB	Double Strand Break
HJ	Holliday Junction
HR	Homologous Recombination
HT	HaloTag
ICL	Interstrand Crosslink
IR	Ionizing Radiation
LE	Loop Extrusion
LEF	Loop Extruding Factor
MALS	Multi-Angle Light Scattering
MMC	Mitomycin C
NGS	Next Generation Sequencing
NHEJ	Non-homologous End Joining
ONA	Oxoid Nutrient Agar
RC	Repair Center
RNA	Ribonucleic Acid
RS	Restriction Site
TAD	Topologically Associated Domain

OVERVIEW OF THE THESIS

Genome integrity is essential for survival of the cell – not only the primary DNA sequence but also the way it is packed within the nucleus or nucleoid. Maintenance of proper three-dimensional genome organisation is a prerequisite for successful gene expression, DNA damage management, as well as information storage and transfer between generations, regardless of the species. Numerous proteins ensure that aforementioned processes are carried out with high fidelity, including members of the Structural Maintenance of Chromosomes (SMC) and SMC-like protein families. Both of them are highly conserved in structure but versatile in function. Despite over three decades of intense research on SMC and SMC-like proteins, several mechanistic details explaining their behaviour on the chromosome and the consequences of their action translocation have not yet been revealed.

I have started my PhD investigating RecN – an SMC-like protein widely present in bacterial genomes. RecN is involved in DNA repair, yet its exact function is not well understood. By that time, the available data was confusing and in some cases contradictory, even to the present day. I had at hand: a few crystal structures of *D. radiodurans* RecN fragments, several biochemical assays from *D. radiodurans*, *E. coli*, *H. influenzae* and *C. crescentus* reporting interactions of the protein with DNA and functional assays strongly pointing to the role of RecN in repair pathway requiring homologous recombination (more in Chapter 2). There is a gap of knowledge regarding interactions between RecN monomers and its tentative, architectural function of bringing broken DNA ends together *in vivo*. Taking advantage of the profound experience in the biology of SMC complexes as well as the relevant methodology in the lab, I attempted to fill this void. I was introducing point mutations, engineering cysteines for site-specific cross-linking experiments and following up with functional viability assays upon exposure to DNA damaging agents. Initially encouraging results confirmed interactions at both extremities of the protein and allowed me to report that formation of multimeric RecN assemblies is possible however biological relevance of the latter remains to be determined. I was able to successfully pick and chemically crosslink single residues as well as hinder these interactions by point mutations. I could confirm the importance of RecN in DNA repair upon introduction of mutations. Unfortunately, the growing amount of data was increasingly incoherent and confusing.

In parallel I started working on another project, focusing on the relationship between Smc size and the speed of translocation. This allowed me to introduce a new technology to the lab – chromosome conformation capture coupled with deep sequencing (3C-seq) to study in detail interactions between chromosomal regions on a genome-wide scale. To be more precise, I have established 3C-seq methodology in the lab for *Bacillus subtilis* (*B. subtilis*) cultures grown in minimal media, including time-course 3C-seq and library preparation as well as subsequent data analysis. Terabytes of sequencing data later, it became clear that with a certain probability Smc complexes translocating on the chromosome meet and interact with one another. The concept of encounters on the DNA track in a crowded cellular environment is not new and has been thoroughly discussed mainly in the context of DNA – RNA polymerases and SMC – RNA polymerase collisions. Nevertheless, it wasn't until recently, that Smc-Smc collisions were addressed themselves. The outcome of such Smc-Smc encounters on 3D genomic organisation and possible physiological consequences for the cells are described in more detail in Chapter 1 and have recently been published in eLife (DOI: 10.7554/eLife.65467).

The general aim of this thesis is to shed light on various aspects of SMC and SMC-like protein biology and their contribution to DNA metabolism in the model organism *B. subtilis*.

CHAPTER 1: Chromosome organisation by the proteins from the SMC family

INTRODUCTION

General remarks on chromosome organisation by SMC complexes

The length of genomic DNA from a single cell dramatically exceeds the size of the cell itself. Hence, the DNA must be compacted in a very precise and organised manner to be available for cellular processes like replication or transcription. Strictly conserved from bacteria to humans, SMC complexes are multisubunit molecular motors, imperative to that process.

In prokaryotes there are three main classes of SMC complexes (also termed as bacterial condensins): MukBEF, MksBEF and Smc-ScpAB. Most bacterial genomes encode a single type of SMC, however there are several examples of bacteria (e.g., *Pseudomonas* and *Aeromonas* species), where two types co-exist and operate in a presumably hierarchical manner (Lioy et al., 2020). Upon Smc complex inactivation, severe defects in chromosome organisation and segregation occur, including formation of anucleate cells, chromosome decondensation and temperature sensitive growth (Gruber et al., 2014; Jensen & Shapiro, 1999).

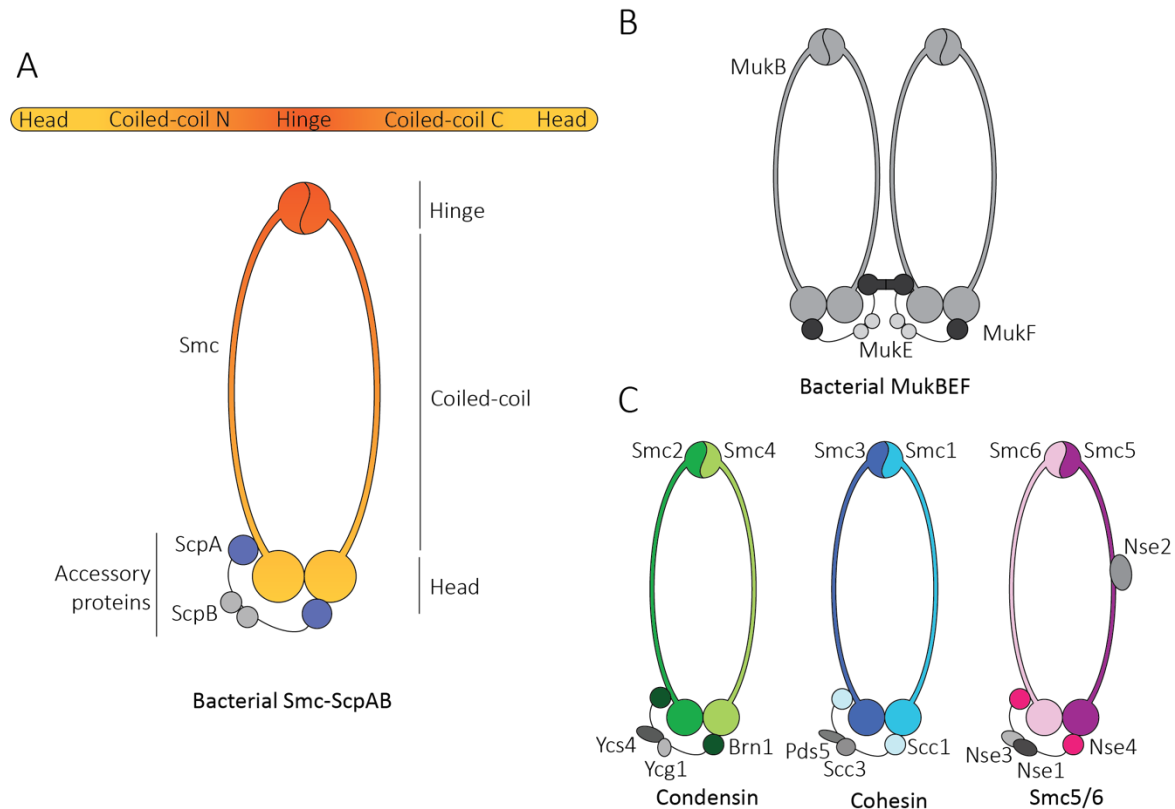


Figure 1. Schematic representation of SMC complexes. Homo- or heterodimeric SMC complexes are composed of two Smc monomers interacting via the

globular hinge domain. The tripartite ring is closed by a kleisin subunit associated asymmetrically with the ATPase head domain. **A.** The canonical bacterial Smc-ScpAB complex. Linear representation of Smc monomer, true for all proteins from the SMC family (upper panel). **B.** The bacterial MukBEF complex. Two dimers interact via the kleisin subunit giving rise to a higher order complex. **C.** Eukaryotic SMC complexes from *S. cerevisiae*. From left to right: condensin, cohesin and Smc5/6 with names of their respective subunits and accessory proteins indicated.

In eukaryotes several specialized SMC complexes coexist in time and space within a single cell (Figure 1C). Cohesin holds sister chromatids together and participates in shaping interphase chromosomes into so called topologically associated domains (TADs) (Szabo et al., 2019; Yatskevich et al., 2019). Condensin is responsible for compacting and structuring mitotic chromosomes to facilitate sister chromatid resolution (T. Hirano, 2016). Finally, the least understood, Smc5/6 is thought to play a role in DNA repair and genome maintenance (Bermúdez-López et al., 2010). Several developmental abnormalities and human diseases have been linked to mutations in SMC complexes. Mutations in cohesin and its loading factor NIPBL lead to Cornelia de Lange syndrome (CdLS) (Deardorff et al., 2007; Krantz et al., 2004) and participate in development of several types of cancer (Leiserson et al., 2015). Mutations in genes encoding subunits of condensin were reported to cause microcephaly (Martin et al., 2016).

3D genome organisation

The first observations of chromosomes were reported towards the end of the 19th century (Flemming, 1882). It then took another century to identify the first SMC complex as a factor contributing to the maintenance of a specific chromosomal structure in *E. coli* (Niki et al., 1991). Even though microscopic observations and genetic studies contributed greatly to uncovering the interdependency of chromosome structure and biological processes, there was a need for more high-throughput approaches. The boom of Chromosome Conformation Capture (3C) technologies in combination with tremendous improvement of Next Generation Sequencing (NGS) quality in the last 10 years (Dekker, 2002 3C-PCR)(Lieberman-Aiden et al. 2009 first HiC experiment)), allowed scientists to study DNA interactions in a more systematic way, on a genome-wide scale and with ever increasing resolution. Together with

extensive DNA polymer simulations and molecular modelling, this greatly accelerated 3D chromosome organisation research. Scientists were able to propose and test the loop extrusion model as a mode of SMC action, discover TADs (or Chromosome Interaction Domains, CIDs, in bacteria), compare chromatin organisation between cell types and follow changes upon mutations in architectural proteins to an extent that was unthinkable before (see below).

The bacterial chromosome

Most bacteria have a single circular genome ranging in size from 0.6 Mb for *Mycoplasma* species (Fraser et al., 1995) to over 14 Mb for *Myxobacteria* species (Han et al., 2013; Reichenbach, 1999). Replication starts at a dedicated single origin and two replication forks proceed in opposite directions to meet at the terminus located *vis a vis* the origin, where replicated sister molecules are eventually resolved. The bacterial genome is relatively 'dense', which means that the ratio of coding sequences (operons) to non-coding regions is high (Rocha, 2008). Interestingly, gene distribution along the bacterial chromosome is not uniform. Highly expressed genes tend to cluster close to the origin region and are often co-oriented with replication. This co-orientation was first observed for *E. coli* ribosomal genes and has likely evolved to minimize unavoidable collisions between DNA and RNA polymerases, moving at strikingly different velocities on the same DNA track (1000 nt/s and 80 nt/s in *E. coli*, respectively) (Bremer & Dennis, 2008; Brewer, 1988; Nomura & Morgan, 1977).

Replication, transcription and segregation happen concomitantly in bacteria and all those processes contribute to 3D genome rearrangements. Discrete chromosomal interaction domains (CIDs), comprising preferentially interacting loci, were revealed for several species. Their sizes range from 30 to 420 kb and their boundaries are somewhat determined by highly expressed genes (Le et al., 2013; Lioy et al., 2020; Marbouty et al., 2015; Mercier et al., 2008).

The segregation of sister chromosomes in bacteria closely follows replication and is coordinated by the SMC complexes. MukBEF, found in enterobacteria and γ -proteobacteria, as well as MksBEF widely scattered among proteobacteria, are presumably loading on the DNA in a sequence independent manner (Petrushenko et al., 2011; Rybenkov, 2014). In most bacteria including *B. subtilis*, however, loading of

the Smc-ScpAB complex is restricted to a few entry sites (*parS*) and mediated by the Smc-loader protein ParB (Gruber & Errington, 2009; Sullivan et al., 2009). The 16-bp *parS* DNA sequences are generally closely juxtaposed and found within a few kb from the replication origin (Livny et al., 2007). After loading, Smc-ScpAB complexes actively translocate to neighbouring loci in both directions and zip up the left and the right chromosome arms (Minnen et al., 2016; Tran et al., 2017; X. Wang et al., 2015, 2017). Unloading of Smc-ScpAB was recently reported to be XerD-dependent and to happen near the replication terminus in *B. subtilis* (Karaboja et al., 2021).

Interphase domains

Eukaryotic chromosomes are highly dynamic and oscillate between a very compact mitotic chromosome conformation and a looser interphase organisation (Figure 2). Chromatin, the assembly of DNA with architectural proteins such as histones, form the basis of these hierarchical structures. Next, at a scale of tens to hundreds of kilobases, interphase chromosomes fold into TADs (Dixon et al., 2012). Certain TADs within each chromosome tend to cluster together forming active “A” and repressed “B” compartments of preferential contacts (Lieberman-Aiden et al., 2009; S. Wang et al., 2016). Finally, uncondensed interphase chromosomes occupy distinct areas (called chromosome territories) within the nucleus (Cremer & Cremer, 2010).

TADs are a hallmark of interphase chromosome organisation. On a molecular level, they are cohesin-dependent regions of increased intra-chromatin interactions and have been first discovered in HiC experiments of mammalian cells (Dixon et al., 2012). Cohesin metabolism on DNA is directed by several factors. NIPBL-MAU2 (or Scc2-Scc4 in yeast) is a cohesin loading factor which also stimulates ATPase activity and loop formation (Ciosk et al., 2000; Davidson et al., 2019). CTCF is a boundary element, enriched specifically at TAD boundaries and preventing cohesin translocation (de Wit et al., 2015; Parelho et al., 2008; Rubio et al., 2008; Wendt et al., 2008). Lastly, a cohesin unloading factor, WAPL, promotes release of cohesin and DNA loop dissolution (Haarhuis et al., 2017). Functionally, TADs were reported to play a role in gene regulation (Dixon et al., 2012; Nora et al., 2012; Rao et al., 2017; Sexton et al., 2012; Sofueva et al., 2013).

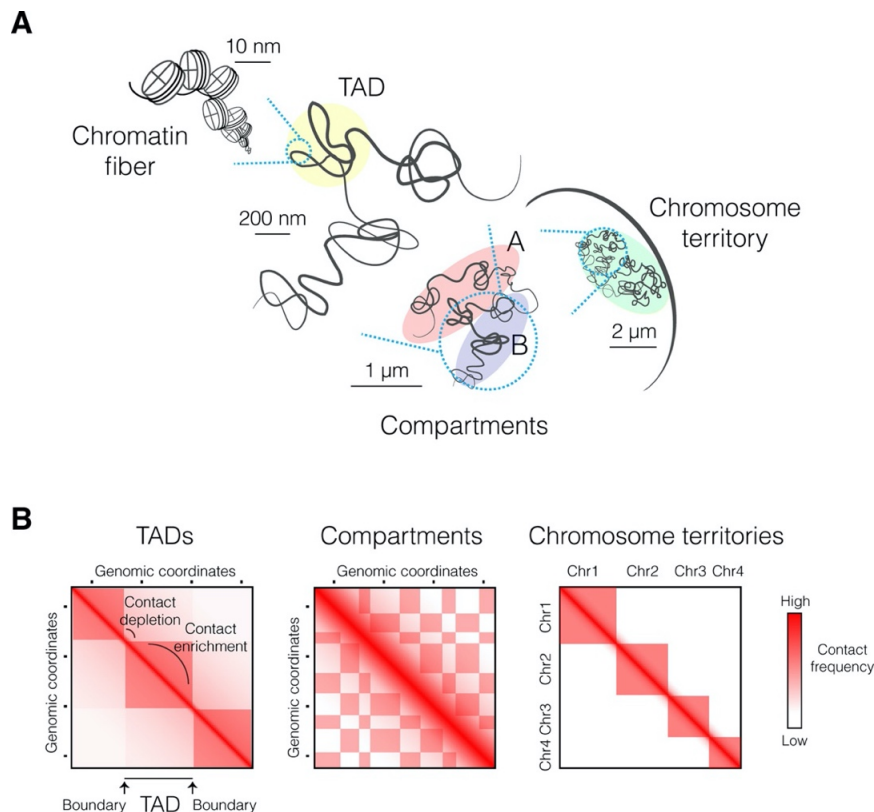


Figure 2. Hierarchical organisation of a eukaryotic genome. A. Scheme of chromosome folding within the nucleus. The 10 nm chromatin fiber is organised in regions of preferred interactions, topologically associated domains (TADs). TADs cluster forming active (A) and inactive (B) compartments within the chromosome territories. **B.** Schemes of HiC maps of different resolutions with features from (A) indicated. Figure source: (Szabo et al., 2019).

The mitotic chromosome

Arguably the most visually striking outcome of SMC action is the mitotic chromosome. In prophase, TAD organisation is lost and expected to be replaced by a homogenous array of consecutive loops condensed around a central axis (Earnshaw & Laemmli, 1983; Gibcus et al., 2018; Marsden & Laemmli, 1979; Naumova et al., 2013). Impressive 10,000-fold compaction of chromatin is mediated by the concerted action of condensin I and II. Condensin II forms relatively big loops of ~400 kb, on which later condensin I establishes smaller, nested loops (~80 kb). Moreover, condensin II gives rise to a so-called axial scaffold, around which the arrays of loops presumably get stacked and are further compacted (Gibcus et al., 2018; Naumova et al., 2013). Nevertheless, the exact mechanism driving high compaction during prometaphase is unknown.

Architecture of SMC complexes

The elongated architecture is a distinctive feature of all canonical SMC complexes (Figure 1). The globular head and hinge domains of Smc proteins are connected via long intramolecular antiparallel coiled coils. Two such monomers dimerize via the hinge domain to form an Smc homodimer (in prokaryotes) or heterodimer (in eukaryotes). Several crystallographic and biochemical studies support at least two states for the SMC complex – a rod conformation with arms closely juxtaposed and a ring conformation with arms apart (M. L. Diebold-Durand et al., 2017; Moreno-Herrero et al., 2005; Soh et al., 2015). Curiously, a discontinuity in the coiled coil arm was recently reported for *E. coli* MukBEF, yeast cohesin and condensin (Bürmann et al., 2019, 2021; B.-G. Lee et al., 2020; Shi et al., 2020), which strongly suggests that an alternative conformation within the complex is also possible. Moreover, a functional SMC complex is completed by a non-SMC kleisin bridging the heads in an asymmetrical manner (Bürmann et al., 2013), and by additional KITE or HAWK subunits bound to the kleisin. Two compartments can be distinguished within such tripartite proteinaceous ring (S-K ring) upon ATP-induced head engagement: S compartment between the coiled coils of two Smc monomers, and K compartment between the engaged Smc heads and the kleisin subunit. Functional tripartite SMC rings were shown to encircle chromosomal DNA (Cuylen et al., 2011; Gligoris et al., 2014; Vazquez Nunez et al., 2019; Wilhelm et al., 2015). Importantly, kleisins are not only functional elements of SMC (M. Hirano & Hirano, 2004; Petrushenko et al., 2006), but also in some cases promote oligomerization of the complexes (Matoba et al., 2005; Petrushenko et al., 2006; Woo et al., 2009). Higher-order structures were reported for MukBEF complexes via the MukF kleisin subunit interactions (dimers of dimers, Figure 1B, Fennell-Fezzie et al., 2005; Yamazoe et al., 1999). Nevertheless, there is no direct evidence supporting oligomerization for other proteins from the canonical SMC family existing in bacteria.

The SMC ATPase cycle

The globular N- and C-terminal domains contain the Walker A and B motifs, respectively. Together with the signature motif, they produce a single head domain with an ABC-ATPase fold (K. P. Hopfner et al., 2000; Lammens et al., 2004; Woo et

al., 2009). Several mutants blocking different steps of the ATPase cycle have been characterized for the canonical members of the SMC protein family (Figure 3): a K-to-A mutation within the Walker A motif abolishes ATP binding, and an E-to-Q mutation within the Walker B motif stabilizes a transition state and inhibits ATP hydrolysis and a S-to-R substitution in the signature motif prevents ATP-dependent head dimerization ('engagement') (M. Hirano & Hirano, 2004; K. P. Hopfner et al., 2000; Minnen et al., 2016; Smith et al., 2002). All these ATPase mutations render SMC complexes non-functional.

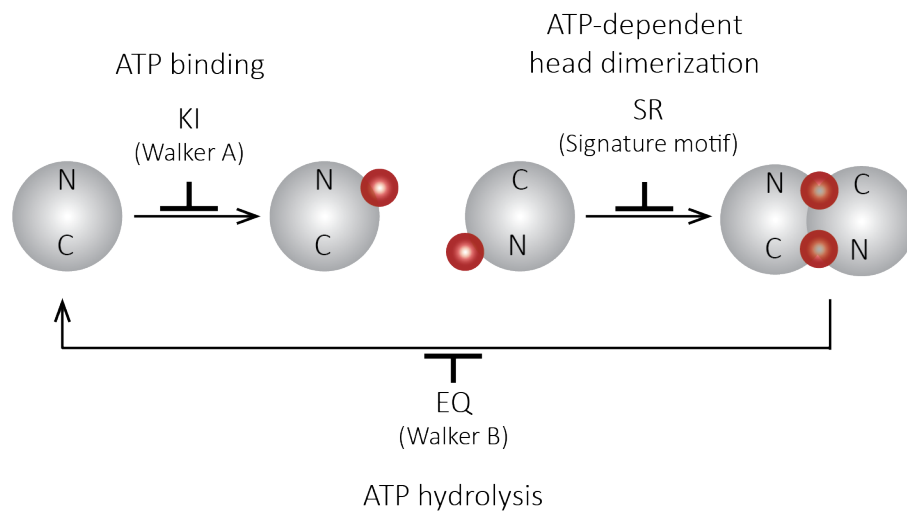


Figure 3. The ATPase cycle of canonical SMC complexes. Mutations affecting ATP binding (KI in Walker A motif), ATP-dependent head dimerization (SR in Signature motif) and ATP hydrolysis (EQ in Walker B) are indicated. Two ATP molecules are sandwiched between SMC heads (in red).

In most of SMC complexes, ATP hydrolysis is stimulated by DNA binding (Chiu et al., 2004; Griese et al., 2010; Griese & Hopfner, 2011; M. Hirano & Hirano, 2006; Taschner et al., 2021; Vazquez Nunez et al., 2019).

Mechanistic models of chromosome folding

A growing body of evidence supports active loop extrusion (LE) as a common mode of action among all members of the SMC family (aka loop extruding factors, LEFs). Several positively charged surfaces within the SMC complex which are potentially important for interactions with DNA were identified: a surface on top of engaged head domains (Rojowska et al., 2014; Seifert et al., 2016), positively charged central channel within the hinge domain (Kurze et al., 2011) and DNA binding sites in the associated

non-SMC subunits (Kschonsak et al., 2017). How these DNA binding sites are coordinated during loop extrusion, however, is not known.

The active LE model implies the LEFs are molecular motors. Previously, purified *S. cerevisiae* condensin was reported to hydrolyse 2 ATP molecules per second in the presence of linear DNA (Terakawa et al., 2017). Translocation was efficient and happened in steps of at least 60 bp per ATP hydrolysis cycle (for comparison, *E. coli* FtsK translocase hydrolyses 2600 ATP/s with step size of ~2 bp/ATP) (Graham et al., 2010; Terakawa et al., 2017). Recently, ATP-dependent loop extrusion events have been recorded in several single molecule experiments: yeast condensin, human cohesin as well as condensin and cohesin from *Xenopus laevis*. DNA loops are reeled at rates of ~1 kb/s in an asymmetric (one-sided) or symmetric (two-sided) manner for condensin and cohesin, respectively (Davidson et al., 2019; Ganji et al., 2018; Golfier et al., 2020; Y. Kim et al., 2019). Nevertheless, the underlying mechanistic details of SMC LE on the DNA remain to be unveiled.

Experimental evidence seems inconsistent with theoretical considerations. If the DNA is reeled in asymmetrically (as reported for yeast condensin, (Ganji et al., 2018)), an obvious outcome includes the presence of unlooped regions, strongly restricting compaction capability. According to molecular modelling experiments, unless LEFs are allowed to traverse one another or employ a switching LE mode (thus becoming two-sided motors), mitotic genome organisation *in vivo* cannot be recapitulated (Banigan et al., 2020; Banigan & Mirny, 2019). Curiously, Smc traversal and Z-loop formation was reported for yeast condensin *in vitro* (E. Kim et al., 2020). Still, the biological relevance of such seemingly hazardous behaviour remains to be determined (Banigan et al., 2020).

Several hypotheses of the loop extrusion model were proposed and are awaiting experimental falsification in the context of compatibility with biological processes.

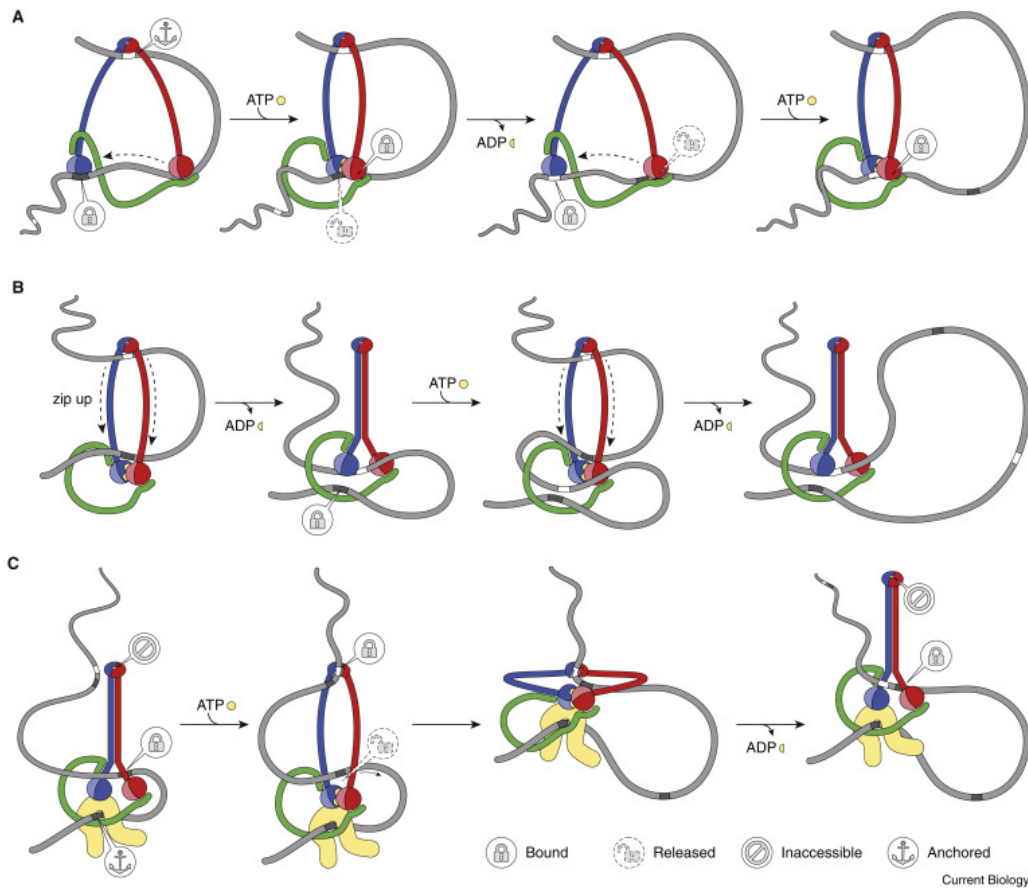


Figure 4. Mechanistic models of chromosome folding. Loop extrusion (LE) by SMC complexes forms the basis of each model. **A.** Sequential walking. **B.** DNA pumping model. **C.** Scrunching model. Figure source: (Hassler et al., 2018)

The Sequential walking model

Inspired by cytoskeletal motor proteins, the sequential walking model assumes “walking” of the head domains along the DNA molecule powered by repeated ATP binding and hydrolysis by the ATPase head domains (Figure 4A). The relatively big step size would span the combined lengths of coiled coil and hinge domains or be restricted by the length of the kleisin subunit bridging the heads (Terakawa et al., 2017). A major setback for this model is the lack of biochemical evidence supporting alternated binding of ATP to each half of the functional ATPase domain. Moreover, it is not clear how the initial loop would be captured and how SMC would stay ‘*in cis*’ on the translocation track given that the heads would only transiently interact with the DNA.

The DNA pumping model

This model assumes DNA loop capture within a ring-shaped SMC complex (topological or pseudo-topological, Figure 4B). ATP-driven conformational ring to rod transitions are expected to promote SMC movement on the DNA, by coordinating availability of DNA binding sites and entrapping DNA within the SMC complex (M. L. Diebold-Durand et al., 2017). The DNA loop captured in the S-compartment would be transferred/pumped to the K-compartment, allowing for gradual enlargement of the loop. How the initial loop would be captured and step size controlled, however, remains unanswered by this model.

The Scrunching model

This model assumes DNA binding to the hinge and head domains in an alternating manner. Moreover, transient interactions between the two mentioned interfaces are expected (Figure 4C). A single cycle would include: DNA binding to disengaged heads, followed by ATP binding, head engagement and opening of the coiled coils allowing for the hinge proximal DNA binding interface to become available. At this point, DNA is transferred from the heads to the hinge due to folding of SMC coiled coils leading to *de novo* loop formation. This model theoretically allows for steps significantly larger than 150 bp (by 50nm coiled coil) and stepping over nucleosomes. However, directionality of movement, coordination of DNA binding surfaces as well as how the SMC complex would manage to stay *'in cis'* is unclear.

In general, LE is a powerful mechanism for organising the chromosome. It allows for establishing long-distance intra-chromosomal contacts *'in cis'*, given stable association of the LEF with the DNA template. None of the models described above explain how loop slippage would be avoided unless an anchor protein is provided. Importantly, the translocation track is decorated with a multitude of other DNA-interacting proteins, such as other LEFs, the DNA replication machinery, the RNA polymerases, etc., which could potentially hinder SMC translocation. It is conceivable that two LEFs reeling in loops initiated at a distance from one another will eventually meet. Does this encounter lead to loop dissolution, DNA exchange between two pre-formed loops or does one complex bypass the other? Recent single molecule experiments with yeast condensin reported SMC-SMC traversal (E. Kim et al., 2020). Molecular simulations are in agreement that traversal could contribute to compacting DNA to a higher degree,

however, formation of knots as a consequence cannot be excluded. So far, there are only two reports addressing Smc-Smc encounters *in vivo* (Anchimiuk et al., 2021; Brandão et al., 2021) with contrasting interpretations.

AIM OF THE STUDY

In Chapter 1, I address the problem of Smc-Smc (i.e., loop extruding enzymes) encounters. I investigate the plasticity of the *Bacillus* segregation system to maintain the characteristic, juxtaposed chromosome organisation. Modifications of the levels of Smc complexes as well as the number and location of loading sites demonstrate that arriving at a specific chromosomal conformation is a finely tuned procedure. Here, I show that in the wild-type situation such Smc-Smc encounters are rare. Perturbations, although not detrimental to cell viability, alter the architecture of the chromosome. Potential consequences for downstream processes are yet to be elucidated.

In the course of my PhD, I have established the 3C-seq technology in the lab for *B. subtilis* cultures grown in minimal media, including time-course 3C-seq and library preparation as well as subsequent data analysis.

RESULTS

A low Smc flux avoids collisions and facilitates chromosome organization in *B. subtilis*

Anna Anchimiuk¹, Virginia S. Liroy², Florian Patrick Bock¹, Anita Minnen³, Frédéric Boccard² and Stephan Gruber*¹

¹Department of Fundamental Microbiology (DMF), Faculty of Biology and Medicine (FBM), University of Lausanne (UNIL), Lausanne, Switzerland

²Université Paris-Saclay, CEA, CNRS, Institute for Integrative Biology of the Cell (I2BC), Gif-sur-Yvette, France

³Max Planck Institute of Biochemistry, Martinsried, Germany

Smc-ScpAB complexes are molecular motors responsible for maintaining a specific chromosome fold in *B. subtilis*: juxtaposition of the right and left chromosome arms. In the paper, the effect of Smc, ParB and *parS* alterations on chromosome organization was studied to give insight on how Smc-ScpAB coordinate in physiological conditions, when multiple loading sites are available. Possibility and consequences of Smc-Smc encounters on the DNA translocation track were evaluated.

In the study we utilized a functional elongated chimeric *BsSpSmc* (*B. subtilis* hinge was replaced with *S. pneumoniae* hinge and 100 amino-acid hinge-proximal coiled coil) and observed that the complexes hyper-accumulated around the loading sites and could not support the known 3D arrangement of the chromosome as judged from ChIP-seq and 3C-seq, respectively. The phenotype could be rescued by limiting the number of loading sites to a single one. Importantly, the ParB time-course experiments with a single *parS* site showed that the modified complexes were proficient in translocating along the chromosome. Therefore, we hypothesize that the increased occupancy of size modified Smcs near the origin region is a result of reduced Smc residency time on the chromosome, leading to increased cytoplasmic pool of Smc, ready to be re-loaded. This in turn likely elevates the probability of Smc-Smc collisions on the chromosome when loading occurs at multiple *parS* sites but not when is restricted to a single *parS* site. In wild type cells the effect of collisions is subdued unless the ratio of Smc per loading site was artificially increased. In this case, similar hyper-accumulation around the loading sites was observed for wild type Smcs by ChIP-seq. Moreover, 3C-seq maps of strains harbouring two equal *parS* sites revealed novel folding patterns with two parallel secondary diagonals emerging. The shape of

the diagonals became distorted when the *parS* sites were placed further apart from each other or the number of Smcs was slightly elevated, suggesting that encounters between Smcs translocating from different *parS* sites cannot be easily resolved and generate tension on the DNA.

Results presented in the paper strongly suggest that in wild type conditions Smc-Smc encounters are avoided by the cells. We propose that several strategies are employed: a small, limited amount of Smc complexes available for loading, as well as the number, the strength, and the clustering of *parS* sites. We demonstrate that aligning the chromosome arms is a finely tuned procedure. Perturbations, although not detrimental to cell viability, alter the architecture of the chromosome, possibly not without consequences for downstream processes, yet to be elucidated.

Specific author contributions to the paper

Anna Anchimiuk

Project conceptualization, investigation: performance and data analysis of ChIP-seq and 3C-seq experiments, optimization and performance of time-course experiments, strain construction, characterization of strains with modified Smc complexes, data curation, methodology, validation and formal analysis, writing and visualization.

Virginia S. Lioy

Investigation: data analysis of 3C-seq experiments, data curation, formal analysis.

Florian Patrick Bock

Investigation: chromosome entrapment assay, formal analysis.

Anita Minnen

Investigation: strain construction and initial ChIP-qPCR regarding *parS* introduction at *amyE* locus.

Frédéric Boccard

Project conceptualization, funding acquisition.

Stephan Gruber

Project conceptualization, writing, visualization, supervision, project administration and funding acquisition.

PUBLICATION

A low Smc flux avoids collisions and facilitates chromosome organization in *B. subtilis*

Anna Anchimiuk, Virginia S. Liroy, Florian P. Bock, Anita Minnen, Frédéric Boccard,
Stephan Gruber

<https://elifesciences.org/articles/65467>

DOI: 10.7554/eLife.65467

A low Smc flux avoids collisions and facilitates chromosome organization in *Bacillus subtilis*

Anna Anchimiuk¹, Virginia S Lioy², Florian Patrick Bock¹, Anita Minnen³, Frederic Boccard², Stephan Gruber^{1*}

¹Department of Fundamental Microbiology, Faculty of Biology and Medicine, University of Lausanne, Lausanne, Switzerland; ²Université Paris-Saclay, CEA, CNRS, Institute for Integrative Biology of the Cell (I2BC), Gif-sur-Yvette, France; ³Max Planck Institute of Biochemistry, Martinsried, Germany

Abstract SMC complexes are widely conserved ATP-powered DNA-loop-extrusion motors indispensable for organizing and faithfully segregating chromosomes. How SMC complexes translocate along DNA for loop extrusion and what happens when two complexes meet on the same DNA molecule is largely unknown. Revealing the origins and the consequences of SMC encounters is crucial for understanding the folding process not only of bacterial, but also of eukaryotic chromosomes. Here, we uncover several factors that influence bacterial chromosome organization by modulating the probability of such clashes. These factors include the number, the strength, and the distribution of Smc loading sites, the residency time on the chromosome, the translocation rate, and the cellular abundance of Smc complexes. By studying various mutants, we show that these parameters are fine-tuned to reduce the frequency of encounters between Smc complexes, presumably as a risk mitigation strategy. Mild perturbations hamper chromosome organization by causing Smc collisions, implying that the cellular capacity to resolve them is limited. Altogether, we identify mechanisms that help to avoid Smc collisions and their resolution by Smc traversal or other potentially risky molecular transactions.

*For correspondence: stephan.gruber@unil.ch

Competing interests: The authors declare that no competing interests exist.

Funding: See page 19

Preprinted: 04 December 2020

Received: 04 December 2020

Accepted: 28 July 2021

Published: 04 August 2021

Reviewing editor: Michael T Laub, Massachusetts Institute of Technology, United States

© Copyright Anchimiuk et al. This article is distributed under the terms of the [Creative Commons Attribution License](https://creativecommons.org/licenses/by/4.0/), which permits unrestricted use and redistribution provided that the original author and source are credited.

Introduction

Members of the family of SMC proteins are ubiquitous in eukaryotes and also present in most bacteria and at least some lineages of archaea. They are crucial for establishing 3D genome organization inside cells, laying the foundation for faithful segregation, recombination, and repair of the chromosomal DNA molecules. Together with kleisin and kite subunits (or kleisin and hawk subunits), SMC proteins form ATP-hydrolyzing DNA motors that actively fold chromosomal DNA molecules apparently by DNA loop extrusion (Yatskevich et al., 2019). Loop extrusion can explain diverse folding phenomena across all domains of life: formation of topologically associated domains (TADs) in interphase, lengthwise compacted chromosomes during mitosis, as well as juxtaposition of the arms of bacterial chromosomes.

Recently, ATP-dependent loop extrusion has been recorded in single-molecule experiments. Purified yeast condensin and vertebrate cohesin extrude DNA loops at rates of ~1 kb/s in an asymmetric (one-sided) or symmetric (two-sided) manner, respectively (Davidson et al., 2019; Ganji et al., 2018; Kim et al., 2019). Nevertheless, the molecular underpinnings of loop extrusion are yet to be discovered. In the case of yeast condensin, two DNA-loop-extruding complexes on the same DNA molecule were reported to occasionally traverse one another in vitro, thus forming interlocking loops (also termed Z loops) (Kim et al., 2020). In principle, the latter behavior could improve the otherwise poor loop coverage achieved by one-sided motors, but on the other hand it likely generates

undesirable DNA entanglements (such as pseudoknots) (Banigan et al., 2020). The biological relevance of Z-loop formation and condensin traversal is yet to be determined.

Two distinct patterns of chromosome organization have been described for bacteria. One relies on MukBEF (or MksBEF) complexes, presumably starting DNA loop extrusion from randomly chosen entry sites on the bacterial chromosome (Lioy et al., 2018; Lioy et al., 2020; Mäkelä and Sherratt, 2020). The second pattern occurs in most bacteria, where Smc-ScpAB complexes start DNA translocation from predefined entry sites, the 16 bp *parS* DNA sequences, which are generally found near the replication origin and are specifically recognized by the Smc-loader protein ParB (Gruber and Errington, 2009; Lin and Grossman, 1998; Minnen et al., 2016; Sullivan et al., 2009). ParB dimers form DNA clamps that self-load onto DNA at *parS* sites (Jalal et al., 2020; Osorio-Valeriano et al., 2019; Soh et al., 2019). As Smc complexes translocate away from the *parS* loading site in both directions (two-sided), they co-align the left and the right chromosome arms that flank the replication origin (Marbouty et al., 2015; Minnen et al., 2016; Tran et al., 2017; Wang et al., 2015; Wang et al., 2017), eventually getting unloaded by XerD near the replication terminus (Karaboja et al., 2021). Bacterial genomes often have one or few closely positioned *parS* sites (separated by a few kb) (Livny et al., 2007). *Bacillus subtilis* (*Bsu*), however, harbors eight *parS* sites scattered over a much wider region of the genome (~0.75 Mb) (Figure 1A).

The two-sided DNA translocation by Smc-ScpAB is thought to have two main functions: (i) it organizes bacterial chromosomes by co-aligning chromosome arms as mentioned above and (ii) supports chromosome individualization presumably by localizing knots and precatenanes (i.e., DNA interwindings) on the replicating chromosome, thus enabling DNA topoisomerases to completely untangle nascent sister DNA molecules efficiently (Bürmann and Gruber, 2015; Orlandini et al., 2019; Racko et al., 2018). This activity might be shared with condensin in eukaryotes (Dyson et al., 2021). The degree of defects in chromosome segregation caused by *smc* deletion is variable among species. In *B. subtilis*, chromosome segregation fails completely in *smc* mutants under nutrient-rich growth conditions but not when cells are grown with more limited nutrient availability (Gruber et al., 2014; Orlandini et al., 2019; Wang et al., 2014). Deletion of *parB* or removal of *parS* sites eliminate chromosome arm alignment, but have only a mild impact on chromosome segregation, demonstrating that chromosome arm alignment is not required for efficient chromosome segregation (and for cell viability) (Lee et al., 2003; Wang et al., 2015) and implying that Smc-ScpAB can use non-*parS* sequences for loading in the absence of ParB/*parS*. For simplicity, we represent the translocating unit of Smc-ScpAB as a single ring; however, we note that other arrangements (such as a double ring) are conceivable.

SMC complexes share a characteristic elongated architecture: a globular head and a hinge domain are connected by a long intramolecular antiparallel coiled coil 'arm' (Figure 1B). The functioning of the complex is restricted to discreet lengths of the coiled coil, the same periodicity of which is observed across diverse species and types of SMC proteins (Bürmann et al., 2017). Two SMC proteins dimerize at the hinge and are bridged at the head domains by a kleisin subunit. This generates annular tripartite SMC-kleisin assemblies that entrap chromosomal DNA double helices (Gligoris et al., 2014; Wilhelm et al., 2015). The kite subunit (ScpB in *B. subtilis*) also forms dimers that associate with the central region of kleisin (ScpA in *B. subtilis*) (Bürmann et al., 2013).

To support the nearly complete alignment of chromosome arms, Smc complexes must keep translocating on the same DNA molecule (i.e., remain in *cis*) and in the same direction for extended periods of time (estimated to be in the range of 40 min in *B. subtilis*). This processivity is thought to rely on the stable entrapment of one or more DNA double helices by the SMC complex guaranteeing lengthy periods of time between association and dissociation events ('chromosome residency') (Gligoris et al., 2014; Wilhelm et al., 2015). The extended nature of the coiled coils would nevertheless permit the SMC complex to overcome relatively big obstacles (~30 nm) without dissociating from DNA. How DNA entrapment might be compatible with the bypass of even larger obstacles on the chromosome remains unclear (Brandão et al., 2019). Moreover, Smc complexes loaded simultaneously at different *parS* sites (Figure 1A) will translocate towards each other and eventually collide. Dedicated mechanisms (such as Smc traversal proposed for purified yeast condensin) might be necessary to resolve such encounters. On the other hand, a translocation mechanism not involving DNA entrapment by the SMC complex would readily facilitate bypassing of obstacles, but it is unclear how directionality of translocation and chromosome association might be maintained in this case.

Figure 1 continued

maps obtained from exponentially growing cultures. Top row: strains with wild-type *parS* sites. Bottom row: strains with a single ^{-9kb}*parS*_{opt} (*parS*-S359) site. All 3C-seq maps presented in this study are split into 10 kb bins and have the replication origin placed in the middle. The interaction score is in log₁₀ scale, the darker the color, the more interactions between given loci (see Materials and methods). (D) Normalized 3C-seq contact maps obtained from exponentially growing cultures carrying all the wild-type *parS* sites and wild-type length Smc (Smc-CC344) with either only hinge replaced by the *S. pneumoniae* sequence (*Spn* hinge, left panel) or the hinge together with 100 amino acids of hinge-proximal coiled coil replaced (*Spn* hinge + CC100, right panel). (E) Scheme for asymmetric loop extrusion starting at ^{-304kb}*parS* (*parS*-334) due to blockage of translocation towards the replication origin by head-on encounters (with other Smc complexes or RNA polymerase) generating an arc of contacts in the 3C-seq maps. (F) Normalized 3C-seq contact maps of elongated Smc (Smc-CC425) carrying *parS*_{opt} sites at -304 kb and -9 kb (left panel) or *parS*_{opt} site at -304 kb only (right panel). Triangles above the contact map point to positions of *parS* sites (dark gray triangles indicate active *parS* sites, light gray triangles for reference are *parS* sites absent in the given experiment).

The online version of this article includes the following figure supplement(s) for figure 1:

Figure supplement 1. Characterization of Smc variants, #1.

Figure supplement 2. Characterization of Smc variants, #2.

Figure supplement 3. Recruitment efficiency of various *parS* sequences.

Here, we studied the effect of Smc, ParB, and *parS* alterations on chromosome organization to explore how Smc-ScpAB load and translocate on a chromosome with multiple loading sites. Based on our results, we propose that Smc complexes rarely meet on the chromosome under physiological conditions. We argue that multiple parameters are fine-tuned to avoid Smc-Smc collisions in the first place. Few Smc complexes are available for loading because most Smc complexes are associated with the chromosome arms for an extended period of time. Artificially increasing the rate of encounters by mildly elevating the levels of Smc complexes *in vivo*, or by altering the efficiency of Smc loading, entrapment and/or translocation, leads to obvious perturbations in chromosome architecture, presumably due to unresolved Smc-Smc collisions. Also, the genomic clustering of strong *parS* sites seems to play a vital role in avoiding Smc collisions in *B. subtilis*. Although we cannot exclude the possibility of dedicated mechanism for the resolution of collisions *per se*, we suggest that an optimized Smc flux helps to eschew such events, presumably to avoid complications emerging from any attempted resolution reaction.

Results

Arm-modified Smc proteins fail to juxtapose chromosome arms

We previously isolated chimeric Smc proteins with elongated and shortened coiled coils that can functionally substitute for the *B. subtilis* Smc (Bürmann *et al.*, 2017). From a collection of 20 constructs, we here identified several elongated Smc proteins, including Smc-CC425 (with a 425 aa coiled coil as compared to the 334 aa in wild-type Smc), which supported normal growth on nutrient-rich medium even in a sensitized background (Δ *parB*) (Figure 1B, Figure 1—figure supplement 2D). A selected Smc variant was tagged with HaloTag ('HT') to evaluate its expression levels. In-gel fluorescence detection showed comparable cellular levels for Smc-HT and Smc-CC425-HT proteins (Figure 1—figure supplement 1A). Chemical cross-linking of cysteine variants of Smc-CC425 moreover indicated that it assembles holo-complexes efficiently, and co-isolation of cross-linked circular species with intact chromosomal DNA implied a only slightly reduced fraction of chromosomally loaded Smc-CC425 (Figure 1—figure supplement 1C; Vazquez Nunez *et al.*, 2019).

We hypothesized that the coiled coil length may influence DNA translocation, particularly when Smc complexes meet and overcome obstacles on the DNA track. To address this, we performed 3C-seq analysis on cells grown in nutrient-poor medium (SMG) at 37°C, supporting growth with a generation time of ~60 min. Encounters between translocating Smc complexes and the replication fork are expected to be rare under these conditions as replication initiates only about every 60 min (Gruber *et al.*, 2014). We found that Smc-CC425 and the other elongated variants failed to support normal chromosome organization (Figure 1C). As revealed by the absence of a secondary diagonal, the co-alignment of chromosome arms was strongly compromised. An arc of contacts on the left arm of the chromosome however was observed in wild-type and mutant 3C-seq maps (see below). A control chimeric protein with wild-type arm length (Smc-CC334 *Spn* hinge+CC100) showed similar growth behavior and 3C-seq maps as the resized variants (Figure 1D, Figure 1—figure supplement

1E). With a shortened Smc protein, Smc-CC253, only residual levels of inter-arm contacts were noticeable, extending only few hundred kb from the replication origin (Figure 1C, Figure 1—figure supplement 1D). Another control chimeric protein with wild-type arm length and only the hinge domain replaced by the corresponding *Streptococcus pneumoniae* sequences (SmC-CC334 Spn hinge) was only moderately affected for chromosome organization (Figure 1D), implying that Smc arm modifications accounted for large parts of the defects in chromosome organization. We conclude that in contrast to wild-type Smc engineered Smc variants are unable to properly co-align the two chromosome arms despite supporting growth, and presumably chromosome segregation, apparently normally.

Removal of all but one *parS* sites rescues chromosome folding by arm-modified Smc

To reveal the cause of the defect in chromosome arm alignment, we sought to characterize the loading and translocation of the modified Smc complexes on the bacterial chromosome. We started by generating strains in which seven *parS* sites were inactivated by mutations, with ^{-9kb}*parS* (*parS*-359) remaining the only *parS* site on the chromosome (along with the weak ^{+1058kb}*parS* site; *parS*-90; see below). As expected from published work (Marbouty et al., 2015; Umbarger et al., 2011; Wang et al., 2015), wild-type Smc efficiently aligned chromosome arms from a single strong *parS* site (Figure 1C). Remarkably, all four Smc proteins with an extended Smc arm displayed clearly increased levels of inter-arm contacts (Figure 1C). Near the replication origin, chromosome arm alignment was comparable to wild type, while the inter-arm contacts were less frequent (or absent) further away from the replication origin with all modified Smc constructs (Figure 1C; for quantification, see Figure 1—figure supplement 2A). The shortened Smc variant (CC253) also displayed more inter-arm contacts when the seven *parS* sites were mutated (Figure 1C). Thus, the removal of seven *parS* sites improved—rather than hindered—chromosome arm alignment by modified Smc proteins.

The arc of contacts detected on the left arm of the chromosome was lost in all strains harboring only the ^{-9kb}*parS* site (Figure 1C; Marbouty et al., 2015). It was also lost when only ^{-304kb}*parS* site (*parS*-334) was mutated but not when its sequence was substituted for the ^{-9kb}*parS* sequence (Figure 1—figure supplement 2B, C). Of note, the ^{-304kb}*parS* site is unique, in being relatively strong as well as distantly located from other strong *parS* sites (Figure 1A). DNA loop extrusion starting from this site is asymmetric, presumably due to a high likelihood of clashes with other Smc complexes and RNA polymerase (see scheme in Figure 1E and see below).

To test the impact of *parS* distribution in a more controlled way, we created strains with two distantly positioned *parS* sites (Figure 1A, lower panel). Since *parS* sites accumulate varying levels of ParB protein (Graham et al., 2014; Minnen et al., 2016), we first identified the *parS* sequences giving highest chromosomal recruitment of ParB and Smc when inserted at the *amyE* locus (+328 kb) in otherwise wild-type cells. The sequence of the ^{-9kb}*parS* site outperformed four other natural *parS* sequences and behaved equally well as an engineered consensus sequence at the ectopic location as judged by ChIP-qPCR (Figure 1—figure supplement 3). We thus used the strong ^{-9kb}*parS* sequence (denoted as *parS*_{opt}) in subsequent experiments. When two *parS*_{opt} sites (^{-9kb}*parS*_{opt} and ^{-304kb}*parS*_{opt}) were combined on the same chromosome, chromosome arm alignment by Smc-CC425 became inefficient, producing a contact map similar to the one obtained with all *parS* sites present (Figure 1F).

RNA polymerase is a known impediment for Smc DNA translocation (Brandão et al., 2019). To dissect the contribution of Smc-Smc and Smc-RNA polymerase encounters in the hindrance of chromosome arm alignment, we treated exponentially growing cells for 15 min with the RNA polymerase inhibitor rifampicin ('rif') (at 25 ng/ml) (Wang et al., 2017). As seen before, the obtained maps became significantly noisier upon rif treatment (Figure 1—figure supplement 2E). The arc originating from ^{-304kb}*parS* in strains carrying Smc-CC425 was less pronounced in the presence of rif, indicating a partial relief of constraints on Smc translocation (Figure 1—figure supplement 2E). This indicates that transcription contributes to the defects observed with Smc-CC425 in the presence of multiple *parS* sites.

Altogether, we conclude that the presence of two or more *parS* sites hampers chromosome organization by Smc-CC425, conceivably because Smc-CC425 protein is more prone to collisions than wild-type Smc or less efficient in resolving them.

An arm-modified Smc protein over-accumulates in the replication origin region

Wild-type Smc-ScpAB displays highest enrichment on the chromosome in the replication origin region with long and shallow gradients of enrichment along both chromosome arms (Gruber and Errington, 2009; Minnen et al., 2016), presumably generated by loading at *parS*, by translocation towards the replication terminus (*ter*) with some Smc being spontaneously unloaded from chromosome arms and the remaining fraction of Smc being unloaded by XerD near *ter* (Karaboja et al., 2021). Removal of seven *parS* sites had only a minor impact on the distribution of wild-type Smc-ScpAB as judged by chromatin immunoprecipitation coupled to deep sequencing (ChIP-seq) using α -ScpB serum (Figure 2A, B, left panels). The chromosomal distribution of Smc-CC425 was markedly different (Figure 2A). It showed hyper-enrichment near the replication origin and poor distribution towards the chromosome arms. Remarkably, the removal of seven *parS* sites substantially reduced the hyper-enrichment near the origin and increased the otherwise relatively low signal on the chromosome arms (Figure 2A, B, right panels, Figure 2—figure supplement 1A). The hyper-enrichment of Smc in the replication origin region thus correlated with poor chromosome arm alignment (Figure 1C). These results suggest that in the presence of multiple *parS* sites the modified Smc coiled coil either impedes Smc translocation provoking frequent collisions and unproductive loop formation or increases the rate of unloading and subsequent reloading events in the origin region. Both hypotheses could equally well explain the hyper-enrichment of Smc-CC425 in that region.

We next synchronized chromosomal loading of Smc and Smc-CC425 at a single *parS* site ($\sim 9^{\text{kb}}$ *parS^{\text{ori}}*) in a population of cells by depleting and repleting ParB protein. These experiments were performed at 30°C to allow sufficient ParB expression from a theophylline riboswitch-regulated *parB* construct. Smc and Smc-CC425 complexes were both found enriched in an ~ 700 kb region centered on the replication origin after 20 min of ParB induction by ChIP-seq analysis using α -ScpB serum (Figure 2C, Figure 2—figure supplement 1B). For wild-type Smc, the enriched region increased in size over time, inferring a constant DNA translocation rate of roughly 500 bp/s at 30°C. Notably, the high enrichment near *parS* disappeared at the later time points as Smc-ScpAB became more broadly distributed on the chromosome. The region of Smc-ScpAB enrichment also broadened in Smc-CC425 during the later time intervals, albeit with an apparently reducing rate. In addition, the origin region remained highly enriched in ScpB also at the later time points. Using 3C-seq, we observed that Smc-CC425 was able to align chromosome arms in this experimental system, yet the alignment did not extend all the way to the *ter* region (Figure 2D). Moreover, the onset of chromosome alignment as well as the rate of progress appeared somewhat reduced when compared to wild-type Smc. Determining a translocation rate for Smc-CC425 from the ChIP-Seq and 3C-Seq data turned out to be difficult because of the lack of a clear moving front particularly at the later time points. Moreover, the translocation rates appeared to reduce at later timer points, possibly due to increased spontaneous unloading of Smc-CC425. Regardless, these experiments demonstrate that Smc-CC425 efficiently accumulated in the replication origin region, but the translocation to distal loci on the chromosome arms was hampered.

A simple explanation for the hyper-accumulation of Smc-CC425 in the replication origin region (in the presence of a single *parS* site) is an increase in spontaneous unloading of translocating Smc. With shorter periods of time spent translocating along the chromosome arms, the cytoplasmic pool of Smc increases and as a consequence so does the flux of loading, which—possibly together with a reduced translocation rate—leads to artificially increased enrichment near the *parS* site(s). This in turn is expected to elevate the probability of Smc-Smc collisions on the chromosome when loading occurs at multiple *parS* sites but not when restricted to a single *parS* site. Such collisions would further exacerbate the Smc hyper-enrichment by hindering Smc translocation away from *parS* sites (Figure 2A, right panel). A reduced chromosome residency time and a reduced translocation rate may thus explain all phenotypic consequences of the Smc arm-modifications. Whether Smc-CC425 has a problem in resolving collisions remains to be established (see Discussion).

Wild-type Smc protein generates overlapping chromosome folding patterns

We next wondered how wild-type Smc proteins co-align chromosome arms when starting DNA loop extrusion at multiple *parS* sites. Wild-type Smc displayed relatively low enrichment in the replication

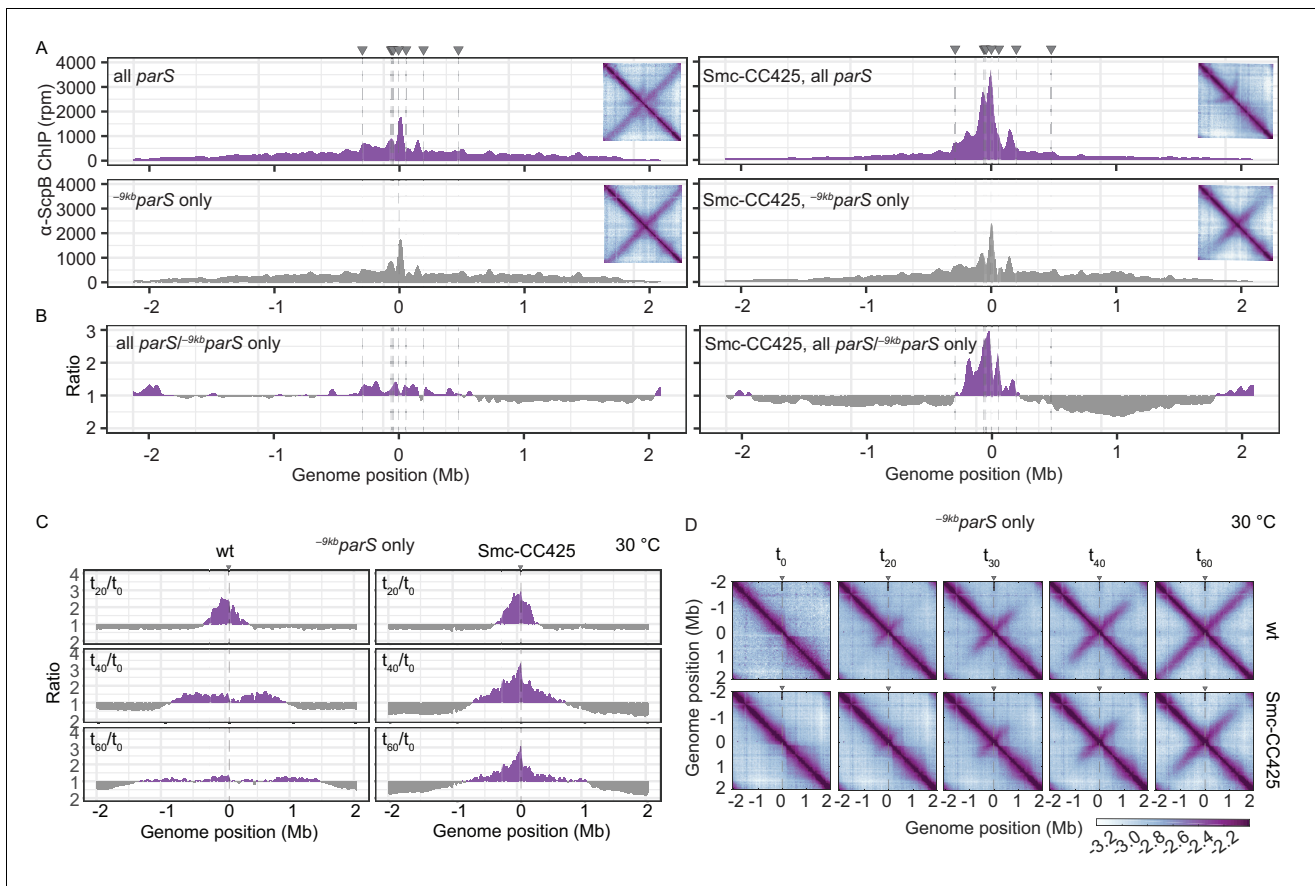


Figure 2. Modified Smc proteins hyper-accumulate in the replication origin region. (A) Read count distribution for chromatin immunoprecipitation coupled to deep sequencing (ChIP-seq) using α -ScpB serum. Left panel: strains carrying wild-type Smc with wild-type *parS* sites (top) or single $-9\text{kb}_{\text{parS}_{\text{opt}}}$ (*parS*-359) site (bottom). Removal of *parS* sites results in a slightly reduced enrichment in the origin region and in turn modestly increased signal mainly on the right arm of the chromosome (supposedly due to the presence of the weak $+1058\text{kb}_{\text{parS}}$ site; *parS*-90). Right panel: strains carrying Smc with elongated coiled coil (Smc-CC425) with wild-type *parS* sites (top) or single $-9\text{kb}_{\text{parS}_{\text{opt}}}$ (*parS*-359) site (bottom). Insets depict corresponding 3C-seq contact maps. All ChIP-seq profiles presented in this study are divided into 1 kb bins and have the replication origin placed in the middle. Dashed lines indicate the position of *parS* sites. (B) Ratio plots of ChIP-seq read counts for wild-type and elongated Smc (Smc-CC425) shown in (A). For each bin, normalized read counts for single $-9\text{kb}_{\text{parS}_{\text{opt}}}$ were compared with respective wild-type *parS* values. If the mutant/wild-type ratio was > 1 , it was plotted above the genome position axis (in violet colors). If the mutant/wild-type ratio was < 1 , the inverse ratio was plotted below the axis (in gray colors). (C) ChIP-seq time-course experiments using α -ScpB serum for strains carrying wild-type (left panel) or elongated Smc (Smc-CC425, right panel). These strains harbor a single loading site, $-9\text{kb}_{\text{parS}_{\text{opt}}}$ (*parS*-359), and a theophylline-inducible *parB* gene. Ratios plots of read counts for a given time point (t_x) versus t_0 are shown. For each bin, normalized read counts were compared with respective t_0 value and the higher value was divided by the lower. If the ratio t_x/t_0 was > 1 , it was plotted above the genome position axis (in violet colors). If the ratio t_0/t_x was > 1 , the inverse ratio was plotted below the axis (in gray colors). (D) Normalized 3C-seq contact maps for the time course experiments with strains carrying wild-type (top panel) or elongated Smc (Smc-CC425, bottom panel), corresponding to (C).

The online version of this article includes the following figure supplement(s) for figure 2:

Figure supplement 1. Enrichment of Smc and Smc-CC425 in the replication origin region.

origin region even when all natural *parS* sites were present (Figure 2A). To understand how collisions between translocating Smc complexes are avoided or resolved, we next aimed to increase the incidence of collisions by positioning two *parS_{opt}* sequences at selected sites in varying genomic distances and performed 3C-seq analysis.

As expected, control strains with a unique *parS_{opt}* sequence at positions -9 kb , at -304 kb , or at $+328\text{ kb}$ (at *amyE*) demonstrated extensive alignment of the respective flanking regions (Figure 3A; Wang et al., 2015; Wang et al., 2017). The $+328\text{ kb}_{\text{parS}_{\text{opt}}}$ site, and to a lesser extent the $-$

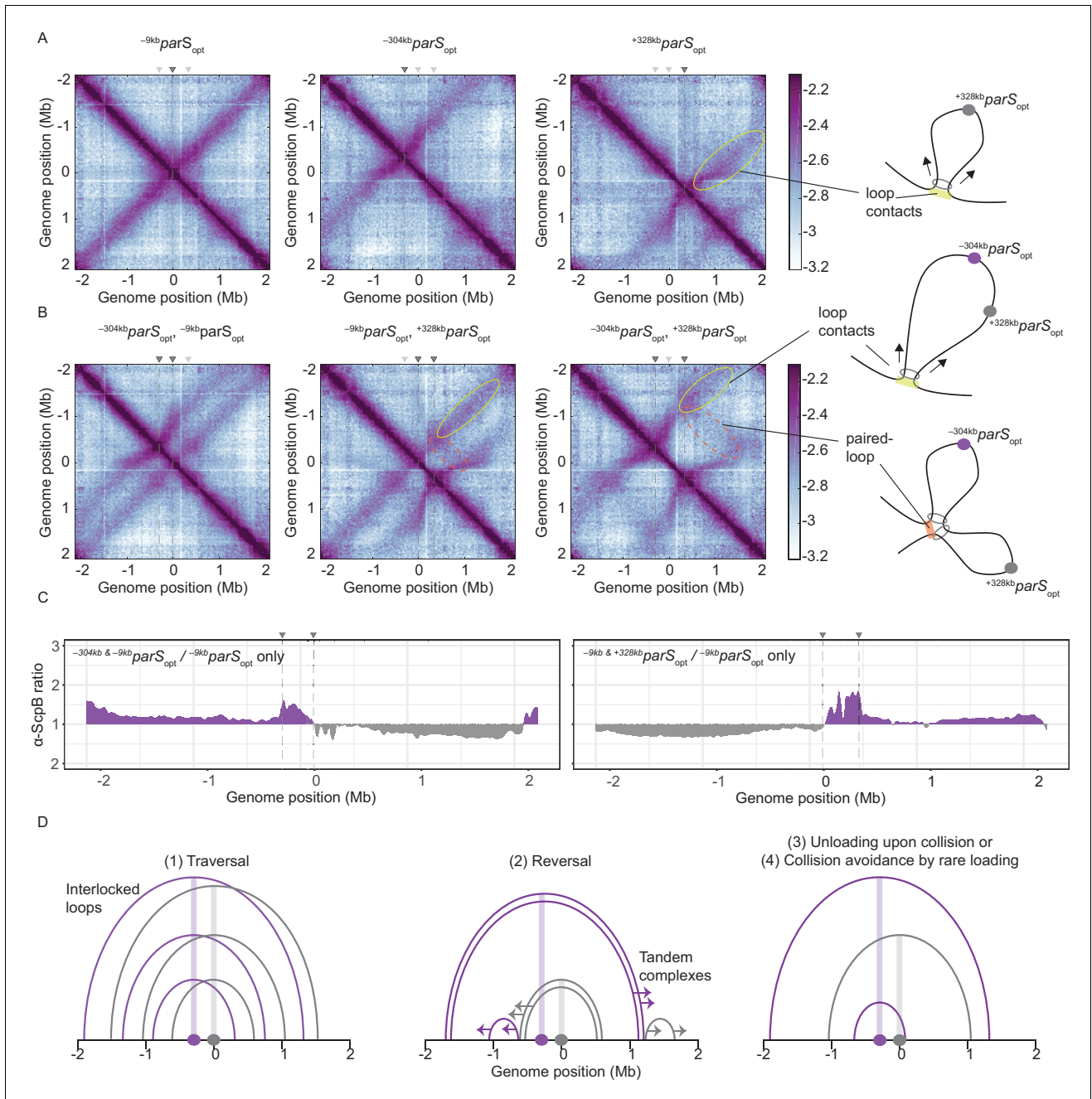


Figure 3. Overlapping chromosome arm alignment patterns for wild-type Smc. (A) Normalized 3C-seq contact maps for strains with a single $parS_{opt}$ site at -9 kb, -304 kb, or $+328$ kb. Dark gray triangles above the contact maps indicate the presence of active $parS$ sites. Light gray triangles for reference are $parS$ sites absent in the given experiment. Schemes depict a ‘loop contact’ that emerges by bidirectional translocation of a Smc unit from a single loading site (yellow), here $+328\text{kb } parS_{opt}$. (B) Normalized 3C-seq contact maps for strains with two $parS_{opt}$ sites spaced by ~ 300 kb (left and middle) or ~ 600 kb (right). Schemes interpreting interactions in the contact maps: loop contacts (in yellow colors) and ‘paired-loop contacts’ that we presume to emerge by collision of two convergently translocating Smc units loaded at opposite $parS$ sites (in orange colors). (C) Ratio plots for CHIP-seq read counts for a strain with two $parS$ sites (left panel: $-304\text{kb } parS_{opt}$ and $-9\text{kb } parS_{opt}$; right panel: $-9\text{kb } parS_{opt}$ and $+328\text{kb } parS_{opt}$) and a control strain with a single $parS$ site ($-9\text{kb } parS_{opt}$). Representation as in **Figure 2B**. (D) Schemes depicting possible scenarios for long-distance contacts emerging by **Figure 3 continued on next page**

Figure 3 continued

bidirectional Smc translocation with collision avoidance and collision resolution: Smc traversal (1), reversal (2), unloading upon collision (3), or low Smc flux (4).

The online version of this article includes the following figure supplement(s) for figure 3:

Figure supplement 1. Wild-type Smc protein generates overlapping chromosome folding patterns.

$^{304\text{kb}}$ *parS*_{opt} site, resulted in asymmetric alignment of the flanking DNA probably due to the presence of clusters of highly transcribed genes (including rDNA operons) in head-on orientation (Brandão *et al.*, 2019). Of note, the frequency of contacts reaching beyond the replication origin is notably reduced with $^{-304\text{kb}}$ *parS*_{opt} or $^{+328\text{kb}}$ *parS*_{opt}, implying that the origin region acts as a semi-permissive barrier for Smc translocation (or a Smc unloading site), as previously noted (Minnen *et al.*, 2016). Note that in the map of Smc-CC425 with a single $^{-304\text{kb}}$ *parS*_{opt} site, only faint signals reaching beyond the origin at the secondary diagonal became visible (Figure 1F), being consistent with the replication origin region being a translocation barrier.

More importantly, when two *parS* sites were combined on the chromosome, striking novel patterns of chromosome organization by wild-type Smc arose (Figure 3B). In all cases, parallel secondary diagonals emerging from the two *parS* sites were detected. The pattern observed with $^{-304\text{kb}}$ *parS*_{opt} and $^{-9\text{kb}}$ *parS*_{opt} can—to a large degree—be explained as a combination of contacts observed in strains with the corresponding single *parS* sites, however, with clearly reduced probability for contacts extending beyond the region demarcated by the *parS* sites. A small but noticeable fraction of Smc complexes however apparently managed to translocate towards and beyond the other *parS* site mostly unhindered (as indicated by the largely unaltered position of the secondary diagonals). Treatment with rif did not significantly alter the contact pattern (apart from generating noisier maps) (Figure 3—figure supplement 1A). The contact maps involving the $^{-304\text{kb}}$ *parS*_{opt} and $^{+328\text{kb}}$ *parS*_{opt} sites showed additional contacts likely representing paired loops originating from collided Smc complexes loaded at opposite *parS* sites (Figure 3B). The presence of such paired loop contacts was less clear for the other *parS* combinations possibly due to background signal and limited resolution of the 3C-seq maps. We conclude that wild-type Smc-ScpAB complexes rarely block one another when loaded from all natural *parS* sites (with the notable exception of $^{-304\text{kb}}$ *parS*). When the distance between two strong *parS* sites was artificially increased, however, impacts arising from collisions and blockage became noticeable. The blockage of Smc translocation was also apparent from ChIP-seq analysis, which demonstrated hyper-enrichment of Smc between two *parS* sites ($^{-304\text{kb}}$ *parS*_{opt} and $^{-9\text{kb}}$ *parS*_{opt} or $^{-9\text{kb}}$ *parS*_{opt} and $^{+328\text{kb}}$ *parS*_{opt}) when compared to the single *parS* control (Figure 3C, Figure 3—figure supplement 1C, D). The effects of collisions on chromosome organization and Smc distribution are thus subdued with wild-type Smc but readily detectable upon repositioning of *parS* sites.

To explain the relatively mild impact of collisions in wild-type cells, we envisaged the following scenarios (Figure 3D, Figure 3—figure supplement 1B): (1) the traversal of Smc complexes generating interlocking loops (Brandão *et al.*, 2020; Kim *et al.*, 2020) (2) the reversal of the translocation of one Smc complex by opposing complexes (Kim *et al.*, 2020), (3) the unloading of one or both complexes upon collision, or (4) collision avoidance either by infrequent loading or (5) by mutually exclusive *parS* usage. The latter hypothesis seemed highly unlikely as all but one *parS* sites would have to remain inactive for extended periods of time. While all other scenarios seemed plausible and may contribute to the process of chromosome organization, one scenario, the avoidance of encounters by infrequent loading, provided an explanation for the defects observed with Smc-CC425 without making additional assumptions.

Increasing the pool of Smc hampers chromosome organization

If Smc-CC425 indeed fails to juxtapose chromosome arms due to an increased flux in the replication origin region, collisions may be rare in wild-type cells because of a high chromosome residency time and a limited pool of soluble Smc complexes, resulting in a low flux of Smc onto the chromosome. If so, artificially increasing the flux of Smc should lead to defects in chromosome organization with multiple *parS* sites but not with a single *parS* site (as observed for Smc-CC425 under normal expression levels) (assuming that most Smc is loaded at *parS*). If Smc complexes, however, were to

efficiently traverse, reverse, or unload one another, then increased Smc levels would not result in defective translocation and chromosome organization.

To test this prediction, we first slightly increased the cellular level of all subunits of the Smc complex by inserting an additional copy of the *smc* gene and of the *scpAB* operon under the control of their respective endogenous promoters into the genome. The increased levels of Smc-ScpAB did not noticeably affect cell growth (**Figure 4—figure supplement 1A**). Immunoblotting suggested a four- to fivefold increase in Smc and ScpB protein levels in the SMC^{high} strain when compared to wild type (**Figure 4A**). Next, we performed 3C-seq analysis. Chromosome arm co-alignment was strongly hampered—rather than improved—by the presence of extra Smc complexes in the cell (**Figure 4B**). A prominent arc was formed at the position of the ^{-304kb}*parS* site, and the secondary diagonal originating in the origin region was weak and diffuse in the SMC^{high} strain. This defect was fully restored, however, by removal of seven *parS* sites (with the remaining strong site being either ^{-9kb}*parS*_{opt} or ^{-304kb}*parS*_{opt}) (**Figure 4C**). Note that an additional feature (a minor secondary diagonal) present on the right arm of the chromosome likely originated from Smc loading at the weak ^{+1058kb}*parS* site. The presence of two strong *parS* sites (^{-9kb}*parS*_{opt} and ^{-304kb}*parS*_{opt}) led to a new pattern of chromosome folding in the SMC^{high} strain. The alignment of DNA flanking the *parS* sites became highly asymmetric, presumably because Smc complexes loaded at opposite *parS* sites hinder each other (**Figure 4D**). Moreover, the contacts corresponding to paired loops became clearly visible (**Figure 4D**). Finally, contacts outside the *parS*-demarcated region were rare and spread out, and their center was shifted away from the *parS* sites. The former indicated that only a few Smc complexes loaded at one *parS* site managed to move beyond the other *parS* site. And if they did, they experienced a strongly reduced translocation rate when moving from *parS* site to the other, presumably due to encounters with and temporary (or partial) blockage by Smc complexes translocating in opposite orientation. Importantly, the hindrance observed with two or all *parS* sites being present was not relieved by treatment with rif, being consistent with the notion that Smc-Smc encounters rather than Smc-RNA polymerase encounters are mainly responsible for the impediment of translocation in SMC^{high} (**Figure 4—figure supplement 1B**).

If Smc-Smc collisions indeed hinder translocation of wild-type Smc, then extra Smc levels may lead to hyper-accumulation of Smc-ScpAB near the replication origin when multiple *parS* sites are present but not with a single *parS* site, as observed for the modified Smc at normal levels of expression (**Figure 2A**). To test this, we performed ChIP-seq with α -ParB and α -ScpB serum in SMC^{high} strains. The α -ParB ChIP-seq demonstrated that the localization of ParB to *parS* sites is, as expected, largely unaffected by the increased levels of Smc (**Figure 4E**; [Minnen et al., 2016](#)). The chromosomal distribution of ScpB was also largely unaffected in SMC^{high} cells harboring a single ^{-9kb}*parS*_{opt} site (**Figure 4—figure supplement 1C**). However, in the presence of two or multiple additional *parS* sites, the enrichment between the *parS* sites increased strongly (**Figure 4E, F**, **Figure 4—figure supplement 1C, D**). The changes in ScpB distribution upon *parS* site removal are remarkably similar in Smc-CC425 and SMC^{high} (compare **Figures 2B** and **4E**), supporting the notion that both modifications lead to more frequent blockage after collisions probably by the same mechanism: an increased flux of Smc in the vicinity of *parS* sites.

Synchronized Smc loading favors Smc collisions

Finally, we synchronized the loading of Smc by induction of ParB with the idea that ParB repletion leads to a transiently elevated Smc flux (from a larger cytoplasmic pool of Smc) and thus increases the likelihood of encounters even with normal cellular levels of Smc-ScpAB. Here, we used a different inducible promoter, the IPTG-inducible *P*_{spank} ([Wang et al., 2017](#)), which enabled us to grow cells at 37°C and compare the results more directly to the experiment with constitutively expressed ParB (**Figure 3B**). We found that the alignment of DNA starting from ^{-9kb}*parS*_{opt} site was indeed hampered when a second *parS* site, ^{-304kb}*parS*_{opt}, was present (**Figure 4G**, **Figure 4—figure supplement 1E**), even more so than with continuous ParB expression (**Figure 3B**). However, we cannot rule out that this effect is mainly caused by competition between the two *parS* sites for Smc loading.

Discussion

Establishing how SMC complexes manage to organize and orderly compact DNA in the crowded environment of a cell is a burning question in the field. SMC complexes translocate along an

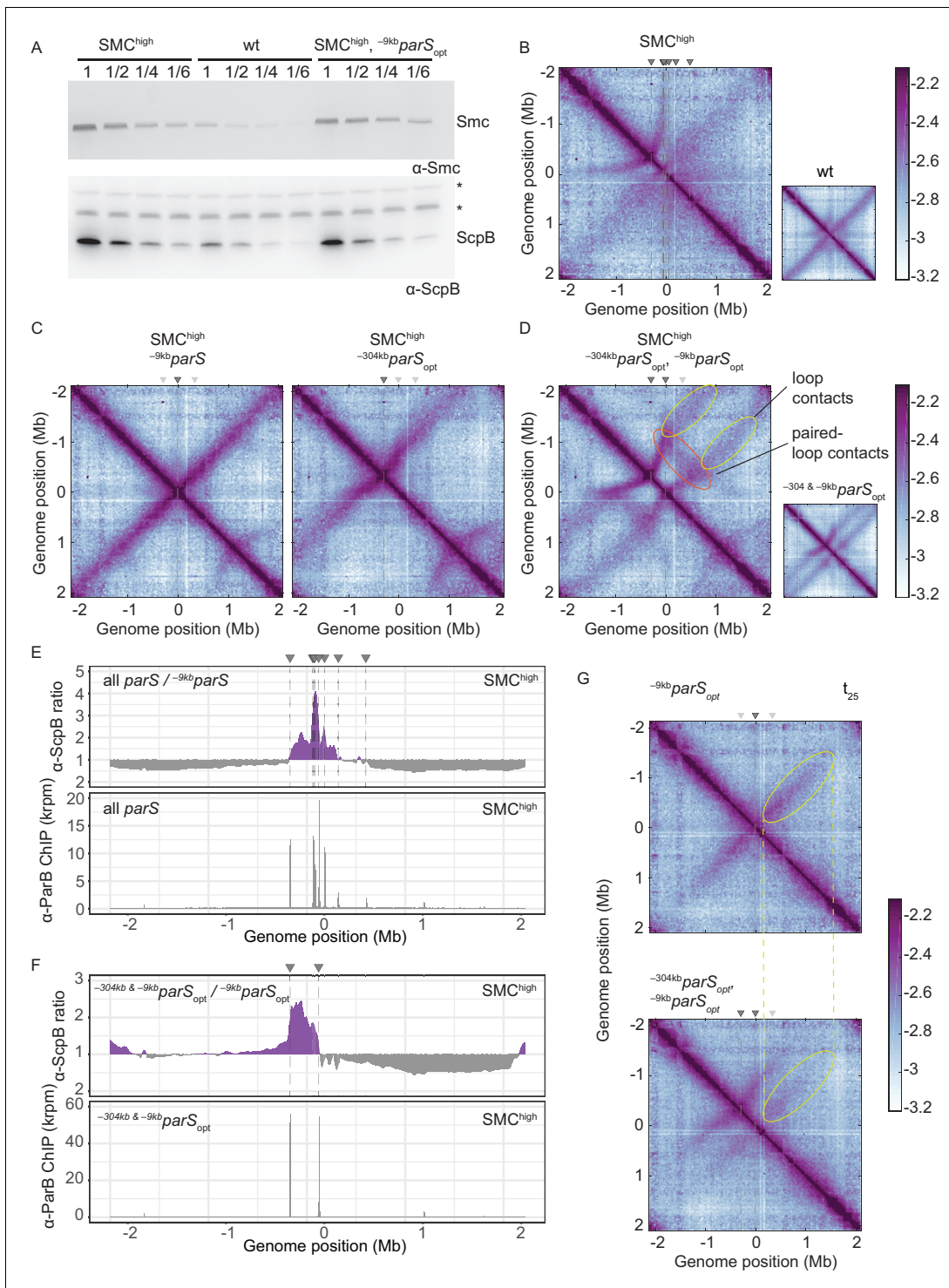


Figure 4. Increasing the cellular pool of Smc hampers chromosome organization. (A) Immunoblotting using α-Smc (top panel) and α-ScpB serum (bottom panel). SMC^{high} denotes strains with extra genes for Smc-ScpAB. Protein extracts of wild-type or SMC^{high} strains (harboring all *parS* sites or single *parS* site) were serially diluted with extracts from Δ*smc* or Δ*scpB* strains as indicated (see Materials and methods). * indicates unspecific bands generated by the α-ScpB serum. (B) Normalized 3C-seq contact map for SMC^{high} strain with all *parS* sites present. Inset shows 3C-seq contact map of a

Figure 4 continued on next page

Figure 4 continued

strain with wild-type protein levels (also displayed in **Figure 1C**) for direct comparison. (C) Normalized 3C-seq contact maps for SMC^{high} strains with *parS_{opt}* at -9 kb only or at -304 kb only. (D) Normalized 3C-seq contact map for SMC^{high} strain with *parS_{opt}* at positions: -9 kb and -304 kb. As in (B), with inset displaying respective control strain with normal Smc expression levels (also shown in **Figure 3B**). (E) Ratio plots for ChIP-seq read counts comparing SMC^{high} strains with all *parS* sites and a single *parS* site ($^{-9\text{kb}}\textit{parS}_{\text{opt}}$). Representation as in **Figure 2B** (top panel). Read count for α -ParB ChIP-seq in SMC^{high} strain (bottom panel). (F) As in (E) involving a SMC^{high} strain with two *parS* sites ($^{-304\text{kb}}\textit{parS}_{\text{opt}}$ and $^{-9\text{kb}}\textit{parS}_{\text{opt}}$) instead of all *parS* sites. (G) Normalized 3C-seq contact maps for time point t_{25} after IPTG-induced ParB expression with a single *parS_{opt}* site (top panel) or two *parS_{opt}* sites (at -9 kb and -304 kb) (bottom panel). Ellipsoids (in yellow colors) mark the position of contacts stemming from loop extrusion originating at $^{-9\text{kb}}\textit{parS}_{\text{opt}}$.

The online version of this article includes the following figure supplement(s) for figure 4:

Figure supplement 1. Synchronized loading of SMC hampers chromosome organization.

unusually flexible, congested and entangled translocation track, that is, the ‘chromatinized’ DNA double helix. The architecture of SMC complexes—one of a kind amongst the collection of molecular motors—is likely a reflection of a unique translocation mechanism. To support the folding of Mb-sized regions of the chromosome, Smc complexes need to keep translocating on the same DNA double helix from initial loading to unloading (a process lasting several tens of minutes in bacteria). Assuming a topological SMC-DNA association (*Glitoris et al., 2014; Wilhelm et al., 2015*), staying on the translocation track in cis is guaranteed as long as the SMC-kleisin ring remains closed, thus preventing the release of DNA.

During translocation, SMC complexes must frequently overcome obstacles on the DNA to translocate fast and far, and to globally organize the chromosome. RNA polymerase is a known obstacle for Smc-ScpAB in *B. subtilis*. It is highly abundant in the replication origin region due to the clustering of highly transcribed genes. Inhibition of RNA polymerase by the chemical inhibitor rif indeed partially relieved the impediment of DNA translocation by Smc. However, defects with SMC^{high} in particular (**Figure 4—figure supplement 1B**) persisted in the presence of rif implying that other obstacles exist. Very large obstructions (>30 nm) could not be overcome while keeping DNA entrapped within the Smc ring but would need to be traversed by dissociating from the translocation track transiently. Such obstacles might include branched DNA structures and protein-mediated DNA junctions (i.e., crossings in the translocation track) as well as other SMC complexes located at the base of a DNA loop.

Traversal and bypassing are not risk-free strategies. When transiently disconnecting from DNA, the complex risks losing directional translocation by wrongly reconnecting with the same DNA double helix or even establishes an unwanted trans-DNA linkage by connecting with a different DNA double helix. Any straying onto the sister DNA molecule (going in trans) would not only defeat the purpose of DNA loop extrusion but actually actively hinder chromosome segregation. Here, we addressed the balance between avoiding and resolving Smc collisions.

Avoiding Smc encounters

In our study, we show that impacts from collisions are barely noticeable in wild-type cells. Under physiological conditions, collisions between Smc-ScpAB complexes are kept at a tolerable level by a low cellular abundance of Smc-ScpAB ~ 30 Smc dimers per chromosome or less (*Wilhelm et al., 2015*), a high DNA translocation rate, an extended time of residency on the chromosome arms, and the preferential usage of a cluster of *parS* sites (spanning ~ 60 kb region of the genome: $^{-68\text{kb}}\textit{parS}$, $^{-63\text{kb}}\textit{parS}$, $^{-49\text{kb}}\textit{parS}$, $^{-9\text{kb}}\textit{parS}$). Thus, multiple parameters are fine-tuned to avoid Smc encounters, possibly rendering the resolution of Smc collisions unnecessary. Occasional loading of Smc at one of the more distal *parS* sites however would quite often lead to collisions, thus resulting in contact maps with an arc-shaped pattern, such as observed for $^{-304\text{kb}}\textit{parS}$ (the strongest of the distal *parS* sites) (**Figure 1C; Brandão et al., 2020**). When strong *parS* sites are artificially moved further away from each other, then impacts from collisions also become noticeable with wild-type Smc (**Figure 3**).

The obvious defects in chromosome organization observed with altered *parS* positioning, elevated Smc levels, or engineered Smc proteins, however, do not substantially impact bacterial growth, suggesting that chromosome segregation is efficiently supported even with Smc collisions (and without chromosome arm alignment being detectable by population-averaging 3C methodology). Colliding Smc complexes might thus efficiently promote DNA disentanglement locally (with

the help of DNA topoisomerases) but hamper the global chromosome folding process, possibly leading to large cell-to-cell variations in chromosome organization with likely knock-on effects on other cellular processes including nucleoid occlusion and cell division.

The presence of multiple types of SMC complexes acting on the same chromosome likely aggravates the issue of collisions. In *Pseudomonas aeruginosa*, the impact of collisions seems to be dealt with by a hierarchy amongst two endogenous SMC complexes and a coordination of SMC activity with chromosome replication (Lioy *et al.*, 2020). Smc-ScpAB appears to limit the loop extrusion activity of MksBEF but not vice versa. When the heterologous *Escherichia coli* MukBEF complex was introduced in place of MksBEF, it blocked the activity of *P. aeruginosa* Smc-ScpAB but not the other way around. The hierarchy is possibly given by the relative abundance of these complexes and differing chromosome association dynamics (residency times).

Resolving Smc encounters?

The parsimonious explanation for our observations—not requiring the involvement of dedicated and potentially hazardous molecular transactions—is that neither wild-type nor modified Smc proteins are able to traverse one another. A recent study describing Smc action in *B. subtilis* by simulations, however, suggested that Smc traversal is needed to accurately recapitulate the relative abundance of long-range contacts observed with natural and artificial arrangements of *parS* sites (similar to **Figure 3B**; Brandão *et al.*, 2020). Briefly, the authors explained the patterns of DNA contact distribution on the basis of estimated or fitted values for Smc abundance (<40 per chromosome), Smc translocation rate (~1 kb/s), Smc-Smc blockage, Smc unloading (~0.0033 s⁻¹), and Smc traversal (~0.05 s⁻¹). While these simulations have apparently successfully predicted changes in contact patterns upon alterations in Smc abundance, we believe that they are not fully conclusive due to substantial uncertainties concerning the involved parameters and the possible existence of unexplored alternative scenarios (e.g., **Figure 3D**). Furthermore, direct observation of Smc traversal and of interlocking DNA loops (Z loops) on the bacterial chromosome is lacking. Also, a basic understanding of the necessary molecular transactions is elusive.

Nevertheless, the idea of Smc traversal is an intriguing proposition with potentially wide implications warranting serious consideration. A putative defect in traversal might contribute to the hyperaccumulation of Smc-CC425 in the replication origin region and the defective chromosome organization with multiple *parS* sites. Assuming the validity of Smc traversal, it is tempting to speculate—on the basis of the observations with Smc-CC425—that the nature and the integrity of the Smc hinge domain and the adjacent coiled coil are critical for the putative bypassing step. How Smc traversal might occur without the risk of establishing unwanted ('trans') DNA linkages yet is totally unclear.

Multiple *parS* sites on the *B. subtilis* chromosome

The presence of multiple *parS* sites likely improves the robustness of the chromosome segregation process (Böhm *et al.*, 2020). Most bacteria have clustered *parS* sites (within 5–40 kb region) and are sensitive to deleting or positioning them outside a tolerance region (Böhm *et al.*, 2020; Lagage *et al.*, 2016; Minnen *et al.*, 2011; Tran *et al.*, 2017). Severe consequences of manipulating *parS* distribution include a longer generation time (when *mksBEF* is missing) (Lagage *et al.*, 2016), an increased number of anucleate cells (Böhm *et al.*, 2020) and elongated cells (Tran *et al.*, 2017). Some of these defects might be related to altered Smc function. In *Caulobacter crescentus*, Smc translocates only ~600 kb away from *parS* (Tran *et al.*, 2017). The partial chromosome arm alignment in *C. crescentus* is reminiscent of the observation with modified Smc proteins in *B. subtilis*. It is tempting to speculate that a shorter chromosome residency time or a lower translocation rate of Smc-ScpAB is acceptable when *parS* sites are tightly clustered or when combined with a single *parS* site. Nevertheless, some bacterial genomes harbor multiple *parS* sites that are quite widely scattered on the genome. From the point of view of collision avoidance, this seems counterproductive. Intriguingly, the scattered *parS* distribution is restricted to few lineages on the phylogenetic tree of bacteria, including Bacilli (Livny *et al.*, 2007). The scattering of *parS* sites likely serves a dedicated purpose in the lifestyles of these bacteria, in *B. subtilis* possibly during sporulation when large chunks of the genome (~1 Mb, i.e., about a quarter of the genome) are captured at the cell pole to promote entrapment of the chromosome in the pre-spore (Wu and Errington, 1998). This process might benefit from the condensation of the replication origin (possibly involving Smc collisions as

observed here) rather than an alignment of chromosome arms. Consistent with this notion, chromosome arm alignment is lost when DNA replication is artificially blocked (as naturally occurring during sporulation) and replaced by smaller loops formed at individual *parS* sites (Marbouty et al., 2015; Wang et al., 2015). A simple explanation for this altered pattern of chromosome folding during replication blockage (and possibly also during sporulation) would be an increased rate of Smc collisions due to an elevated (Smc) protein-to-DNA ratio.

Altogether, our results strongly suggest that the process of Smc DNA translocation is finely tuned to keep the probability of Smc encounters at a low level, presumably to enable extensive DNA loop extrusion without the need to resolve Smc collisions.

Materials and methods

***B. subtilis* strains and growth**

B. subtilis 1A700 or PY79 isolate was used for experiments. Naturally competent *B. subtilis* was transformed via homologous recombination as described in Diebold-Durand et al., 2019 and selected on SMG-agar plates with appropriate antibiotic selection. Transformants were next checked by PCR and, if required, Sanger sequencing. Genotypes of strains used in this study are listed in Table 1. More detailed information on how strains with mutated or wild-type *parS* sites were generated is provided in Supplementary file 3. Relevant, key plasmid maps are deposited in Mendeley Data DOI: 10.17632/kvjd6nj2bh.2.

For spotting assays, the cells were cultured in SMG medium at 37°C to stationary phase and 9^{-2} and 9^{-5} -fold dilutions were spotted onto ONA (~16 hr incubation) or SMG (~36 hr incubation) agar plates.

Immunoblotting

Cells were cultured in 150 ml of minimal media (SMG) at 37°C until mid-exponential phase ($OD_{600} = 0.022\text{--}0.025$). Pellets were collected by filtration, washed, and resuspended in 1 ml PBSG (PBS supplemented with 0.1% glycerol). 1.25 OD_{600} units of each sample were resuspended in 50 μ l PBS containing 400 units of ReadyLyse lysosome (Epicentre), 12.5 units Benzonase (Sigma) and a protease-inhibitor cocktail (PIC, Sigma), and incubated for 30 min at 37°C. Next, 4 \times Loading Dye containing DTT (200 mM final) was added and samples were incubated for 5 min at 95°C. Protein extracts from tested strains were mixed with Δ *scpB* or Δ *smc* extracts as follows: tested strain only, 1:1 vol of tested strain with Δ , 1:4, 1:6. 5 μ l of mixed protein extracts were run on Novex WedgeWell 4–12%, Tris-Glycine gels in 1 \times Laemmli buffer.

Proteins were transferred onto a PVDF membrane (Immobilon-P, Merck Millipore) using wet transfer. Membranes were blocked with 5% (w/v) milk powder in TBS with 0.05% Tween20. 1:2000 or 1:5000 dilutions of rabbit polyclonal sera against *B. subtilis* ScpB or Smc were used as primary antibodies for immunoblotting, respectively. The membrane was developed with HRP-coupled secondary antibodies and chemiluminescence (Amersham ECL Western Blotting Detection Reagent) and visualized on a FUSION FX7 (Vilber).

Chromatin immunoprecipitation (ChIP)

ChIP samples were prepared as described previously (Bürmann et al., 2017). Briefly, cells were cultured in 200 ml of minimal media (SMG) at 37°C until mid-exponential phase ($OD_{600} = 0.022\text{--}0.030$) and fixed with buffer F (50 mM Tris-HCl pH 7.4, 100 mM NaCl, 0.5 mM EGTA pH 8.0, 1 mM EDTA pH 8.0, 10% [w/v] formaldehyde) for 30 min at room temperature (RT) with occasional shaking. Cells were harvested by filtration and washed in PBS. Each sample was adjusted for 2 OD_{600} units (2 ml at $OD_{600} = 1$) and resuspended in TSEMS lysis buffer (50 mM Tris pH 7.4, 50 mM NaCl, 10 mM EDTA pH 8.0, 0.5 M sucrose and PIC [Sigma], 6 mg/ml lysozyme from chicken egg white [Sigma]). After 30 min of incubation at 37°C with vigorous shaking, protoplasts were washed again in 2 ml TSEMS, resuspended in 1 ml TSEMS, split into three aliquots, pelleted, and, after flash freezing, stored at -80°C until further use.

For time-course experiments, 1 l preculture was first grown until mid-exponential phase ($OD = 0.022\text{--}0.030$) and next appropriate culture volumes were added to fresh pre-warmed SMG so that at given time points 200 ml of culture at mid-exponential could be processed. The cultures were

Table 1. List of strains and genotypes used in the study.

BSG	Genotype	Origin
1002	1A700, smc ftsY::ermB, trpC2	The Gruber Laboratory
1007	1A700, Δsmc ftsY::ermB, trpC2	The Gruber Laboratory
1018	1A700, smc(<i>Streptococcus pneumoniae</i> hinge) ftsY::ermB, trpC2	The Gruber Laboratory
1050	1A700, ΔparB::kanR, trpC2	The Gruber Laboratory
1471	1A700, smc(E1118Q) ftsY::ermB, ΔamyE::parS-359 + tetO qPCR primer seq::cat, trpC2	This study
1489	1A700, specR::scpA ΔscpB, trpC2	The Gruber Laboratory
1541	1A700, smc(E1118Q) ftsY::ermB, ΔamyE::parS-355 + tetO qPCR primer seq::cat, trpC2	This study
1542	1A700, smc(E1118Q) ftsY::ermB, ΔamyE::parS-354 + tetO qPCR primer seq::cat, trpC2	This study
1543	1A700, smc(E1118Q) ftsY::ermB, ΔamyE::parS-90 + tetO qPCR primer seq::cat, trpC2	This study
1544	1A700, smc(E1118Q) ftsY::ermB, ΔamyE::parS-optimal + tetO qPCR primer seq::cat, trpC2	This study
1711	1A700, specR::scpA ΔscpB, trpC2	The Gruber Laboratory
2090	1A700, smc(1-438, 487-684, 733-1186) ftsY::ermB, trpC2	Bürmann et al., 2017
2092	1A700, smc(1-399, 487-684, 772-1186) ftsY::ermB, trpC2	Bürmann et al., 2017
2093	1A700, smc(1-395, 487-684, 776-1186) ftsY::ermB, trpC2	Bürmann et al., 2017
2210	1A700, smc-HaloTag (C61V, C262A) ftsY::tetL yIqB, trpC2	The Gruber Laboratory
2352	1A700, smc(1-395, SpnSmc(398-768), 776-1186) ftsY::ermB, trpC2	Bürmann et al., 2017
2934	PY79: Δ7-parS, parAB::kanR	This study
3026	PY79: Δ7-parS(parS359+), ΔparB::kanR, amyE::(PhbsB short 5'UTR-theo E+ -parB (mtparS))::CAT	This study
3216	PY79: Δ7-parS(parS359+), ΔparB::kanR, smc(1-476 SpnSmc(398-768) 695-1186) ftsY::ermB, amyE::(PhbsB short 5'UTR-theo E+ - parB (mtparS))::CAT	This study
3425	1A700, smc(1-488), SpnSmc(398-768), smc(682-1186) ftsY::ermB, trpC2	This study
3426	1A700, smc(1-482), SpnSmc(398-768), smc(689-1186) ftsY::ermB, trpC2	This study
3427	1A700, smc(1-476), SpnSmc(398-768), smc(695-1186) ftsY::ermB, trpC2	This study
3428	1A700, smc(1-472), SpnSmc(398-768), smc(699-1186) ftsY::ermB, trpC2	This study
3429	1A700, ΔparB::kanR, smc(1-488), SpnSmc(398-768), smc(682-1186) ftsY::ermB, trpC2	This study
3430	1A700, ΔparB::kanR, smc(1-482), SpnSmc(398-768), smc(689-1186) ftsY::ermB, trpC2	This study
3431	1A700, ΔparB::kanR, smc(1-476), SpnSmc(398-768), smc(695-1186) ftsY::ermB, trpC2	This study
3432	1A700, ΔparB::kanR, smc(1-482), SpnSmc(398-768), smc(689-1186) ftsY::ermB, trpC2	This study
3636	PY79: Δ7-parS, parAB::specR, smc(1-476 SpnSmc(398-768) 695-1186) ftsY::ermB	This study
3674	1A700, Δ1-parS(mtparS334)	This study
3770	PY79: smc::tet, parAB::kanR	This study
3785	1A700, ΔparB::kanR, smc(1-395, SpnSmc(398-768), 776-1186) ftsY::ermB, trpC2	This study
3786	1A700, ΔparB::kanR, smc(1-399, 487-684, 772-1186) ftsY::ermB, trpC2	This study
3787	1A700, ΔparB::kanR, smc(1-395, 487-684, 776-1186) ftsY::ermB, trpC2	This study
3790	1A700, Δ7-parS(parS359+), smc::specR	This study
3791	1A700, mtparS334 to parS359	This study
3798	1A700, Δ1-parS(mtparS334), smc(1-476), SpnSmc(398-768), smc(695-1186) ftsY::ermB	This study
3801	1A700, Δ7-parS, smc(1-488), SpnSmc(398-768), smc(682-1186) ftsY::ermB	This study

Table 1 continued on next page

Table 1 continued

BSG	Genotype	Origin
3802	1A700, $\Delta 7$ -parS, smc(1-482), SpnSmc(398-768), smc(689-1186) ftsY::ermB	This study
3803	1A700, $\Delta 7$ -parS, smc(1-476), SpnSmc(398-768), smc(695-1186) ftsY::ermB	This study
3804	1A700, $\Delta 7$ -parS, smc(1-472), SpnSmc(398-768), smc(699-1186) ftsY::ermB	This study
3805	1A700, $\Delta 6$ -parS (mtparS334 to parS359), smc::ermB	This study
3815	1A700, $\Delta 8$ -parS, parAB(mtparS359)::kanR, smc::specR	This study
3840	1A700, $\Delta 7$ -parS(parS359+), Δ parB::kanR, smc::specR	This study
3841	1A700, $\Delta 7$ -parS(parS359+), Δ parB::kanR, smc(1-488), SpnSmc(398-768), smc(682-1186) ftsY::ermB	This study
3842	1A700, $\Delta 7$ -parS(parS359+), Δ parB::kanR, smc(1-482), SpnSmc(398-768), smc(689-1186) ftsY::ermB	This study
3843	1A700, $\Delta 7$ -parS(parS359+), Δ parB::kanR, smc(1-476), SpnSmc(398-768), smc(695-1186) ftsY::ermB	This study
3844	1A700, $\Delta 7$ -parS(parS359+), Δ parB::kanR, smc(1-472), SpnSmc(398-768), smc(699-1186) ftsY::ermB	This study
3863	PY79: smc(1-476), SpnSmc(398-768), smc(695-1186) ftsY::ermB, parAB::kanR	This study
3878	1A700, $\Delta 6$ -parS(parS359+, parS334->359+), smc(1-476), SpnSmc(398-768), smc(695-1186) ftsY::tetR	This study
3879	1A700, $\Delta 7$ -parS(parS334->359+), parAB::kanR, smc::ermB	This study
3882	1A700, $\Delta 7$ -parS(parS334->359+), parAB::kanR, smc(1-476), SpnSmc(398-768), smc(695-1186) ftsY::specR	This study
3932	1A700, $\Delta 7$ -parS(parS359+), smc(1-395, 487-684, 776-1186) ftsY::ermB	This study
4083	1A700, $\Delta 6$ -parS(parS359+), smc::specR, Δ amyE::parS-359 + tetO qPCR primer seq::cat	This study
4090	1A700, $\Delta 7$ -parS, parAB::kanR, smc::specR, Δ amyE::parS-359 + tetO qPCR primer seq::cat	This study
4091	1A700, $\Delta 6$ -parS(parS334->359+), parAB::kanR, smc::ermB, Δ amyE::parS-359 + tetO qPCR primer seq::cat	This study
4100	1A700, Δ amyE::smc::CAT, qoxD-specR::scpAB-ywcE, trpC2	This study
4137	1A700, $\Delta 6$ -parS (mtparS334 to parS359), smc::ermB, Δ amyE::smc::CAT, qoxD-specR::scpAB-ywcE	This study
4143	1A700, $\Delta 7$ -parS(parS359+), smc::ermB, Δ amyE::smc::CAT, qoxD-specR::scpAB-ywcE	This study
4146	1A700, $\Delta 7$ -parS(parS334->359+), parAB::kanR, smc::ermB, Δ amyE::smc::CAT, qoxD-specR::scpAB-ywcE	This study
4152	1A700, $\Delta 7$ -parS(parS359+), Δ parB::kanR, smc::specR, Δ amyE::(Pspank-optRBS-parB(mtparS)-lacI)::CAT	This study
4427	1A700, $\Delta 6$ -parS (mtparS334 to parS359), Δ parB::kanR, smc::specR, Δ amyE::(Pspank-optRBS-parB(mtparS)-lacI)::CAT	This study
4798	1A700, smc(1-476), SpnSmc(398-768), smc(695-1186)-TEV-HaloTag ftsY::ermB, specR::scpA(E52C, H235C), trpC2	This study
4837	1A700, smc(S152C, R1032C)-TEV-HaloTag ftsY::ermB, specR::scpA(E52C, H235C), trpC2	This study
4838	1A700, smc(1-476)(S19C, S152C), SpnSmc(398-768), smc(695-1186)(R1032C)-TEV-HaloTag ftsY::ermB, specR::scpA(E52C, H235C), trpC2	This study
4867	1A700, smc(1-476)(S152C), SpnSmc(398-768), smc(695-1186)(R1032C)-TEV-HaloTag, specR::scpA(E52C, H235C), trpC2	This study
4869	1A700, smc(S19C, S152C, R1032C)-TEV-HaloTag ftsY::ermB, specR::scpA(E52C, H235C), trpC2	This study

induced with 2 mM theophylline (P_{theo} promoter). Due to characteristics of the theophylline switch, the pre-culture as well as induction was performed at 30°C.

For ChIP-qPCR, each pellet was resuspended in 2 ml of buffer L (50 mM HEPES-KOH pH 7.5, 140 mM NaCl, 1 mM EDTA pH 8.0, 1% [v/v] Triton X-100, 0.1% [w/v] Na-deoxycholate, 0.1 mg/ml RNaseA and PIC [Sigma]) and transferred to 5 ml round-bottom tubes. Cell suspensions were sonicated 3×20 s on a Bandelin Sonoplus with a MS72 tip (90% pulse and 35% power output). Next, lysates were transferred into 2 ml tubes and centrifuged 10 min at 21,000 g at 4°C. 800 μ l of supernatant was used for IP and 200 μ l was kept as whole-cell extract (WCE).

For IP, first, antibody serum was incubated with Protein G coupled Dynabeads (Invitrogen) in 1:1 ratio for 2.5 hr at 4°C with rotation. Next, beads were washed in buffer L and 50 μ l were aliquoted to each sample tube. Samples were incubated for 2 hr at 4°C with rotation, followed by a series of washes with buffer L, buffer L5 (buffer L containing 500 mM NaCl), buffer W (10 mM Tris-HCl pH 8.0, 250 mM LiCl, 0.5% [v/v] NP-40, 0.5% [w/v] sodium deoxycholate, 1 mM EDTA pH 8.0), and buffer TE (10 mM Tris-HCl pH 8.0, 1 mM EDTA pH 8.0). Finally, the beads were resuspended in 520 μ l buffer TES (50 mM Tris-HCl pH 8.0, 10 mM EDTA pH 8.0, 1% [w/v] SDS). 300 μ l of TES and 20 μ l

of 10% SDS were also added to WCE. Both tubes were incubated O/N at 65°C with vigorous shaking to reverse formaldehyde crosslinks.

Phenol-chloroform extraction was performed to purify the decrosslinked DNA. Samples were transferred to screw cap 1.5 ml tubes and first mixed vigorously with 500 µl of phenol equilibrated with buffer (10 mM Tris-HCl pH 8.0, 1 mM EDTA). After centrifugation (10 min, RT, 13,000 rpm), 450 µl of the aqueous phase was transferred to a new screw cap tube and mixed with equal volume of chloroform, followed by centrifugation. 400 µl of aqueous phase was recovered for DNA precipitation with 2.5× volume of 100% ethanol, 0.1× volume of 3 M NaOAc, and 1.2 µl of GlycoBlue and incubated for 20 min at –20°C. Next, samples were centrifuged for 10 min at 20,000 g at RT and pellets obtained pellets were resuspended in 10 µl of EB (Qiagen) shaking at 55°C for 10 min and finally purified with a PCR purification kit, eluting in 50 µl EB.

For qPCR, 1:10 and 1:1000 dilutions in water of IP and WCE were prepared, respectively. Each 10 µl reaction was prepared in duplicate (5 µl Takyon SYBR MasterMix, 1 µl 3 µM primer pair, 4 µl of DNA) and run in Rotor-Gene Q machine (Qiagen). Primer sequences are listed in **Table 2**. Data was analyzed using PCR Miner server (<http://ewindup.info>) (Zhao and Fernald, 2005).

For IP of samples for ChIP-seq, the procedure was the same as for ChIP-qPCR, except for resuspending the pellets in 1 ml of buffer L and sonication in a Covaris E220 water bath sonicator for 5 min at 4°C, 100 W, 200 cycles, 10% load, and water level 5.

For deep sequencing, the DNA libraries were prepared by Genomic Facility at CIG, UNIL, Lausanne. Briefly, the DNA was fragmented by sonication (Covaris S2) to fragment sizes ranging from 220 to 250 bp. DNA libraries were prepared using the Ovation Ultralow Library Systems V2 Kit (NuGEN) including 15 cycles of PCR amplification. 5–10 million single-end sequence reads were obtained on a HiSeq2500 (Illumina) with 150 bp read length.

Processing of ChIP-seq reads

Reads were mapped to *B. subtilis* genome NC_000964.3 (for 1A700) or NC_0022898 (for PY79) with bowtie2 using –very-sensitive-local mode. Subsequent data analysis was performed using Seqmonk (<http://www.bioinformatics.babraham.ac.uk/projects/seqmonk/>) and R. The bin size used is 1 kb. For the enrichment plots, the data was smoothed using Local Polynomial Regression Fitting (loess).

Generation of chromosome conformation capture (3C) libraries

3C libraries were prepared as previously described (Marbouty et al., 2015). Minimal media (SMG) was used instead of LB. Briefly, cells were grown in 400 ml of SMG medium to exponential phase ($OD_{600} = 0.022\text{--}0.030$) and fixed with fresh formaldehyde (3% final concentration) for 30 min at RT, followed by 30 min at 4°C, and quenched for 30 min with 0.25 M glycine at 4°C. Fixed cells were harvested by filtering, washed in fresh SMG, frozen in liquid nitrogen, and stored at –80°C until further use.

Samples for RNAP inhibition experiment were prepared as other 3C libraries with additional rifampicin treatment before harvesting. Exponentially growing cultures were split in 2 × 400 ml cultures (two technical replicates for each, treated sample and untreated control). One was treated with 25 ng/µl rifampicin for 15 min (duration and concentration of treatment as in Wang et al., 2017) and respective control sample was left to grow for 15 min without treatment.

Table 2. List of oligos used for the qPCR.

Locus	Oligo name1	Oligo sequence1	Oligo name2	Oligo sequence2
<i>parS354</i>	STG495	ttgcagctaactgccatttg	STG496	aaaactgaacaggggtcacg
<i>parS355</i>	STG493	taattcatcatcgctcaaa	STG494	aatgccgattacgagtttgc
<i>parS359</i>	STG097	aaaaagtgtattgaggagcag	STG098	agaaccgcatcttcacagg
<i>parS90</i>	STI587	gccattgggcatcagtatg	STI588	ataagcgacaccttgcctgt
<i>dnaA</i>	STG199	gatcaatcggggaaagtgtg	STG200	gtagggcctgtgattttgtg
<i>amyE</i>	STG220	aatcgtaactcggcgctgtc	STG221	catcatcgctcatccatgtc
<i>ter</i>	STG099	tccatctcctcgtcctacg	STG100	attctgctgatgtgcaatgg

For time-course experiments, 2 l preculture was first grown until mid-exponential phase ($OD = 0.022\text{--}0.030$) and next appropriate culture volumes were added to fresh pre-warmed SMG so that at given time points 2×200 ml of culture at mid-exponential could be collected (two technical replicates). The cultures were induced with 2 mM theophylline or 1 mM IPTG, depending on the promoter used, P_{theo} or P_{spank} , respectively. Due to the characteristics of the theophylline switch, the pre-culture as well as induction was performed at 30°C.

Frozen pellets were resuspended in 600 μ l 1 \times TE and incubated at RT for 20 min with 4 μ l of Ready-lyze lysozyme (35 U/ μ l, Tebu Bio). Next, SDS was added to a final concentration of 0.5% and incubated at RT for 10 min. 50 μ l of lysed cells were aliquoted to eight tubes containing 450 μ l of digestion mix (1 \times NEB 1 buffer, 1% triton X-100, and 100 U HpaII enzyme [NEB]) and incubated at 37°C for 3 hr with constant shaking. Digested DNA was collected by centrifugation, diluted into four tubes containing 8 ml of ligation mix (1 \times ligation buffer: 50 mM Tris-HCl, 10 mM MgCl₂, 10 mM DTT), 1 mM ATP, 0.1 mg/ml BSA, 125 U T4 DNA ligase 5 U/ml, and incubated at 16°C for 4 hr. Ligation reaction was followed by O/N decrosslinking at 65°C in the presence of 250 μ g/ml proteinase K (Eurobio) and 5 mM EDTA.

DNA was precipitated with 1 vol of isopropanol and 0.1 vol of 3 M sodium acetate (pH 5.2, Sigma) at -80°C for 1 hr. After centrifugation, the DNA pellet was resuspended in 1 \times TE at 30°C for 20 min. Next, DNA was extracted once with 400 μ l phenol-chloroform-isoamyl alcohol solution and precipitated with 1.5 vol cold 100% ethanol in the presence of 0.1 vol 3 M sodium acetate at -80°C for 30 min. The pellet was collected and resuspended in 30 μ l TE with RNaseA at 37°C for 30 min. All tubes were pooled and the resulting 3C library was quantified on gel using ImageJ.

Processing of libraries for Illumina sequencing

1 μ g of 3C library was suspended in water (final volume 130 μ l) and sonicated using Covaris S220 (following the manufacturer's recommendations to obtain 500 bp target size). Next, DNA was purified with Qiagen PCR purification kit, eluted in 40 μ l EB, and quantified using NanoDrop. 1 μ g of DNA was processed according to the manufacturer's instructions (Paired-End DNA sample Prep Kit, Illumina, PE-930-1001), except that DNA was ligated to custom-made adapters for 4 hr at RT, followed by inactivation step at 65°C for 20 min. DNA was purified with 0.75 \times AMPure beads and 3 μ l were used for 50 μ l PCR reaction (12 cycles). Amplified libraries were purified on Qiagen columns and pair-end sequenced on an Illumina platform (HiSeq4000 or NextSeq).

Processing of PE reads and generation of contact maps

Sequencing data was demultiplexed, adapters trimmed, and PCR duplicates removed using custom scripts. Next, data was processed as described at https://github.com/axelcournac/3C_tutorial. Briefly, bowtie2 in -very sensitive-local mode was used for mapping for each mate. After sorting and merging both mates, the reads of mapping quality >30 were filtered out and assigned to a restriction fragment. Uninformative events like recircularization on itself (loops), uncut fragments, and religations in original orientation were discarded (Cournac et al., 2012) and only pairs of reads corresponding to long-range interactions were used for generation of contact maps (between 5 and 8% of all reads). The bin size used is 10 kb. Next, contact maps were normalized through the sequential component normalization procedure (SCN, Cournac et al., 2012). Subsequent visualization was done using MATLAB (R2019b). To facilitate visualization of the contact matrices, first we applied to the SCN matrices the \log_{10} and then a Gaussian filter ($H = 1$) to smooth the image. The scale bar next to the maps represents the contact frequencies in \log_{10} —the darker the color, the higher the frequency of contacts between given loci.

Expression analysis of HaloTagged proteins

Cells were cultured at 37°C in 200 ml SMG to exponential phase ($OD_{600} = 0.022\text{--}0.030$) and harvested by filtration. Next, they were washed in cold PBS supplemented with 0.1% (v/v) glycerol ('PBSG') and split into aliquots of a biomass equivalent to 1.25 OD_{600} units. Cells were centrifuged for 2 min at 10,000 g, resuspended in 40 μ l PBSG containing 75 U/ml ReadyLyse Lysozyme, 750 U/ml Sm nuclease, 5 μ M HaloTag TMR Substrate and protease inhibitor cocktail ('PIC') and incubated at 37°C for 30 min to facilitate lysis. After lysis, 10 μ l of 4 \times LDS-PAGE with DTT (200 mM final) buffer

was added, samples were incubated for 5 min at 95°C, and resolved by SDS-PAGE. Gels were imaged on an Amersham Typhoon scanner with Cy3 DIGE filter setup.

Chromosome co-entrapment assay

Microbead entrapment followed the developments reported in *Vazquez Nunez et al., 2019*. Cells containing the Smc alleles with cysteines at the desired positions were inoculated in SMG medium to $OD_{600} = 0.004$ and grown to mid-exponential phase ($OD_{600} = 0.02$) at 37°C. Cells were mixed with ice for rapid cooling and harvested by filtration. A cell mass equivalent of OD_{600} units of 3.75 was resuspended in 121 μ l PBSG and incubated with a final concentration of 1 mM BMOE for 10 min. Reactions were quenched by the addition of β -mercaptoethanol to a final concentration of 32.6 mM. 45 μ l of cross-linked cells were retained as 'Input' sample. 1 μ l of PIC and 9 μ l Dynabeads Protein G were added to 90 μ l of the remaining cell fraction. Samples for entrapment were mixed with 100 μ l 2% low-melt agarose at a temperature of 45°C before being mixed rapidly with 700 μ l mineral oil. Resulting Agarose microbeads were washed once in 1 ml RT PBSG by centrifugation at 10,000 rpm for 1 min. Beads were subsequently resuspended in 300 μ l PBSG and mixed with EDTA pH 8 (1 mM final), 5 μ l PIC, Halo TMR ligand (5 μ M final), as well as ReadyLyse lysozyme to a final concentration of 40 U/ μ l. Input samples were mixed with 5 μ l of a master mix containing 0.9 μ l PBSG, 0.5 μ l PIC, 2.5 μ l 1:100 Benzonase, 0.5 μ l Halo TMR ligand, as well as 0.6 μ l of a 1:10 dilution of ReadyLyse lysozyme. Input as well as Entrapment samples were incubated for 25 min at 37°. All subsequent steps were undertaken to protect from light as much as possible. Input samples were mixed with 50 μ l 2 \times LDS loading dye. Entrapment samples were washed twice with 1 ml PBSG by centrifugation at 10,000 rpm, 1 min, RT. Microbeads were then washed three times in TES under gentle (500 rpm) shaking, first for 1 hr with two subsequent washing steps for 30 min each. Preparations were resuspended in 1 ml TES and incubated on a rolling incubator overnight at 4°C. Subsequently, the beads were washed twice with 1 ml PBS before being resuspended in 100 μ l PBS. 5 μ l Benzonase were added (750 U/ml final concentration), and samples were incubated at 37°C under light shaking for 1 hr. To free the preparations from agarose, the samples were first heated to 70°C for 1 min before incubating on ice for 5 min. Agarose was removed from the sample content by centrifugation, first with 21,000 rpm at 4°C for 15 min, then with 14,000 rpm at RT for 5 min. Supernatant liquid was transferred to spin columns and centrifuged for 1 min, 10,000 rpm, ambient temperature. The resulting solution was brought to 1 ml total volume with water and mixed to final concentrations of 33 mg/ml BSA and 0.02% (w/v) deoxycholate before resting on ice for 30 min. Trichloroacetic acid was added to a final concentration of 8.8% preceding a 1 hr incubation on ice. Precipitated protein was spun down (21,000 rpm, 4°C, 15 min), resuspended in 10 μ l 1 \times LDS loading dye and brought to neutral pH by μ l-wise addition of 1 M Tris solution. 5 μ l of input material and all of the 'eluate' samples were loaded on Tris-acetate gels and run at 35 mA. Gels were scanned using Amersham Typhoon Imager with the Cy5 filter settings.

Acknowledgements

We thank Hugo Brandao, Leonid Mirny, and Xindan Wang for sharing unpublished data and comments on the manuscript. We are grateful to Frank Bürmann and all members of the Gruber laboratory for stimulating discussions and critical feedback. We thank Marc Garcia-Garcera and Björn Vessman for continuous support with R and Python and the Genomic Technologies Facility (GTF, UNIL, Lausanne) and Next Generation Sequencing Core Facility (CNRS, I2BC, Gif-sur-Yvette) for ChIP-seq library preparation and deep sequencing. This work was supported by funding from the European Research Council (Horizon 2020 [ERC CoG 724482](https://doi.org/10.1016/j.cel.2020.05.010)) (SG) and the Agence Nationale pour la Recherche (ANR-CE12-0013-01) and the Association pour la Recherche contre le Cancer (FB).

Additional information

Funding

Funder	Grant reference number	Author
H2020 European Research Council	724482	Stephan Gruber

Agence Nationale de la Recherche ANR-CE12-0013-01 Frederic Boccard

Association pour la Recherche contre le Cancer Frederic Boccard

The funders had no role in study design, data collection and interpretation, or the decision to submit the work for publication.

Author contributions

Anna Anchimiuk, Conceptualization, Data curation, Formal analysis, Validation, Investigation, Visualization, Methodology, Writing - original draft, Writing - review and editing; Virginia S Lioy, Data curation, Software, Formal analysis, Visualization, Methodology; Florian Patrick Bock, Resources, Investigation; Anita Minnen, Data curation, Investigation; Frederic Boccard, Supervision, Funding acquisition, Methodology, Writing - review and editing; Stephan Gruber, Conceptualization, Formal analysis, Supervision, Funding acquisition, Visualization, Writing - original draft, Project administration, Writing - review and editing

Author ORCIDs

Anna Anchimiuk  <https://orcid.org/0000-0002-2899-9413>

Stephan Gruber  <https://orcid.org/0000-0002-0150-0395>

Decision letter and Author response

Decision letter <https://doi.org/10.7554/eLife.65467.sa1>

Author response <https://doi.org/10.7554/eLife.65467.sa2>

Additional files

Supplementary files

- Supplementary file 1. Information about replicates for each relevant figure panel.
- Supplementary file 2. List of strains sorted according to relevant figure panels and ordered in the way they are presented.
- Supplementary file 3. Details of strain construction. Key plasmid maps for generating the strains are deposited in Mendeley Data DOI: 10.17632/kvjd6nj2bh.2.
- Supplementary file 4. Table listing strains for which 3C-seq maps were generated with reference to the figure panels, genotype, and number of valid reads.
- Transparent reporting form

Data availability

All deep sequencing data has been deposited to the NCBI GEO database and will be available at GEO Accession number: GSE163573 All other raw data will be made available via Mendeley Data <https://doi.org/10.17632/kvjd6nj2bh.2>.

The following datasets were generated:

Author(s)	Year	Dataset title	Dataset URL	Database and Identifier
Anchimiuk A, Lioy VS, Boccard F, Gruber S	2020	GEO_Smc_collisions	https://www.ncbi.nlm.nih.gov/geo/query/acc.cgi?acc=GSE163573	NCBI Gene Expression Omnibus, GSE163573
Anchimiuk A, Gruber S	2021	Smc_collisions	https://data.mendeley.com/datasets/kvjd6nj2bh/2	Mendeley Data, 10.17632/kvjd6nj2bh.2

References

- Banigan EJ**, van den Berg AA, Brandão HB, Marko JF, Mirny LA. 2020. Chromosome organization by one-sided and two-sided loop extrusion. *eLife* **9**:e53558. DOI: <https://doi.org/10.7554/eLife.53558>, PMID: 32250245
- Böhm K**, Giacomelli G, Schmidt A, Imhof A, Koszul R, Marbouty M, Bramkamp M. 2020. Chromosome organization by a conserved condensin-ParB system in the actinobacterium *Corynebacterium glutamicum*. *Nature Communications* **11**:1485. DOI: <https://doi.org/10.1038/s41467-020-15238-4>, PMID: 32198399
- Brandão HB**, Paul P, van den Berg AA, Rudner DZ, Wang X, Mirny LA. 2019. RNA polymerases as moving barriers to condensin loop extrusion. *PNAS* **116**:20489–20499. DOI: <https://doi.org/10.1073/pnas.1907009116>, PMID: 31548377
- Brandão HB**, Ren Z, Karaboja X, Mirny LA, Wang X. 2020. DNA-loop extruding SMC complexes can traverse one another in vivo. *bioRxiv*. DOI: <https://doi.org/10.1101/2020.10.26.356329>
- Breier AM**, Grossman AD. 2007. Whole-genome analysis of the chromosome partitioning and sporulation protein Spo0J (ParB) reveals spreading and origin-distal sites on the *Bacillus subtilis* chromosome. *Molecular Microbiology* **64**:703–718. DOI: <https://doi.org/10.1111/j.1365-2958.2007.05690.x>, PMID: 17462018
- Bürmann F**, Shin HC, Basquin J, Soh YM, Giménez-Oya V, Kim YG, Oh BH, Gruber S. 2013. An asymmetric SMC-kleisin bridge in prokaryotic condensin. *Nature Structural & Molecular Biology* **20**:371–379. DOI: <https://doi.org/10.1038/nsmb.2488>, PMID: 23353789
- Bürmann F**, Basfeld A, Vazquez Nunez R, Diebold-Durand ML, Wilhelm L, Gruber S. 2017. Tuned SMC arms drive chromosomal loading of prokaryotic condensin. *Molecular Cell* **65**:861–872. DOI: <https://doi.org/10.1016/j.molcel.2017.01.026>, PMID: 28238653
- Bürmann F**, Gruber S. 2015. SMC condensin: promoting cohesion of replicon arms. *Nature Structural & Molecular Biology* **22**:653–655. DOI: <https://doi.org/10.1038/nsmb.3082>, PMID: 26333713
- Cournac A**, Marie-Nelly H, Marbouty M, Koszul R, Mozziconacci J. 2012. Normalization of a chromosomal contact map. *BMC Genomics* **13**:436. DOI: <https://doi.org/10.1186/1471-2164-13-436>, PMID: 22935139
- Davidson IF**, Bauer B, Goetz D, Tang W, Wutz G, Peters JM. 2019. DNA loop extrusion by human cohesin. *Science* **366**:1338–1345. DOI: <https://doi.org/10.1126/science.aaz3418>, PMID: 31753851
- Diebold-Durand ML**, Bürmann F, Gruber S. 2019. High-Throughput allelic replacement screening in *Bacillus subtilis*. *Methods in Molecular Biology* **2004**:49–61. DOI: https://doi.org/10.1007/978-1-4939-9520-2_5, PMID: 31147909
- Dyson S**, Segura J, Martínez-García B, Valdés A, Roca J. 2021. Condensin minimizes topoisomerase II-mediated entanglements of DNA in vivo. *The EMBO Journal* **40**:e105393. DOI: <https://doi.org/10.15252/embj.2020105393>, PMID: 33155682
- Ganji M**, Shaltiel IA, Bisht S, Kim E, Kalichava A, Haering CH, Dekker C. 2018. Real-time imaging of DNA loop extrusion by condensin. *Science* **360**:102–105. DOI: <https://doi.org/10.1126/science.aar7831>, PMID: 29472443
- Gligoris TG**, Scheinost JC, Bürmann F, Petela N, Chan KL, Uluocak P, Beckouët F, Gruber S, Nasmyth K, Löwe J. 2014. Closing the cohesin ring: structure and function of its SMC3-kleisin interface. *Science* **346**:963–967. DOI: <https://doi.org/10.1126/science.1256917>, PMID: 25414305
- Graham TG**, Wang X, Song D, Etson CM, van Oijen AM, Rudner DZ, Loparo JJ. 2014. ParB spreading requires DNA bridging. *Genes & Development* **28**:1228–1238. DOI: <https://doi.org/10.1101/gad.242206.114>, PMID: 24829297
- Gruber S**, Veening JW, Bach J, Blettinger M, Bramkamp M, Errington J. 2014. Interlinked sister chromosomes arise in the absence of condensin during fast replication in *B. subtilis*. *Current Biology* **24**:293–298. DOI: <https://doi.org/10.1016/j.cub.2013.12.049>, PMID: 24440399
- Gruber S**, Errington J. 2009. Recruitment of condensin to replication origin regions by ParB/Spo0J promotes chromosome segregation in *B. subtilis*. *Cell* **137**:685–696. DOI: <https://doi.org/10.1016/j.cell.2009.02.035>, PMID: 19450516
- Jalal AS**, Tran NT, Le TB. 2020. ParB spreading on DNA requires cytidine triphosphate in vitro. *eLife* **9**:e53515. DOI: <https://doi.org/10.7554/eLife.53515>, PMID: 32077854
- Karaboja X**, Ren Z, Brandão HB, Paul P, Rudner DZ, Wang X. 2021. XerD unloads bacterial SMC complexes at the replication terminus. *Molecular Cell* **81**:756–766. DOI: <https://doi.org/10.1016/j.molcel.2020.12.027>, PMID: 33472056
- Kim Y**, Shi Z, Zhang H, Finkelstein IJ, Yu H. 2019. Human cohesin compacts DNA by loop extrusion. *Science* **366**:1345–1349. DOI: <https://doi.org/10.1126/science.aaz4475>, PMID: 31780627
- Kim E**, Kerssemakers J, Shaltiel IA, Haering CH, Dekker C. 2020. DNA-loop extruding condensin complexes can traverse one another. *Nature* **579**:438–442. DOI: <https://doi.org/10.1038/s41586-020-2067-5>, PMID: 32132705
- Lagage V**, Boccard F, Vallet-Gely I. 2016. Regional control of chromosome segregation in *Pseudomonas aeruginosa*. *PLOS Genetics* **12**:e1006428. DOI: <https://doi.org/10.1371/journal.pgen.1006428>, PMID: 27820816
- Lee PS**, Lin DC, Moriya S, Grossman AD. 2003. Effects of the chromosome partitioning protein Spo0J (ParB) on oriC positioning and replication initiation in *Bacillus subtilis*. *Journal of Bacteriology* **185**:1326–1337. DOI: <https://doi.org/10.1128/JB.185.4.1326-1337.2003>, PMID: 12562803
- Lin DC**, Grossman AD. 1998. Identification and characterization of a bacterial chromosome partitioning site. *Cell* **92**:675–685. DOI: [https://doi.org/10.1016/s0092-8674\(00\)81135-6](https://doi.org/10.1016/s0092-8674(00)81135-6), PMID: 9506522
- Lioy VS**, Cournac A, Marbouty M, Duigou S, Mozziconacci J, Espéli O, Boccard F, Koszul R. 2018. Multiscale structuring of the *E. coli* Chromosome by Nucleoid-Associated and Condensin Proteins. *Cell* **172**:771–783. DOI: <https://doi.org/10.1016/j.cell.2017.12.027>

- Lioy VS**, Junier I, Lagage V, Vallet I, Boccard F. 2020. Distinct activities of bacterial condensins for chromosome management in *Pseudomonas aeruginosa*. *Cell Reports* **33**:108344. DOI: <https://doi.org/10.1016/j.celrep.2020.108344>, PMID: 33147461
- Livny J**, Yamaichi Y, Waldor MK. 2007. Distribution of centromere-like parS sites in Bacteria: insights from comparative genomics. *Journal of Bacteriology* **189**:8693–8703. DOI: <https://doi.org/10.1128/JB.01239-07>, PMID: 17905987
- Mäkelä J**, Sherratt DJ. 2020. Organization of the *Escherichia coli* chromosome by a MukBEF axial core. *Molecular Cell* **78**:250–260. DOI: <https://doi.org/10.1016/j.molcel.2020.02.003>, PMID: 32097603
- Marbouty M**, Le Gall A, Cattoni DI, Cournac A, Koh A, Fiche JB, Mozziconacci J, Murray H, Koszul R, Nollmann M. 2015. Condensin- and Replication-Mediated bacterial chromosome folding and origin condensation revealed by Hi-C and Super-resolution imaging. *Molecular Cell* **59**:588–602. DOI: <https://doi.org/10.1016/j.molcel.2015.07.020>, PMID: 26295962
- Minnen A**, Attaiech L, Thon M, Gruber S, Veening JW. 2011. SMC is recruited to oriC by ParB and promotes chromosome segregation in *Streptococcus pneumoniae*. *Molecular Microbiology* **81**:676–688. DOI: <https://doi.org/10.1111/j.1365-2958.2011.07722.x>, PMID: 21651626
- Minnen A**, Bürmann F, Wilhelm L, Anchimiuk A, Diebold-Durand ML, Gruber S. 2016. Control of smc coiled coil architecture by the ATPase heads facilitates targeting to chromosomal ParB/parS and release onto flanking DNA. *Cell Reports* **14**:2003–2016. DOI: <https://doi.org/10.1016/j.celrep.2016.01.066>, PMID: 26904953
- Orlandini E**, Marenduzzo D, Michieletto D. 2019. Synergy of topoisomerase and structural-maintenance-of-chromosomes proteins creates a universal pathway to simplify genome topology. *PNAS* **116**:8149–8154. DOI: <https://doi.org/10.1073/pnas.1815394116>, PMID: 30962387
- Osoerio-Valeriano M**, Altegoer F, Steinchen W, Urban S, Liu Y, Bange G, Thanbichler M. 2019. ParB-type DNA segregation proteins are CTP-Dependent molecular switches. *Cell* **179**:1512–1524. DOI: <https://doi.org/10.1016/j.cell.2019.11.015>, PMID: 31835030
- Racko D**, Benedetti F, Goundaroulis D, Stasiak A. 2018. Chromatin loop extrusion and chromatin unknotting. *Polymers* **10**:1126. DOI: <https://doi.org/10.3390/polym10101126>
- Soh YM**, Davidson IF, Zamuner S, Basquin J, Bock FP, Taschner M, Veening JW, De Los Rios P, Peters JM, Gruber S. 2019. Self-organization of parS centromeres by the ParB CTP hydrolase. *Science* **366**:1129–1133. DOI: <https://doi.org/10.1126/science.aay3965>, PMID: 31649139
- Sullivan NL**, Marquis KA, Rudner DZ. 2009. Recruitment of SMC by ParB-parS organizes the origin region and promotes efficient chromosome segregation. *Cell* **137**:697–707. DOI: <https://doi.org/10.1016/j.cell.2009.04.044>, PMID: 19450517
- Tran NT**, Laub MT, Le TBK. 2017. SMC progressively aligns chromosomal arms in *Caulobacter crescentus* but is antagonized by convergent transcription. *Cell Reports* **20**:2057–2071. DOI: <https://doi.org/10.1016/j.celrep.2017.08.026>, PMID: 28854358
- Umbarger MA**, Toro E, Wright MA, Porreca GJ, Baù D, Hong SH, Fero MJ, Zhu LJ, Marti-Renom MA, McAdams HH, Shapiro L, Dekker J, Church GM. 2011. The three-dimensional architecture of a bacterial genome and its alteration by genetic perturbation. *Molecular Cell* **44**:252–264. DOI: <https://doi.org/10.1016/j.molcel.2011.09.010>, PMID: 22017872
- Vazquez Nunez R**, Ruiz Avila LB, Gruber S. 2019. Transient DNA occupancy of the SMC interarm space in prokaryotic condensin. *Molecular Cell* **75**:209–223. DOI: <https://doi.org/10.1016/j.molcel.2019.05.001>, PMID: 31201090
- Wang X**, Tang OW, Riley EP, Rudner DZ. 2014. The SMC condensin complex is required for origin segregation in *Bacillus subtilis*. *Current Biology* **24**:287–292. DOI: <https://doi.org/10.1016/j.cub.2013.11.050>, PMID: 24440393
- Wang X**, Le TB, Lajoie BR, Dekker J, Laub MT, Rudner DZ. 2015. Condensin promotes the juxtaposition of DNA flanking its loading site in *Bacillus subtilis*. *Genes & Development* **29**:1661–1675. DOI: <https://doi.org/10.1101/gad.265876.115>, PMID: 26253537
- Wang X**, Brandão HB, Le TB, Laub MT, Rudner DZ. 2017. *Bacillus subtilis* SMC complexes juxtapose chromosome arms as they travel from origin to terminus. *Science* **355**:524–527. DOI: <https://doi.org/10.1126/science.aai8982>, PMID: 28154080
- Wilhelm L**, Bürmann F, Minnen A, Shin H-C, Toseland CP, Oh B-H, Gruber S. 2015. SMC condensin entraps chromosomal DNA by an ATP hydrolysis dependent loading mechanism in *Bacillus subtilis*. *eLife* **4**:e06659. DOI: <https://doi.org/10.7554/eLife.06659>
- Wu LJ**, Errington J. 1998. Use of asymmetric cell division and spoIIIE mutants to probe chromosome orientation and organization in *Bacillus subtilis*. *Molecular Microbiology* **27**:777–786. DOI: <https://doi.org/10.1046/j.1365-2958.1998.00724.x>, PMID: 9515703
- Yatskevich S**, Rhodes J, Nasmyth K. 2019. Organization of chromosomal DNA by SMC complexes. *Annual Review of Genetics* **53**:445–482. DOI: <https://doi.org/10.1146/annurev-genet-112618-043633>, PMID: 31577909
- Zhao S**, Fernald RD. 2005. Comprehensive algorithm for quantitative real-time polymerase chain reaction. *Journal of Computational Biology* **12**:1047–1064. DOI: <https://doi.org/10.1089/cmb.2005.12.1047>, PMID: 16241897

CHAPTER 2:
Characterization of *BsRecN* and its role in
DNA repair

INTRODUCTION

DNA damage and repair

Damage to the genetic information stored in DNA is unavoidable. It can be triggered by extrinsic as well as intrinsic factors including ionizing radiation (IR), reactive oxygen species, genotoxic compounds or collapsing forks during DNA replication. The consequences include cell cycle arrest, altered cellular fitness and eventually cell death. In human cells, oxidative stress leads to an impressive number of 10'000 lesions per cell per day (Ames et al., 1993). Loss of genome integrity puts survival of the cell at stake, therefore the mechanisms for dealing with damage must be efficient and robust.

In eukaryotes, surveillance mechanisms/checkpoints have been described during which the cellular state is evaluated before committing to the next stage of the cell cycle (Hartwell & Weinert, 1989). In bacteria, accumulation of DNA damage leads to SOS-regulon activation. It is a tightly regulated system that allows for expression of repair-specific proteins to tackle the DNA damage. Different repair pathways can be employed: nucleotide excision repair (NER), translesion DNA synthesis (TLS), homologous recombination (HR) and non-homologous end joining (NHEJ) leading to either error-free or error-prone repair. In this thesis, I will only describe the last two pathways and will not discuss the other ones. The conservation level of DNA repair systems between taxa is tremendous. Nevertheless, the sensitivity towards damage, and hence the number and functions of genes engaged in managing the damage differ considerably (Rocha et al., 2005).

Double Strand Breaks (DSBs) and their repair

Double strand breaks (DSBs) are among the most deleterious types of DNA damage. Even a single DSB leads to cell death if left unrepaired. Two principally different processes resolving DSBs are described below (Figure 5). Commitment to a given repair pathway depends primarily on the stage of the cell cycle and on the genomic location of the damage (whether the DSB is inflicted within the replicated segment of the chromosome).

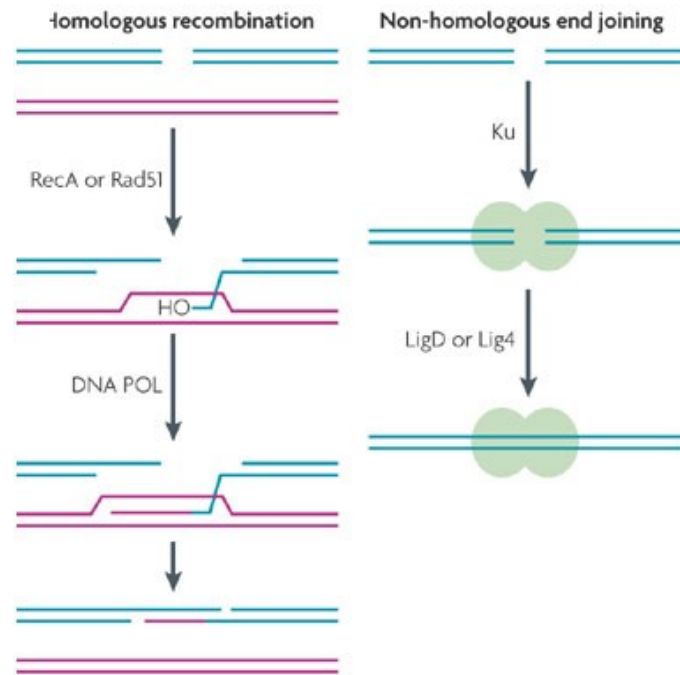


Figure 5. Schematic overview of two main pathways involved in double strand break repair (DSB repair): error-free homologous recombination (HR) and error-prone non-homologous end joining (NHEJ). Commitment to HR begins with RecA (Rad51) binding to an end-processed ssDNA overhang. The RecA-nucleoprotein complex then invades the double-stranded intact template and promotes D-loop formation. DNA polymerase fills missing information based on template sequence. Branch migration and endonucleolytic Holliday junction (HJ) resolution eventually result in two intact daughter chromosomes. When an intact copy is not available, NHEJ is a repair pathway of choice. Broken ends are recognized and bound by the Ku protein. LigD (Lig4) directly ligates the ends together with minimal processing. Figure source: (Shuman & Glickman, 2007).

Non-homologous End Joining (NHEJ)

NHEJ does not require a homologous DNA template for repair. The two ends of DSBs are brought together by the end-binding protein Ku and are then sealed by a specialized DNA ligase Lig4 (Ku and LigD in bacteria). Depending on whether the ends are re-ligated with or without prior end-processing, NHEJ can be faithful or mutagenic. In eukaryotes, NHEJ is the repair pathway of choice during the G1 phase of the cell cycle (Hendrickson, 1997). Interestingly, in mammalian cells up to 70% of site directed DSBs are repaired by NHEJ (Liang et al., 1998).

Although the presence of NHEJ proteins was reported for many bacterial species (e.g., *Mycobacterium*, *Pseudomonas*, *Bacillus* and *Agrobacterium*), commitment to NHEJ is

relatively poorly understood. Neither Ku nor LigD are essential under laboratory growth conditions unless the cells enter stationary phase (Weller et al., 2002) or commit to sporulation (S. T. Wang et al., 2006).

Homologous recombination (HR)

If a homologous template is available, a DSB is likely to be repaired by error-free homologous recombination (HR). In bacteria, two alternative HR pathways exist, likely supplementing one another: RecBCD- (AddAB in *B. subtilis*) and RecFOR-dependent (Amundsen & Smith, 2003). The conserved steps during DSB repair can be divided into three main stages (presynapsis, synapsis and postsynapsis) including the following steps (Figure 6):

- (i) DSB recognition and processing by an exonuclease to create 3' single-stranded DNA (ssDNA) ends;
- (ii) loading of a recombinase such as RecA (Rad51 in eukaryotes) onto ssDNA and nucleoprotein filament formation;
- (iii) strand invasion and D-loop formation to pair the ssDNA with an intact homologous DNA segment;
- (iv) DNA synthesis using the 3'-OH of the invading strand;
- (v) branch migration, endonucleolytic resolution of the crossover junction, resulting in the formation of two intact daughter chromosomes.

HR is the most prevalent repair pathway in prokaryotes. In eukaryotes, DSB repair mediated by HR occurs mainly during the late S and G2 phases of the cell cycle when sister chromatids are present.

A significant challenge and still unanswered question regarding HR is how the homology partner is recognized and subsequently maintained in proximity to the damaged ends. Is the damaged end travelling or is the intact template brought to the break? Are there dedicated areas within the cell where DNA damage is addressed and processed (aka 'repair centers')? The dense cellular environment does not seem like a particularly easy space to scan for a homologous template in a random manner, and thus a dedicated system for facilitating template search and keeping both DNA regions in proximity must exist. Proteins from the SMC or SMC-like families seem like obvious and attractive candidates.

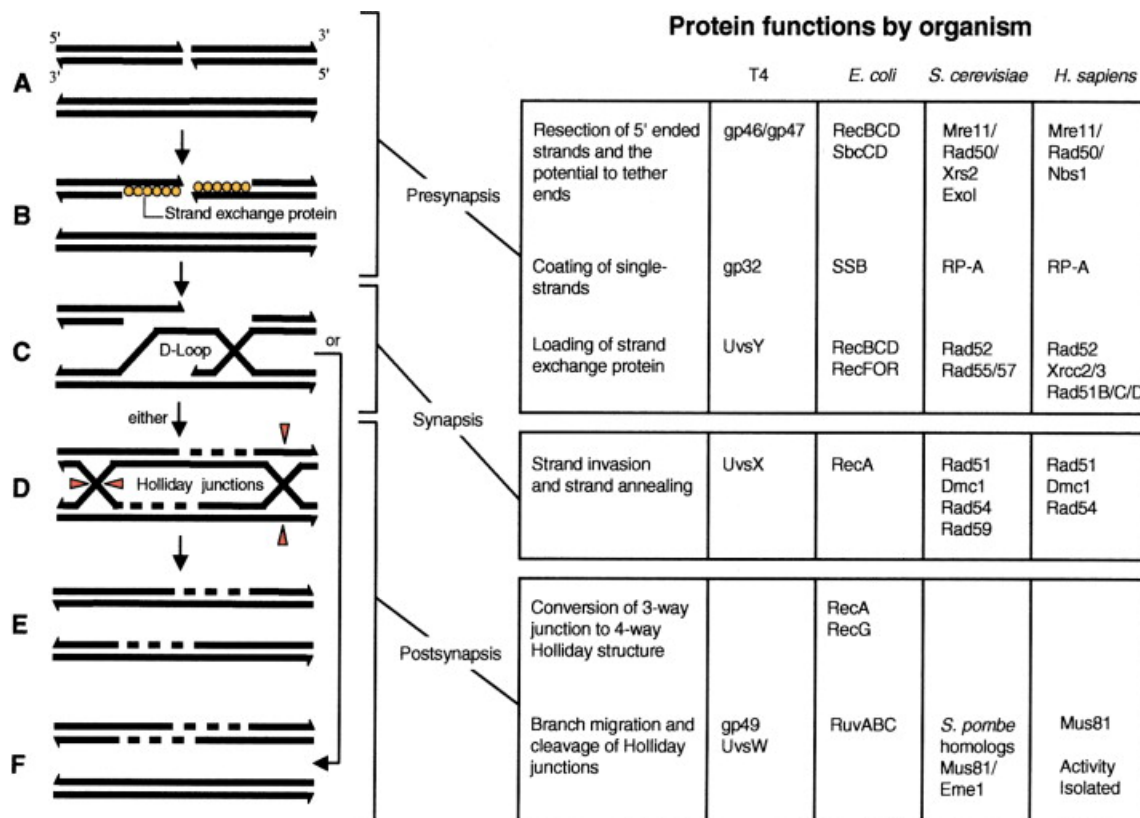


Figure 6. A detailed HR scheme with a list of proteins involved in individual steps of repair across species. A and B, end processing. C, D-loop formation (three-way junction). D, Holliday junction formation (four-way junction). E, branch migration. F, ejection of invading strand after priming DNA synthesis. Figure source: (Cromie & Leach, 2001)

Mitomycin C (MMC) for random DSB induction

Mitomycin C (MMC) is a compound widely used in DNA repair studies to induce DSBs in a random manner. It is a naturally occurring antibiotic produced by *Streptomyces caespitosus*. MMC halts DNA synthesis by reacting specifically with guanine residues resulting in covalent intra- or inter-strand crosslinks (Figure 7) (Noll et al., 2006). Resolution of the interstrand crosslinks (ICLs) begins with a nick made next to it (by UvrABC). If the nick is encountered by a replication fork, a DSB is formed.

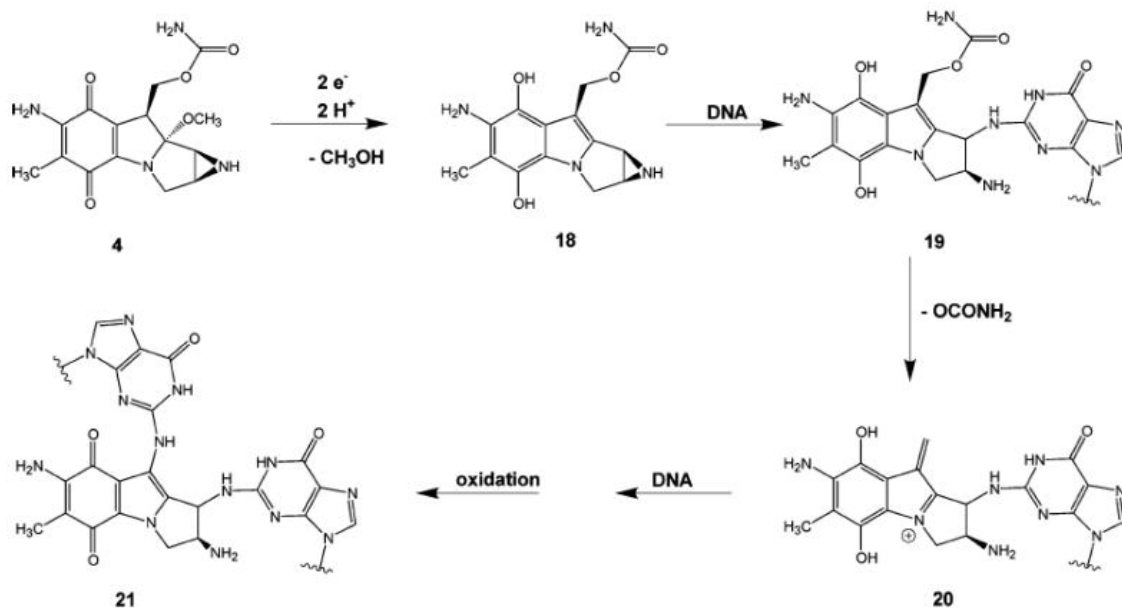


Figure 7. Mitomycin C (MMC) activation and the resulting cross-link formation with DNA. **4**, MMC. **18**, hydroquinone intermediate. **19**, DNA monoadduct. **20**, vinylogous hydroquinone methide intermediate. **21**, interstrand cross-link. Figure source: (Noll et al., 2006)

I-SceI endonuclease for site-specific induction of DSBs

In the DNA repair field, I-SceI proved to be a powerful tool for creating site-specific chromosomal DSBs. It involves a homing megaendonuclease from *S. cerevisiae*, initially reported to be responsible for intron mobility in mitochondria of yeast (Jacquier & Dujon, 1985; Plessis et al., 1992). The enzyme cuts dsDNA with high sequence specificity. The recognition site is asymmetric and relatively long (12–40 bp). Cleavage at the recognition sequence results in a 4 bp overhang with a 3'-OH terminus (Plessis et al., 1992). This system contributed greatly to the identification of the genetic determinants and molecular mechanisms of HR and NHEJ (Haber, 1995; Meddows et al., 2004, 2005; Siegl et al., 2010).

The role of SMC-like proteins in DNA repair

In bacteria

Several SMC-like proteins are involved in DNA repair in bacteria: SbcCD (Connelly et al., 2003), SbcEF (Krishnamurthy et al., 2010) and RecN (Meddows et al., 2005). Their absence renders cells sensitive to MMC, H_2O_2 or IR, but only moderately sensitive to UV radiation, suggesting that they are mainly involved in DSB repair (Alonso et al.,

1993; Dervyn et al., 2004; Funayama et al., 1999; Mascarenhas et al., 2006; Sargentini & Smith, 1985; Stohl & Seifert, 2006). SbcCD is reported to be an initiator of recombinational repair. The complex processes DNA ends (preparing them for end-resection) before the RecA recombinase can load and facilitate HR. SbcCD was shown to act at sites where replication forks converge *in vivo*, to recognize DNA hairpin structures *in vitro*, and cleave them leading to DSB formation (Connelly et al., 1998, 2003; Connelly & Leach, 1996; Trujillo & Sung, 2001; Wendel et al., 2018). A single study of *B. subtilis* SbcE indicated its potential role in transformation and MMC-induced damage repair (replication-independent foci formation upon MMC treatment) (Krishnamurthy et al., 2010). Finally, RecN, a protein widely spread among bacterial species, participating in DSB repair via HR. More on the importance of RecN and its participation in DNA damage repair is described below.

In eukaryotes

S. cerevisiae and human Rad50-Mre11 (MRX and MRN complexes, respectively) are structural and functional homologs of *E. coli* SbcCD and archaeal *P. furiosus* Rad50-Mre11. Due to their role in end-resection they are functionally similar to *E. coli* helicase-nuclease RecBCD (Karl-Peter et al., 2000; Sharples & Leach, 1995). The MRX/MRN complex participates not only in DSB repair, but also in processes controlling replication fork dynamics and telomere maintenance (reviewed in (Syed & Tainer, 2018)).

MRN/MRX was reported to act early in DSB repair by regulating and coordinating the choice of repair pathway. Specifically, its endo- and exonuclease activities are required for end processing in a variant of NHEJ called microhomology-mediated end joining (Sharma et al., 2015). The resected by MRN/MRX DNA ends can become a substrate for Exo1 and/or Dna2 nucleases producing long 3' ssDNA tails (similarly to RecBCD in bacteria, (Shibata et al., 2014)) and subsequent loading of Rad51 recombinase (the bacterial RecA homolog) to promote strand exchange in HR (Baumann & West, 1999; Gupta et al., 1999; Ogawa et al., 1993). Moreover, structural studies of the complex strongly support an architectural role of the Rad50 subunit in tethering DSB ends to link sister chromatids in HR and DNA ends in NHEJ (K.-P. Hopfner et al., 2002).

Architecture of SMC-like proteins

In contrast to canonical SMCs described in a previous chapter, SMC-like proteins lack a globular hinge domain and instead have alternative ways for dimerization (Figure 8) (K.-P. Hopfner et al., 2002). RecN dimerizes via hydrophobic interactions between the coiled coils. The arrangement of monomers (or dimers for that matter) within a complex is not clear. SbcC/Rad50 dimer formation is mediated via a zinc-hook, and the exact nature of SbcE dimerization, or whether it is relevant at all, has not yet been determined. The sizes of SMC-like complexes differ significantly, from 240 amino acid long coiled coils of RecN to over 900 amino acid coiled coils of mammalian Rad50.

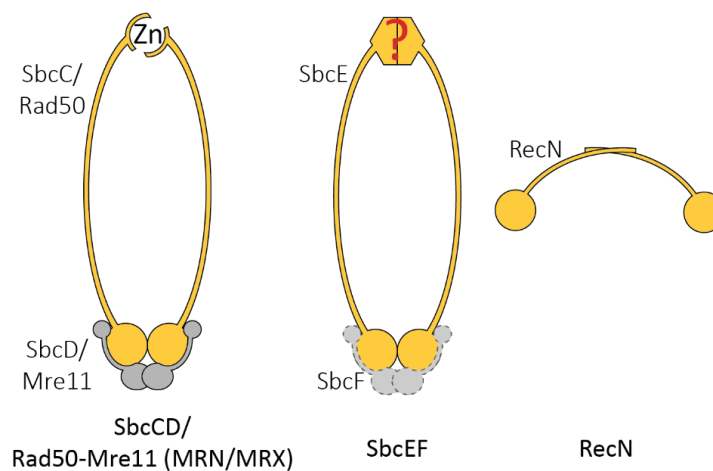


Figure 8. Scheme of homodimeric SMC-like proteins: SbcCD (Rad50-Mre11 in eukaryotes), SbcEF and RecN. SbcC monomers (ortholog of eukaryotic Rad50) dimerize via a zinc-hook. At the head domain, the complex interacts symmetrically with the Mre11 nuclease. The nature of dimerization and positioning of accessory proteins in unknown for SbcEF complex. RecN has a significantly shorter coiled coil compared to other proteins from the SMC family. Two monomers dimerize via hydrophobic interactions at the coiled coils. No accessory proteins were reported so far.

Focus on RecN and its role in DSB repair

General information

RecN was first identified in *E. coli* 37 years ago as a 62 kDa protein involved in DSB repair ((Lloyd et al., 1983; Picksley et al., 1984). It is a major SOS response protein (Finch et al., 1985). RecN homologs are widely distributed amongst almost all bacterial genomes suggesting a highly conserved function. Nevertheless, models derived from

different species using a variety of techniques (genetics, biochemistry and structural biology) are confusing and sometimes conflicting.

Phenotype of RecN mutants

As mentioned before, RecN deletion confers sensitivity to IR, MMC and I-SceI in various species: *H. influenzae* (Sweetman et al., 2005), *B. subtilis* (Alonso et al., 1993), *D. radiodurans* (Funayama et al., 1999), *H. pylori* (G. Wang & Maier, 2008) and *E. coli* (Meddows et al., 2005; Picksley et al., 1984). Interestingly, *H. influenzae* RecN could functionally substitute for *E. coli* RecN *in vivo* (Grove et al., 2009). Overexpression of RecN in untreated cells does not perturb chromosomal disposition (Vickridge et al., 2017) however, upon damage, it leads to cell filamentation and defective nucleoid partitioning (Nagashima et al., 2006).

The sensitivity to DNA damage differs among bacterial species. While a single DSB does not elicit an SOS response in *C. crescentus* or *B. subtilis* it is enough to do so in *E. coli* (Badrinarayanan et al., 2015; Pennington & Rosenberg, 2007; Simmons et al., 2009). Importantly, when the DSB is induced at two or more distantly located sites in *E. coli*, the presence of RecN becomes critical for survival (Meddows et al., 2005). Nevertheless, the mechanism of RecN recruitment to the lesion and tentative coordination of several broken ends at a single location is a burning question that has to be addressed.

In eukaryotes, cohesin was reported to be involved in DSB repair after replication is completed (Sjögren & Nasmyth, 2001; Ström et al., 2004). In *S. cerevisiae*, a single DSB induces the formation of a large domain of cohesin binding near the lesion (Unal et al., 2004). In *E. coli*, compaction and decompaction of the nucleoid was reported to be RecN dependent (Odsbu & Skarstad, 2014). Moreover, similarly to cohesin, RecN was reported to maintain sister chromatid interactions (SCI) upon MMC treatment in *E. coli* (Vickridge et al., 2017). This phenotype is dependent on RecA and is activated specifically upon DNA damage (Vickridge et al., 2017). Thus, RecN might be important for preventing segregation upon damage to facilitate repair and accelerate the return to normal growth. In *C. crescentus*, RecN was reported to participate in bringing broken ends in proximity to undamaged homologous template and re-segregation of loci to original positions in response to an I-SceI induced DSB (Badrinarayanan et al., 2015).

The idea of ordered re-zipping between homologous loci to global alignment of the chromosome is favoured (Vickridge et al., 2017).

Structural information

Only few crystal structures are available for RecN: *D. radiodurans* RecN (*DrRecN*) head (PDB: 4ABY), RecN coiled coil (PDB: 4ABX) and RecN head with a fragment of the coiled coil (PDB: 4AD8) (Pellegrino et al., 2012). Sequence analysis revealed that RecN's coiled coils are substantially shorter compared to other SMCs. Based on the crystal structures they are also predicted to be rigid and unlikely to form a ring-shaped dimer encircling DNA (Pellegrino et al., 2012). RecN is suggested to form a rather elongated dimeric conformation (300 Å) with heads facing opposite directions in respect to one another (Pellegrino et al., 2012). Interestingly, several studies report multimeric structures for RecN as judged from gel filtration and analytical ultracentrifugation (Grove et al., 2009; Keyamura & Hishida, 2019; Kidane et al., 2004; Sanchez & Alonso, 2005). Nevertheless, it is currently unknown how RecN monomers are arranged at the site of damage and whether those multimeric assemblies reported *in vitro* are biologically relevant.

RecN presence in time and space

In some bacteria like *E. coli*, RecN belongs to the SOS-regulon and its expression is tightly regulated. It is one of the most abundant transcripts in the SOS response (Courcelle et al., 2001; Picksley 1984). GFP-RecN was found to localise in discrete foci on the *E. coli* nucleoid following DNA damage and was rapidly degraded by the ClpX protease after repair completion (Nagashima 2006). RecN is thought to act after RecA, as RecA is required for formation of nucleoid associated RecN foci (Keyamura et al., 2013).

In contrast, in *B. subtilis*, RecN expression is SOS-independent (Au et al., 2005) and the protein is constitutively present in the cell. Due to this fact, until recently RecN was thought to be one of the first responders to DSB in *B. subtilis*, even before RecA (Ayora et al., 2011). Recently, another study showed that indeed large RecN-GFP foci are formed early, but they assemble at the periphery of the cell, possibly forming aggregates (McLean et al., 2021). Similarly to *E. coli*, the damage-induced nucleoid associated RecN-GFP focus formation requires end processing and RecA presence

(McLean et al., 2021). Single-molecule imaging showed that RecN assemblies are in general short-lived and that RecN fluctuates between mobile and immobile fractions upon DNA damage induction (Rösch et al., 2018).

Interaction partners?

Both RecN and RecA are undeniably important for recombinational repair of DSBs. Interestingly, the two proteins were reported to co-precipitate when using anti-RecA antibody in *E. coli* and *D. radiodurans* cell extracts (Uranga et al., 2017; Vickridge et al., 2017). Still, the notion of a direct physical interaction between RecN and RecA proteins is controversial (Keyamura et al., 2013; Klimova & Sandler, 2020; Vickridge et al., 2017). Also, no accessory proteins have so far been reported for RecN.

Biochemistry of RecN

RecN is a member of the SMC-like protein family and as such possesses highly conserved residues in the ATPase head domain (see more about ATPase cycle in Introduction to Chapter 1). Surprisingly, biochemical experiments (DLS, MALS) performed for *D. radiodurans* RecN indicate that the mutation of the conserved lysine in the Walker A motif renders the protein deficient in ATP hydrolysis, while the glutamate appears to be important for both, ATP binding and ATP hydrolysis (Pellegrino et al., 2012). The K-to-A hydrolysis effect was also shown for other species (Grove et al., 2009). RecN foci are formed in this mutant, but cells are sensitive to I-SceI induced breaks, a phenotype resembling $\Delta recN$ in *E. coli* (Grove et al., 2009; Keyamura et al., 2013). Moreover, establishing a stable transition state (2 ATP molecules bound but hydrolysis blocked) in *DrRecN* could only be obtained when mutating both residues (Pellegrino et al., 2012).

H. influenzae RecN exhibits low ATPase activity (comparable to the one reported for other SMC proteins) of less than 2 ATP molecules hydrolysed per RecN monomer per minute, and seems to be insensitive to the presence of DNA (Grove et al., 2009). Purified *B. subtilis* RecN and *D. radiodurans* RecN, however, were shown to bind to DNA and have DNA-stimulated ATPase activity *in vitro* (Pellegrino et al., 2012; Reyes et al., 2010; Sanchez & Alonso, 2005; Uranga et al., 2017).

Numerous studies attempted at labelling RecN as a cohesin-like protein because of its potential DNA end-joining activity (Pellegrino et al., 2012; Reyes et al., 2010), ssDNA binding (Sanchez & Alonso, 2005, *B. subtilis*), and participation in D-loop formation (Uranga et al., 2017, *D. radiodurans*). In general, difficulties in purification of RecN in *E. coli* due to poor solubility of the protein render interpretation of many biochemical experiments questionable. Taking this into account, it remains elusive whether RecN plays a structural or enzymatic role in DSB repair. Careful characterization of the RecN protein will likely provide additional information on the role of SMC proteins in DNA repair.

AIM OF THE STUDY

In Chapter 2, I investigate the architecture and involvement of *B. subtilis* RecN (BsRecN) in DNA repair. I strive to determine how RecN monomers interact *in vivo* and what role this factor plays in DSB management. Several residues reporting interactions between coiled coils of RecN monomers as well as head engagement and their contribution to survival were determined. Moreover, there seems to be a pattern in RecN-sensitive DNA repair depending on the position of the break. Work presented in this thesis lays a solid foundation for further, possibly high-throughput research.

RESULTS

RecN is involved in repair of Mitomycin C induced damage as previously reported

In *B. subtilis*, RecN is expressed in the cells at any given time, also prior to the DNA damage (Figure 1A, (Au et al., 2005)). Here, I investigated how different DNA repair pathway mutants deal with a constant exposure to damage.

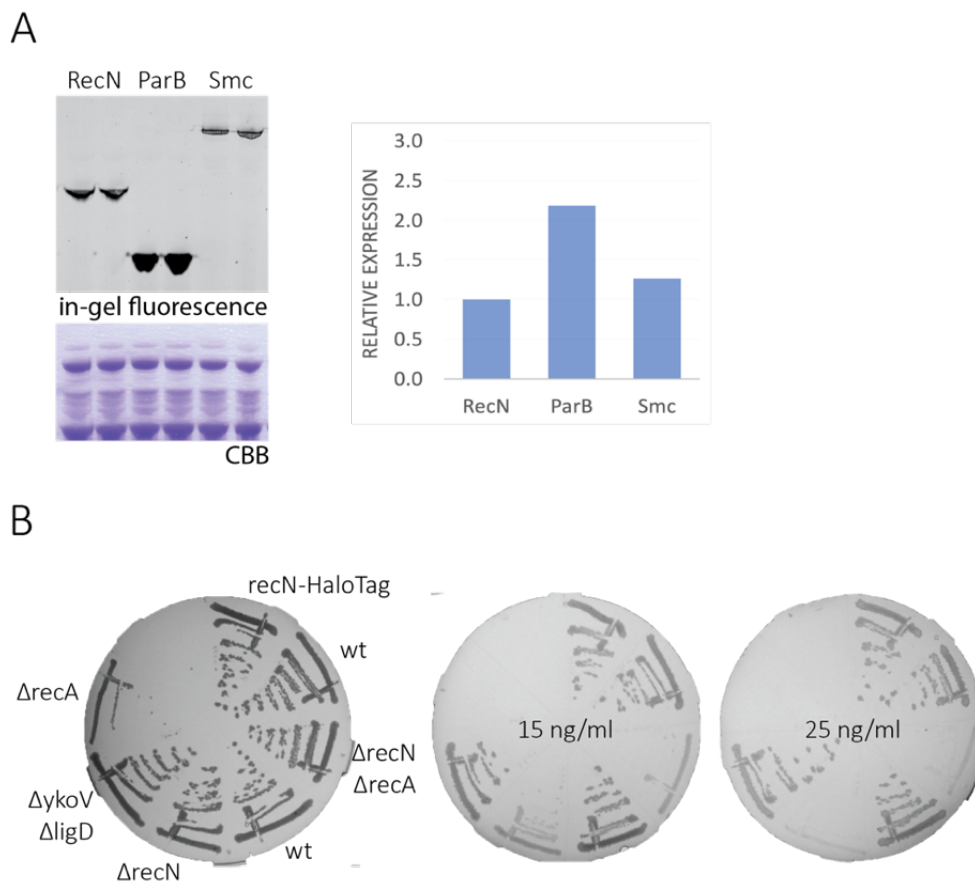


Figure 1. RecN is constitutively expressed in *B. subtilis* and is involved in MMC-induced DNA break repair. **A.** Cellular expression levels of HaloTagged ('HT') versions of RecN, ParB and Smc (top panel) and subsequent Coomassie Brilliant Blue (CBB) staining (bottom panel). Two technical replicates for each sample were loaded. On the right, quantification of the gel. **B.** Viability streaking assay on ONA plates supplemented with 0, 15 or 25 ng/ml MMC for strains with deletions in genes involved in HR (*recA*, *recN*) or NHEJ (*ykoV*, *ligD*) and controls (wild-type RecN, RecN-HT).

As reported before, Δ *recA* cells grow slowly even without external source of damage and become unviable on plates supplemented with MMC (Figure 1B, (Mascarenhas et

al., 2006)). Sensitivity of $\Delta recA$ cells even without the induction of breaks is likely due to failure in dealing with replication-related damage. The wild-type strain was proficient in dealing with MMC induced damage, even at 25 ng/ml concentration of MMC and C-terminal HaloTag (HT) fusion to RecN maintained a wild type-like level of activity (Figure 1B). Deletion of genes encoding proteins involved in non-homologous end joining (NHEJ), $\Delta ykoV \Delta ligD$, did not influence the strains' ability to cope with MMC-induced lesions, suggesting that this pathway is not utilized in MMC-induced damage response (Figure 1B). A $\Delta recN$ strain, however, was sensitive to MMC. Surprisingly, the double $\Delta recA \Delta recN$ mutant grew significantly better than the single $\Delta recA$ mutant, even in the presence of MMC (Figure 1B, see Discussion). This experiment confirms the role of RecN in MMC-induced DSB repair and that the sub-lethal MMC concentrations allow to monitor RecN's role in the DNA repair.

Studying architecture of RecN *in vivo*

Smc proteins are known to form ring-shaped complexes that co-entrap DNA molecules and/or extrude DNA loops (see Introduction). Interactions between two *BsSmc* monomers within a dimeric complex were thoroughly studied using high throughput cysteine cross-linking with reporter cysteines for head-head interactions and hinge dimerization being described (M. L. Diebold-Durand et al., 2017; Minnen et al., 2016; Vazquez Nunez et al., 2019). In the case of RecN, the relative orientation of RecN monomers and whether RecN is capable of capturing DNA remains elusive. Here, I utilize site-specific cysteine cross-linking to better understand *BsRecN* architecture *in vivo*. In this method, the side chains of a closely juxtaposed pair of cysteines become covalently linked upon addition of a thiol-specific bis-maleimide compound (BMOE). Moreover, I investigate interactions between RecN monomers in the context of mutations relevant for proteins activity.

Identifying residues for testing dimerization at the coiled coils

Chain rather than ring formation around the region affected by DSB was proposed for RecN. Nevertheless, so far, this has not been addressed *in vivo*. Here, combining the knowledge from available structures of *D. radiodurans* RecN (*DrRecN*) and sequence conservation, I picked candidate residues in *BsRecN* for reporting dimerization between the coiled coils of the RecN monomers.

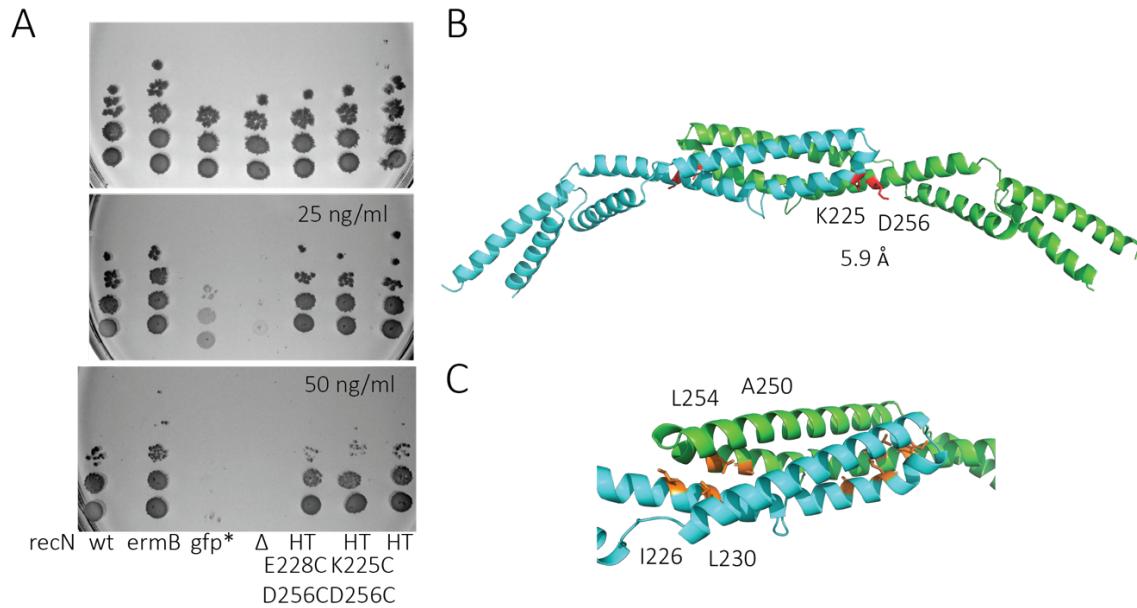


Figure 2. *BsRecN* monomers dimerize via coiled coil interactions. **A.** Viability spotting assay on ONA plates supplemented with 0, 25 or 50 ng/ml MMC for strains carrying pairs of reporter cysteines for coiled coil interface (E228C, D256C or K225C, D256C) coupled with a N-terminal HT. gfp* *recN* frameshift mutant. **B.** Model of *BsRecN* coiled coils interacting at the dimerization interface based on the structural data from *DrRecN*. Residues that proved to be the most efficient in reporting dimerization in cysteine cross-linking experiments are marked in red (K225, D256). α C- α C distance between pairs of residues is indicated. **C.** Close up of the dimerization interface of the same model as in B. with residues selected for mutagenesis, potentially leading to disrupting interactions at this interface marked in orange.

To this end, based on the PDB: 4ABX structure of the coiled coil domain of *DrRecN*, following cysteine residues were engineered in the *recN* sequence by allelic replacement: E228 and D256 (5.4 Å, α C- α C distance between pairs of residues), K225 and D256 (5.9 Å) or Q241 at symmetry axis (6.8 Å) (Figure 2B). The single mutant (Q241C) was non-viable on plates containing MMC. The two cysteine combinations were well tolerated by *B. subtilis* implying that the mutant proteins are functional (Figure 2A). Additional introduction of a C-terminal HaloTag, to allow for in-gel fluorescence detection of RecN mutants, did not influence the sensitivity of the mutants to MMC compared to wild-type (Figure 2A). Importantly, both cysteine combinations reported specific and robust BMOE cysteine cross-linking, reaching an efficiency of 70-80% (Figure 3A, 3B), visible as a shift in the SDS-PAGE gel corresponding to the formation of a dimeric complex. DNA damage induction with MMC did not influence

cysteine cross-linking, implying unaltered dimer formation (Figure 3B, see more below). The K225C and D256C mutant was approximately 10% more efficient in reporting dimerization when compared to E228C and D265C and therefore it was selected for subsequent assays. As expected, single mutations could not report dimerization, confirming the specificity of the reaction (Figure 3C). Thus, I was able to show that RecN monomers interact at the coiled coils to form dimeric complexes *in vivo*, validating the phenomenon observed for protein fragments in a crystal (Pellegrino et al., 2012). The high efficiency of cross-linking suggests that a large fraction of the protein exist as a dimer.

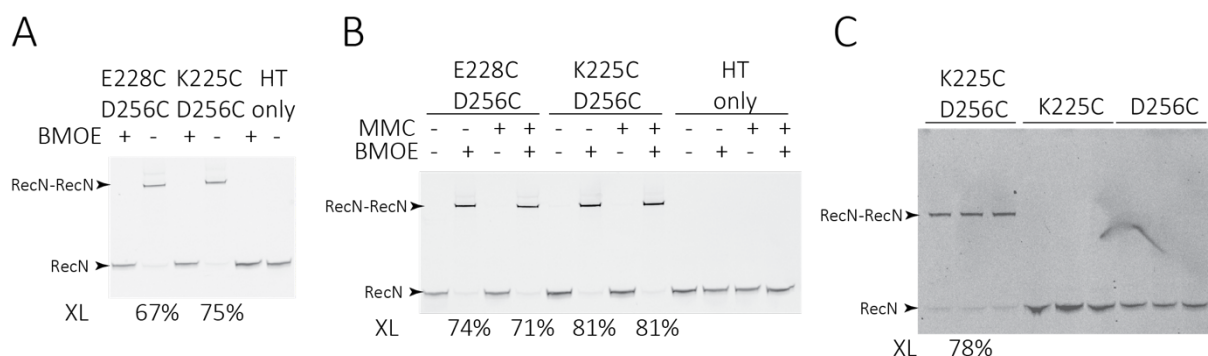


Figure 3. In-gel fluorescence reports efficient site-specific BMOE cross-linking at the dimerization interface and can only be reported when two residues are mutated to cysteines. A. Comparison of two double mutants: E228C, D256C and K225C, D256C. Monomeric species (lower bands) shift upon BMOE addition to a single dimeric species (upper band). **B.** DNA damage induction with MMC does not influence dimeric species formation. **C.** Single mutants in the dimerization interface do not support dimer formation. Three technical replicates were loaded on the gel. Numbers below each gel indicate the percentage of cross-linked species (XL).

Is the dimerization important for RecN's function in DSB repair?

Mutations in the Smc hinge domain render the protein non-functional and abolish distinct foci formation in *B. subtilis* cells (T. Hirano, 2002; Minnen et al., 2016). After establishing RecN dimerization via coiled coil interactions, now I wondered what the role of these interactions for DNA repair is. To assess that, first I disrupted the dimerization interface by point mutations. Hydrophobic dimerization interface candidate residues I226, L230, A250, L254 were selected for mutagenesis into glutamate (Figure 2C) using allelic replacement.

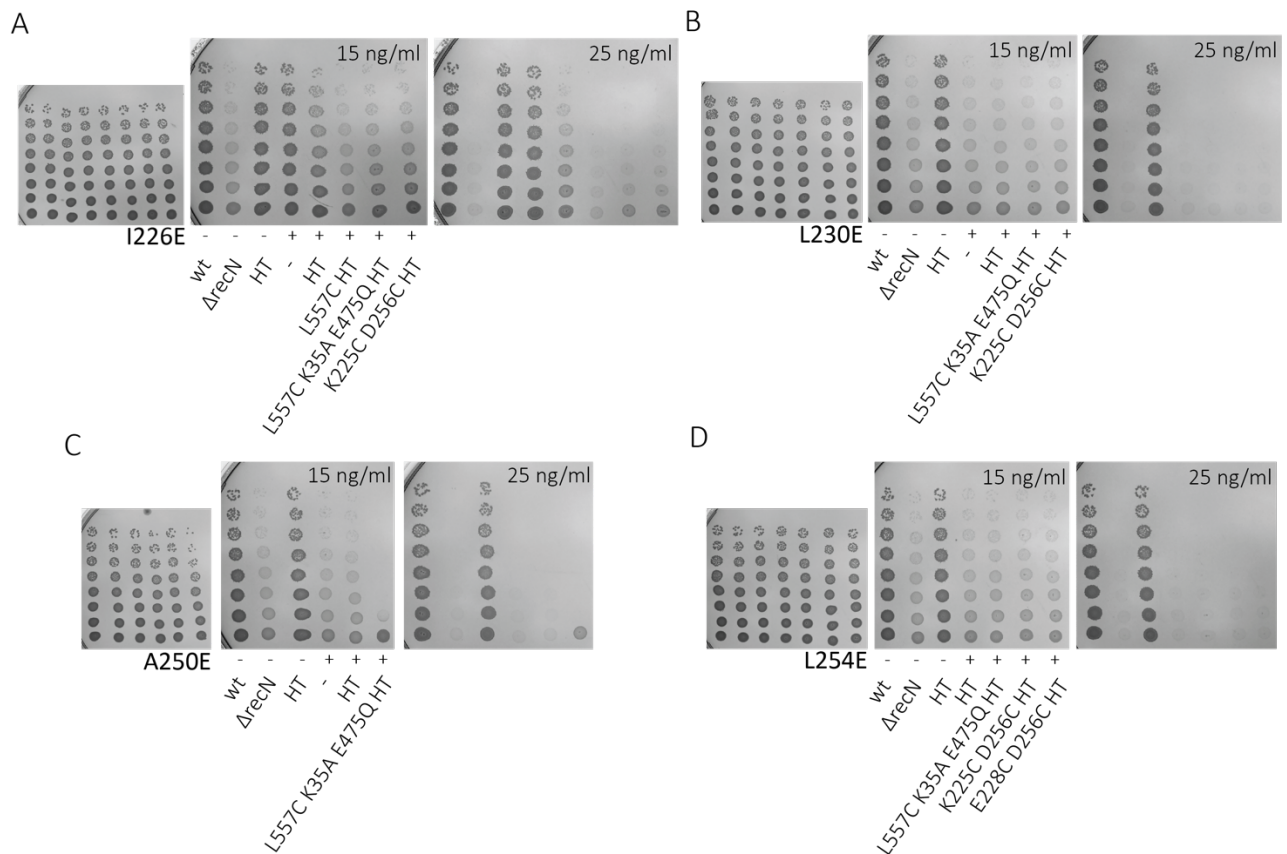


Figure 4. Single point mutation in the part of the coiled coil mediating dimerization can render the strain sensitive to DNA damage. Viability spot assays for different strain variants. **A.** I226E, **B.** L230E, **C.** A250E, **D.** L254E. Some combinations could not be obtained for given mutants.

Here, the strains were grown to higher OD (late exponential phase) before preparing serial dilutions and plating on ONA media supplemented with 0, 15 or 25 ng/ml MMC.

L230E, A250E and L254E point mutations rendered the strains sensitive to MMC (Figure 4B-D), resulting in a phenotype similar to $\Delta recN$. This suggests that the integrity of the coiled coil region is crucial for RecN's function. Moreover, L230E and L254E either completely abolished or severely reduced crosslinking (c. 8%) at the dimerization interface when combined with K225C and D256C, respectively (Figure 5). I226E on its own did not influence the sensitivity to MMC (Figure 4A). Curiously, combining I226E with a HT and K225C, D256C negatively impacted the strains viability, but only slightly the crosslinking efficiency (Figure 4A, 5). The observed DNA damage sensitivity thus correlates well with the cross-linking efficiency of the interface. Taken together, these results suggest that the dimerization of RecN at the coiled coil is essential for the DNA repair.

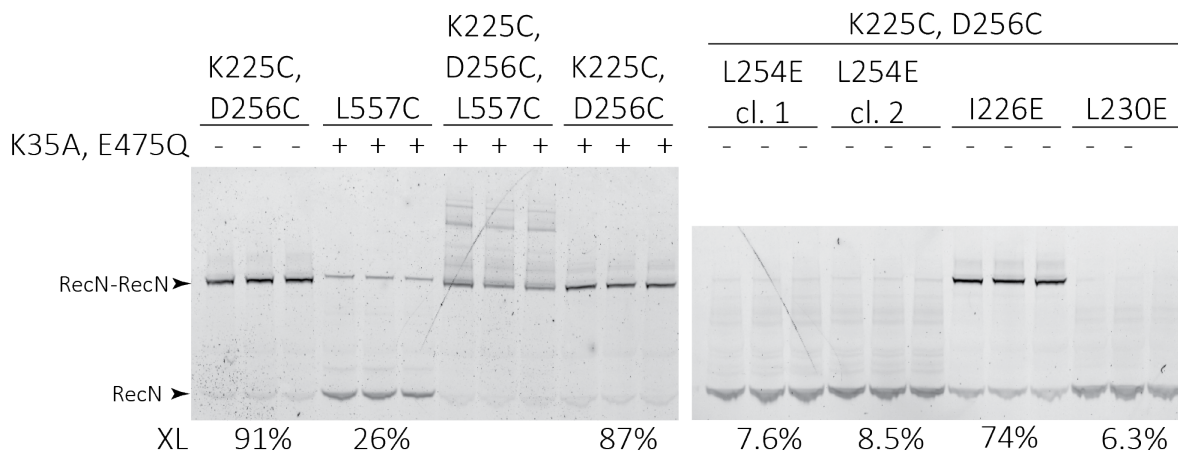


Figure 5. Interactions at the dimerization interface can be inhibited by point mutations. In-gel fluorescence for BMOE site-specific cross-linking for the dimerization interface, head domain, with or without the ‘transition state’ mutation (left panel, see more in main text below) and dimerization interface mutants (right panel). For each sample, three technical replicates were loaded on the gel. Numbers below each gel indicate the percentage of cross-linked species (XL).

ATPase activity is crucial for RecN’s function in DSB repair

The energy for SMC undertakings comes from ATP binding and hydrolysis within the globular ATPase head domain. I aimed to explore the consequences of perturbing the ATPase cycle of the RecN in *B. subtilis*. To do so, lysine (K35 – referred to as ‘KA’) and glutamate (E475 – referred to as ‘EQ’) residues in the NBD were mutated to alanine and glutamine, respectively. The two single mutants and the corresponding double mutant were generated by allelic replacement and tested for sensitivity to MMC.

As expected, the KA mutant produced a $\Delta recN$ -like phenotype (Figure 6A). The EQ mutation rendered the cells more sensitive to MMC when compared to wild type, however, surprisingly, the cells were slightly more resistant to MMC than the $\Delta recN$ strain (not completely inviable upon exposure to 15 or even 25 ng/ml MMC, Figure 6A). Therefore, either the EQ mutation is not essential in DNA repair function of RecN or it affects the ATPase cycle differently than in canonical SMC proteins.

The double mutant was as sensitive to DNA damage as the $\Delta recN$ variant when exposed to MMC (Figure 6B, 7D). Oddly, this sensitivity could be somewhat rescued by introducing a HT, which perhaps influences positioning of the heads in respect to each other (Figure 6A, 6B). The double mutant (K35A and E475Q) showed wild type-

like RecN expression as judged from HT version of the protein (Figure 7B). The results obtained above suggest that completing the ATP cycle is essential for the RecN function.

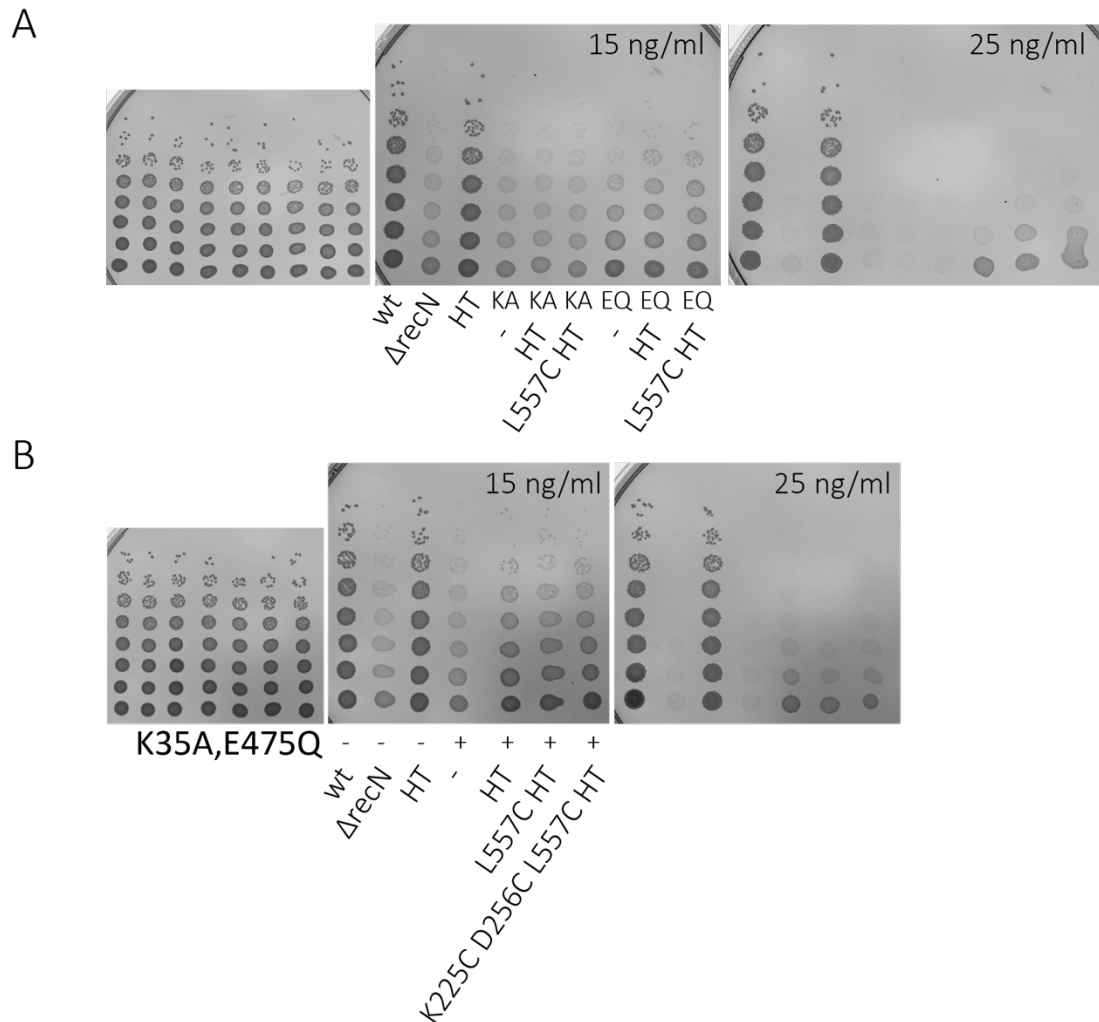


Figure 6. Mutations in the Walker A and Walker B motif of ATPase domain of *BsRecN* have distinct influence on viability of the cells. A. Viability spotting assay of constant exposure to 15 or 25 ng/ml MMC on ONA plates for strains carrying single mutations in the catalytic site of the head domain: either K35A, or E475Q. **B.** Same as in **A.**, just here the double mutant strain (K35A, E475Q) and its variants are tested.

Here, the strains were grown to higher OD (late exponential phase) before preparing serial dilutions and plating on solid media.

Identifying residues to report cross-linking at the head domain

Above I managed to establish reporters for coiled coil interactions. I also showed that the RecN ATPase is important for cell viability upon DNA damage. Here, I ventured to determine reporters for one state of the ATPase, the dimerization of the head domain.

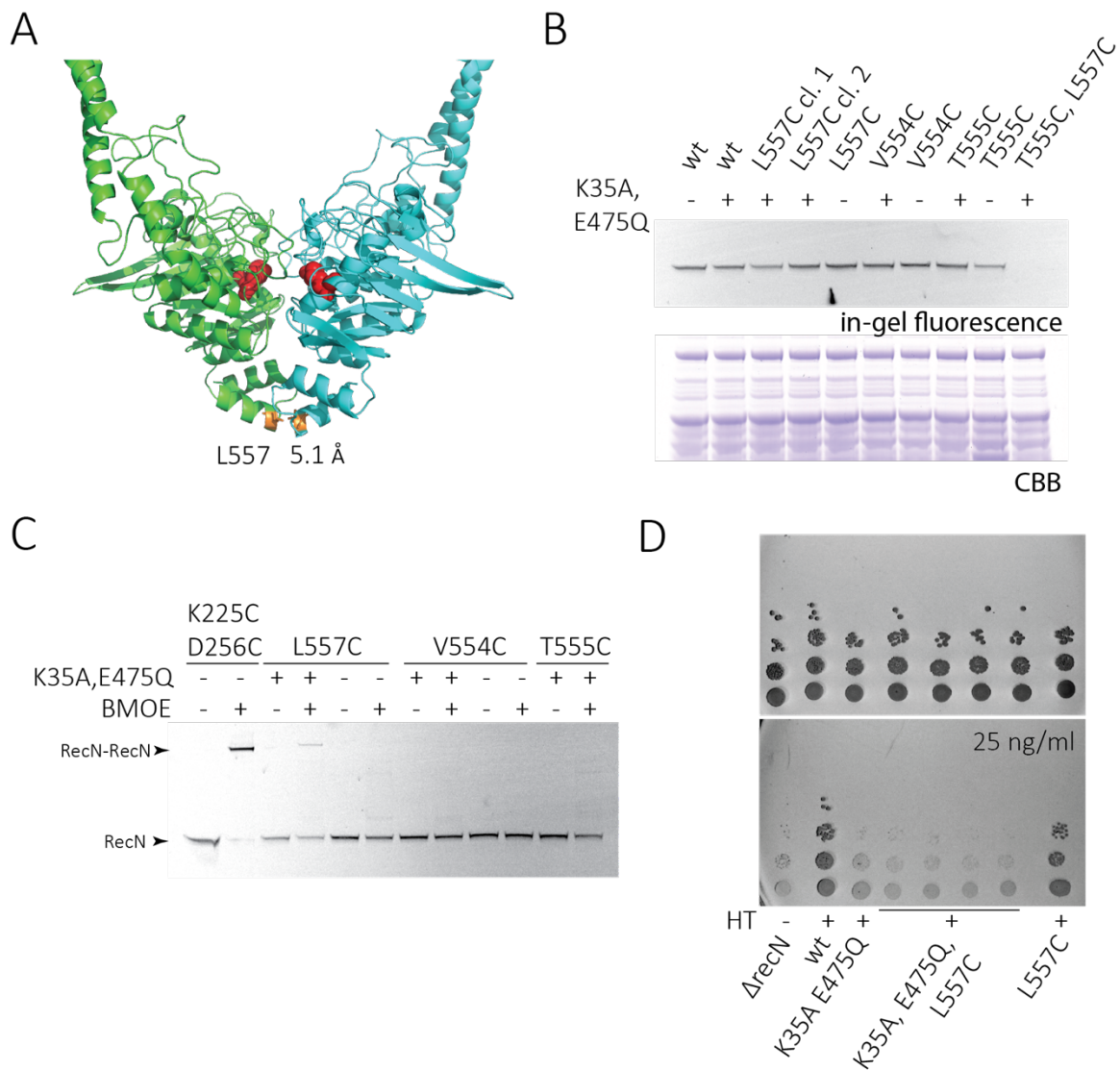


Figure 7. *BsRecN* head domain interactions are hardly detectable by cross-linking. **A.** Model of engaged *BsRecN* heads based on structural data from *DrRecN* and Rad50/Mre11 from *M. jannaschii* and *C. thermophilum*. Residues involved in interactions with ATP represented as red spheres. Residue that proved to be the most efficient in reporting dimerization in cysteine cross-linking experiments is marked in orange (L557). **B.** Cellular expression levels of HaloTagged ('HT') versions of wild-type, single mutants L557, V554, T555 and double mutant T555, L557 (upper panel) and subsequent Coomassie Brilliant Blue (CBB) staining (bottom panel). **C.** In-gel fluorescence for BMOE site-specific cross-linking for head domain mutants with or without transition state mutations. Dimerization interface mutant (K225C, D256C) as a cross-linking control. **D.** Viability spotting assay on ONA plates supplemented with 0 or 25 ng/ml MMC for variants of L557C mutant.

PDB: 4ABY (*DrRecN* head dimer structure) and PDB: 4AD8 (*DrRecN* head and head-proximal coiled coil fragment) structures were used for homology modelling of *BsRecN*

heads. PDB: 5DNY (*M. jannaschii*) and PDB: 5DA9 (*C. thermophilum*) ATP γ S-bound Rad50/Mre11 complexes were used to approximate possible conformation of ATP-engaged *BsRecN* heads (Figure 7A). The C-terminal Helix-turn-helix domain at the bottom of the heads seemed like a promising mutagenesis target. V554 (19.8 Å), T555 (8.6 Å) and L557 (5.1 Å) residues were selected to be mutated to cysteines (Figure 5A). Of note, T555 is relatively well conserved among diverged bacterial species (sequence alignment in Pellegrino et al., 2012). All variants, except for the T555C, L557C double mutant, were expressed to near wild-type levels (Figure 7B). Introduction of L557C into otherwise wild-type RecN did not influence *B. subtilis* viability and sensitivity to MMC (Figure 7D). Notably, none of the tested residues allowed me to detect head engagement in otherwise wild-type strain backgrounds (Figure 7C).

The K35A and E475Q double mutant, with L557C residue at the head domain allowed for robust reporting of head engagement, maintaining the heads in a presumably engaged form as reported by cross-linking (28% cross-linking efficiency, Figure 5, 7C, 8A, see below). As expected, the cross-linking efficiency at the head domain was very low for single EQ (3.6%) and undetectable for single KA mutant (Figure 8A). This result suggests that indeed both mutations within the ATPase pocket are a prerequisite for efficient head engagement. Taken together, the above experiments imply that establishing a stable transition state (2 ATP molecules bound but hydrolysis blocked) requires two mutations in the ATPase domain as previously suggested for *DrRecN* (see Introduction). The RecN monomers likely engage at head interface rarely, and possibly in a very transient manner.

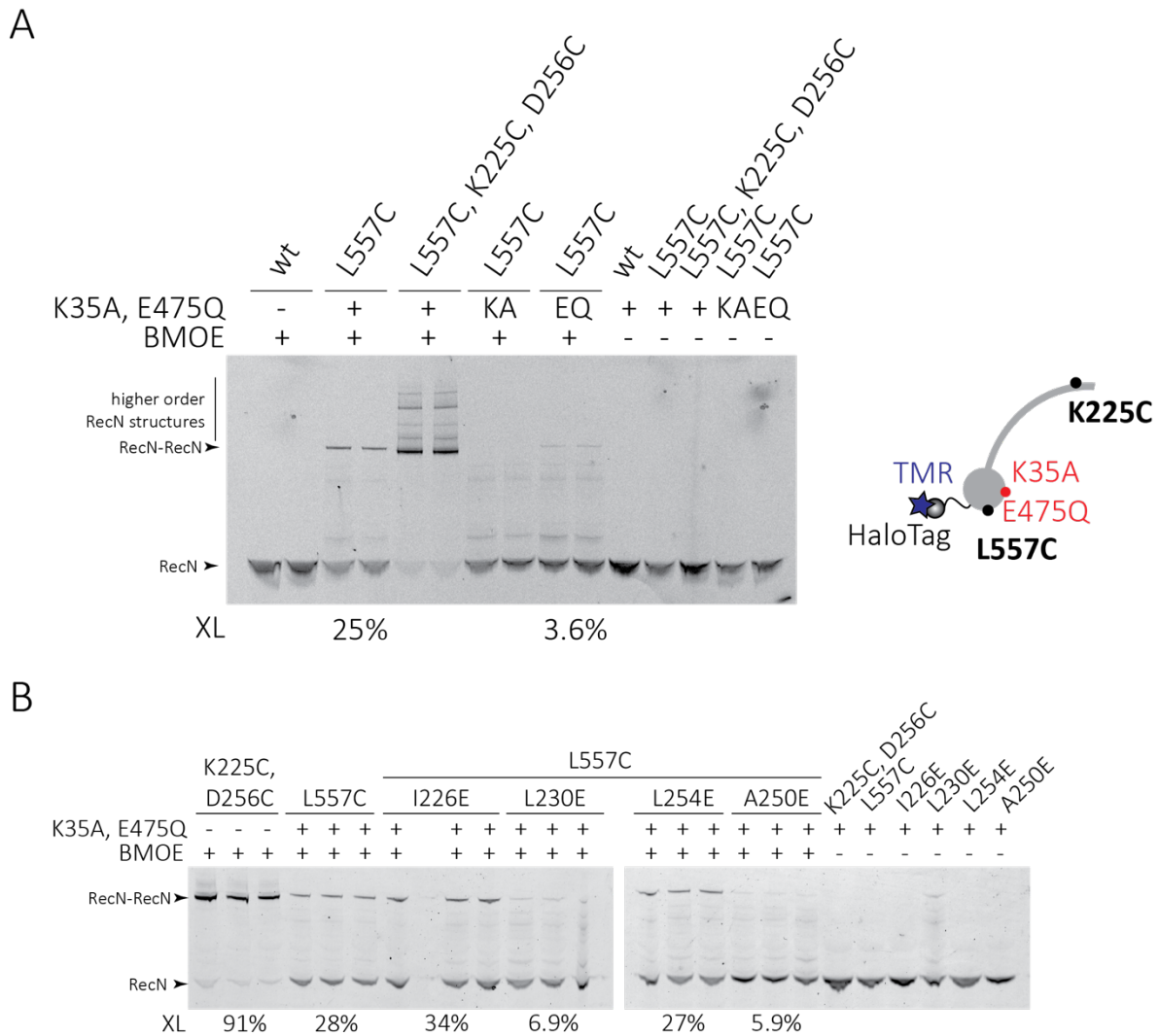


Figure 8. *BsRecN* head domain interactions are stabilized by a double mutant in the ATPase head domain and are sensitive to mutations in the coiled coil. A. In-gel fluorescence for BMOE site-specific cross-linking for head domain mutants with or without transition state mutations. The contribution of single mutants in the catalytic site of the head domain on cross-linking efficiency was assessed. Right panel shows a schematic representation of RecN monomer associated with a HT and residues involved in cross-linking indicated in bold black, mutations in the ATPase fold shown in red. TMR was the substrate for in-gel visualisation using the HT. **B.** In-gel fluorescence for BMOE site-specific cross-linking for dimerization interface mutants with transition state mutations. The contribution of point mutations to glutamate on cross-linking efficiency at the head domain was assessed.

Numbers below each gel indicate the percentage of cross-linked species (XL).

Do interactions at the coiled coil influence head engagement?

In wild type *BsSmc* head-head interactions are hardly detectable using a cysteine reporter (K1151) analogously positioned as L557C (Minnen et al., 2016), but could be

observed in the transition state mutant. Interestingly, hinge mutants boosted head engagement in the *BsSmcEQ* mutant and caused extra toxicity (Minnen et al., 2016), implying that dimerization at the hinge hindered head engagement. Here, I ventured to examine the interplay between the two extremities of the protein and whether coiled coil interface disruption boosts head engagement between RecN monomers.

To do so, I investigated cross-linking efficiency at the head domain in presence of mutations disrupting the dimerization interface at the coiled coils and the transition state mutations (Figure 8B). Conversely to what was observed in *BsSmc*, disrupting the interactions between coiled coils did not promote head engagement (Figure 8B) – it remained at the same level (L254E) or dropped (6.9% in L230E mutant vs 27% in unmodified coiled coil). This suggests that the opening of the coiled coils promotes dissociation of the RecN heads. Thus, RecN seems to be an outlier from the SMC-like protein family.

Can RecN form multimeric structures?

Certain studies report RecN-dependent ‘repair center’ (RC) formation (Kidane et al., 2004; Rösch et al., 2018), which conceivably requires several RecN molecules to interact with each other or other proteins in the assembly, presumably creating a scaffold facilitating homology search.

To assess whether higher-order RecN interactions using the known protein-protein interfaces are possible, cysteine mutations at both extreme interfaces were combined with the hydrolysis (‘transition state’) double mutant. The obtained strain was sensitive to MMC (Figure 6B). Interestingly, besides a dimer band seen in previous experiments, several higher molecular weight bands appeared on the gel upon BMOE addition (Figure 5, 8A). This suggests that a multimeric assembly of RecN monomers is possible *in vivo*: heads of two RecN dimers can engage to form tetramers or higher order structures with K35A and E475Q. However, no such structures were observed without the ATPase mutations, raising doubts about the physiological relevance of such assemblies.

DNA damage does not noticeably change interactions between RecN monomers.

If RecN was to play a structural role during DNA repair (e.g., bringing/holding broken ends in proximity), changes in head engagement and in coiled coil interactions might occur when DNA is damaged. Increase or decrease in interactions between monomers possibly could be monitored using engineered cysteine reporters upon damage induction. Despite numerous attempts including varying concentrations and exposure times to MMC or introduction of a single break, rich or poor growth media, different growth temperatures, no noticeable changes in the cross-linking efficiency neither at the dimerization interface, nor between the head domains were detected (Figure 9, 10). The inability to pinpoint the right conditions could suggest that in *B. subtilis* the interactions between RecN monomers are so minute/transient that changes cannot be detected using our system.

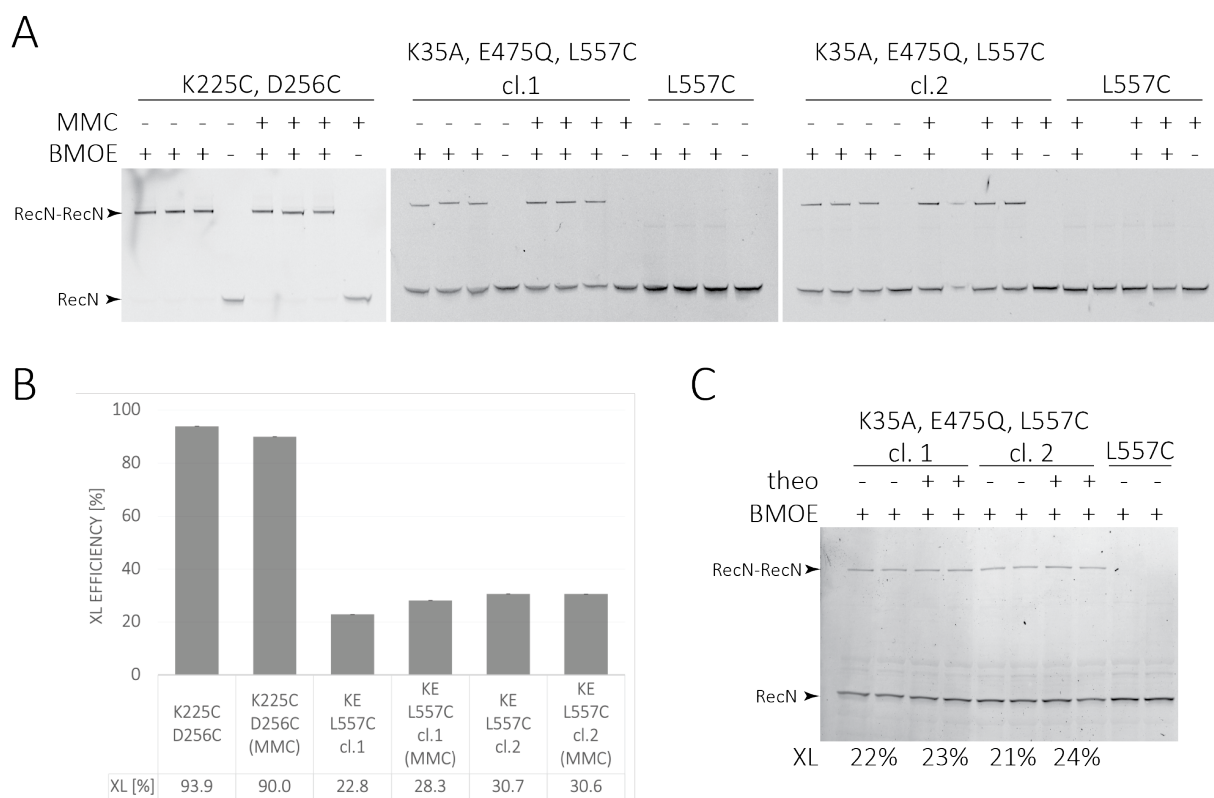


Figure 9. Transient damage induction does not promote changes in interactions between RecN monomers. A. In-gel fluorescence for BMOE site-specific cross-linking for dimerization interface and head domain mutants with or without transient MMC treatment (300 ng/ml MMC for 20 minutes). Two independently obtained clones of K35A, E475Q, L557C were tested. Three technical replicates for each sample were loaded. **B.** Quantification of dimeric band formation for treated and untreated samples presented in **A.** **C.** In-gel

fluorescence for BMOE site-specific cross-linking for head domain mutants with or without induction of a single cut at *cgeD* locus (2 mM theophylline treatment for 40 minutes at 30 °C). Two independently obtained clones of K35A, E475Q, L557C were tested. Two technical replicates for each sample were loaded. Numbers below each gel indicate the percentage of cross-linked species (XL).

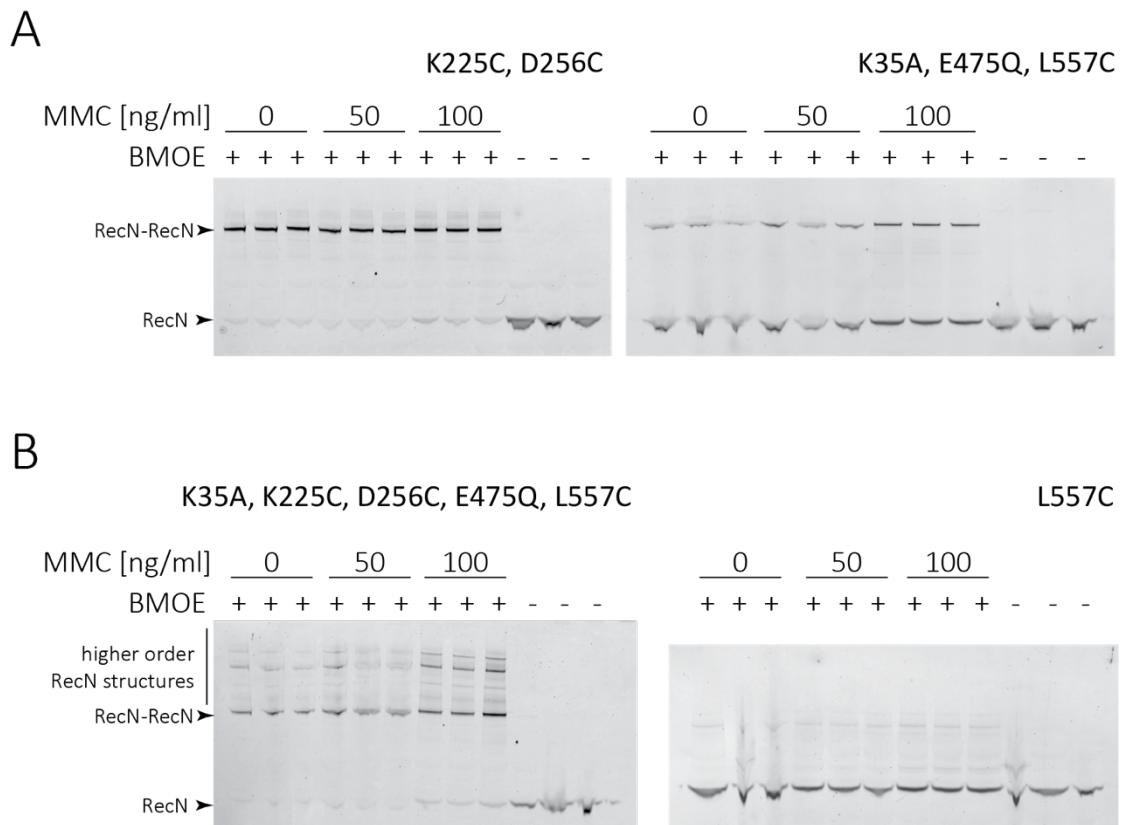


Figure 10. Investigating influence of exposure to different MMC concentrations on efficiency of cross-linking. Cells were treated for 30 minutes with indicated MMC concentrations. Tested interfaces are indicated above each gel in bolder text: **A.** dimerization interface (left panel) and head domain (right panel). **B.** Cysteine reporters at both extremities of RecN (left panel) and head domain without transition state mutations (right panel). Three technical replicates for each sample were loaded.

Is there a link between the position of DSB and requirement for RecN?

In *E. coli* survival of the cells challenged with more than one DSB depends on the presence of RecN (see Introduction, Meddows et al., 2005b). Possibly, RecN allows for faithful repair when several broken ends have to be coordinated in the cell. In the section above, no changes in cross-linking could be observed upon MMC treatment. Perhaps, I have not found the right time and place of RecN's action. MMC induces

DSBs at random chromosomal locations therefore, in an attempt to better understand spatio-temporal behaviour of RecN, I employed the I-SceI endonuclease under a theophylline-inducible promoter (Figure 11A, (Meddows et al., 2005)) to create DSBs in a highly controlled manner. In brief, a I-SceI gene cassette was introduced at the nonessential *amyE* locus. To ensure tight regulation of I-SceI expression, P_{divIVA} promoter was coupled with a theophylline switch. *B. subtilis* genome is free of endogenous I-SceI recognition sites, avoiding the risk of genome fragmentation by the meganuclease. One or two recognition sites were introduced at different positions on the chromosome (Figure 11B). Wild-type and $\Delta recN$ combinations were prepared to assess the importance of RecN in repair of site-specific DSBs at given locus/loci.

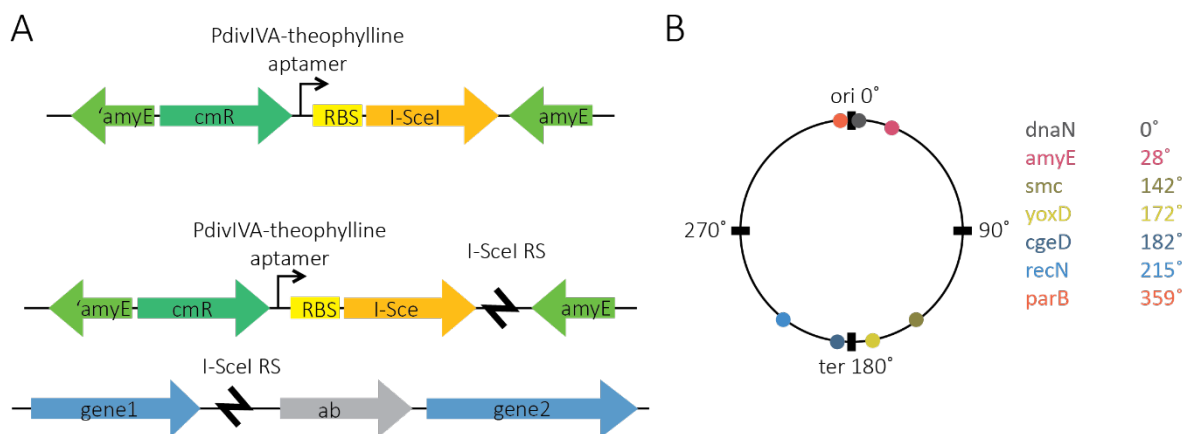


Figure 11. I-SceI meganuclease for site-specific DSB induction at different positions on *B. subtilis* chromosome. **A.** Cartoon depicting the cloning strategy for introducing I-SceI cassette into non-essential *amyE* locus with or without a Restriction Site (I-SceI RS) (top and middle panel, respectively), as well as introducing RS at other intergenic regions (lowest panel). **B.** Circular representation of *B. subtilis* genome with positions in degrees and loci in vicinity of which RS were introduced marked with colored circles (left panel) together with a list of loci and their respective chromosomal positions (right panel).

Two approaches were used to induce DSBs by I-SceI: either 40 min treatment with 2 mM theophylline in a liquid culture or plating on media containing 2 mM theophylline. The transient exposure did not reveal measurable differences suggesting efficient repair when breaks are only transiently present, or insufficient expression of I-SceI (Figure 12A, middle panel).

Resistance to DSBs strictly depended on the incubation temperature (data not shown). After careful consideration, it appeared to be an intrinsic feature of the theophylline switch which, for reasons we did not follow up on, allows for higher expression at lower temperature (30 vs 37°C). Of note, this knowledge was utilized in the elongated SMC project described in Chapter 1.

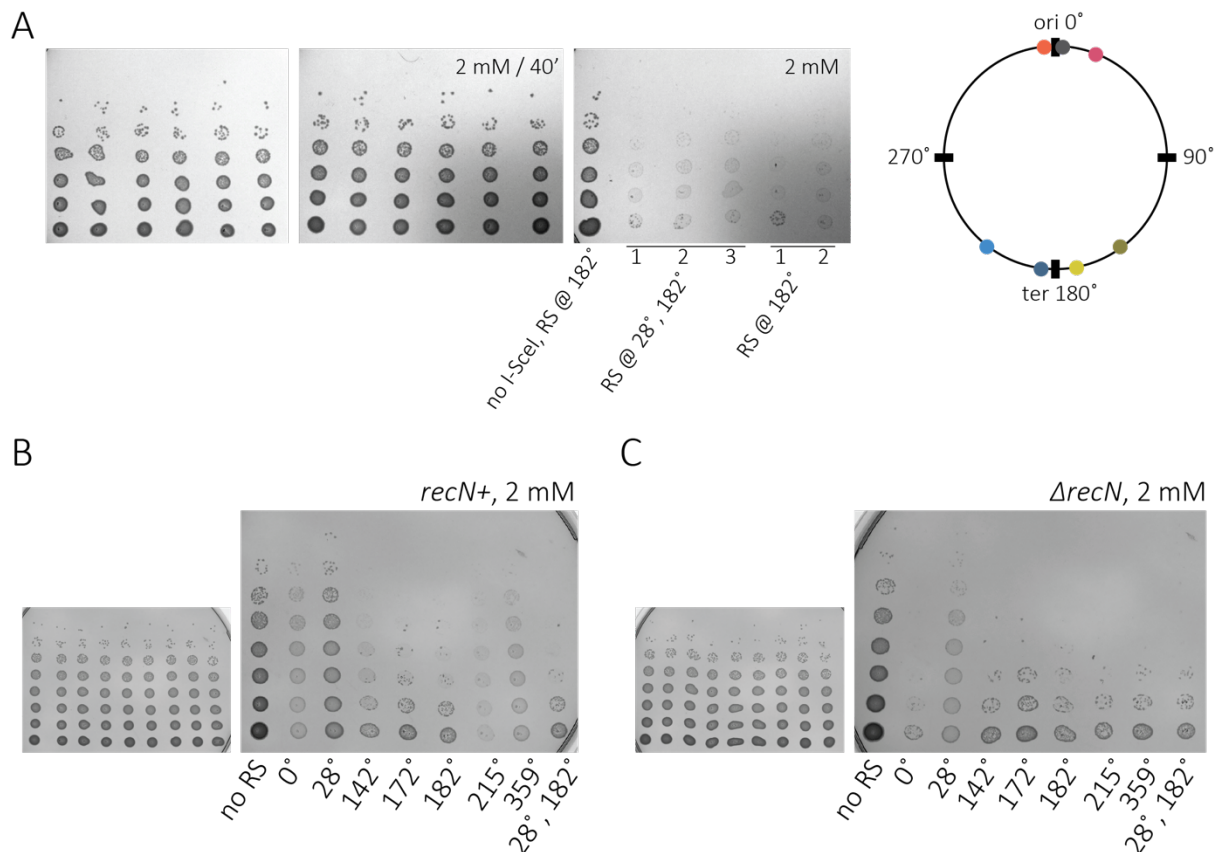


Figure 12. Is there a link between the position of DSB and requirement for RecN? **A.** Viability spotting assay for strains with a single origin-distal RS or two RS. Two types of viability assay were performed: transient induction for 40 minutes with 2mM theophylline (middle panel) or constant exposure to damage on ONA plates supplemented with 2mM theophylline (right panel). 10-fold serial dilutions of strains prior to damage induction serve as a control (left panel). Inset depicts *B. subtilis* chromosome with marked loci in the vicinity of which RSs were introduced (as in Figure 8B), for facilitated view. **B.** Viability spotting assay on ONA plate supplemented with 2mM theophylline for constant induction of I-SceI meganuclease and directed DSB induction at *ori*-proximal and/or *ori*-distal locus/loci. **C.** Same as in B. except that now strains with RecN deletion are being tested. Insets show untreated samples (grown on ONA without theophylline inducer).

Plates containing 2 mM theophylline incubated at 30 °C revealed striking results – a single cut-site at the *ori*-distant *cgeD* (182°) locus was detrimental (Figure 12A). The outcome was similar when two cut-sites were introduced, at *amyE* (28°) and *cgeD* (182°) (Figure 12A). A single cut-sites at close to the origin of replication were tolerated much better by the cell (Figure 12B). To test whether this depends on RecN presence, I deleted the gene. Lack of RecN led to inability to repair DSBs in all cases (with an exception of *amyE*, see below) implying that repair is indeed RecN dependent, and that the pathway is highly sensitive to distance from *ori*, presumably because of template availability (Figure 12B-C). In rich media, *B. subtilis* performs multi-fork replication which means that another round of replication starts before the previous one finished. Effectively leading to more copies of origin proximal DNA being available compared to terminus region and so a homologous template would be easier to find. Curiously, cuts at *amyE* locus were tolerated substantially better than other tested *ori*-proximal regions. Supposedly, as speculated in Chapter 1, direct vicinity of the origin of replication is a peculiar, busy and crowded region. *amyE*, positioned more than 300 kb away from the *ori*, might be already out of this busy zone and therefore could be targeted easily by HR machinery. Additional tests to evaluate cutting ‘sensitivity zones’ should be performed to confirm these findings.

DISCUSSION

Concerted Smc action is responsible for maintaining specific chromosomal architecture.

SMC complexes are essential for chromosome organisation, nevertheless mechanistic details of their action are not yet well understood. Those tripartite rings actively translocate along the DNA double helix, compacting it and allowing for efficient segregation of sister chromatids to daughter cells. In Chapter 1 and annexed article, I show that maintenance of specific chromosomal architecture in *B. subtilis* is dependent on homeostasis between the number of available Smc complexes and their turnover on the chromosome, as well as the disposition of *parS* sites.

In most bacteria, the Smc translocation process starts from dedicated entry sites, called *parS* sites, localized in the vicinity of replication origin (Livny et al., 2007). Close juxtaposition of several *parS* sites likely contributes to robustness of Smc loading, by marking the proper loading area, and avoiding unspecific loading when *parS* sequence becomes unavailable e.g., because of a mutation or possibly gets blocked by nucleoid associated proteins (NAPs). On the other hand, availability of several entry sites raises a question about what happens when Smc complexes get loaded at two (or more) *parS* sites simultaneously and eventually meet one another (see below).

Numerous studies address RNAP-SMC or replication-transcription conflicts (Busslinger et al., 2017; Heinz et al., 2018; Merrikh et al., 2012; Rowley et al., 2019), with Smc-Smc encounters only now comes into the spotlight of investigation. Several possible scenarios of Smc-Smc encounters can be envisioned including: 1. Smc blocking (with or without subsequent unloading), 2. Reversal of one of the Smc complexes upon meeting, 3. Traversal of one Smc complex over the other, 4. General collision avoidance.

Here and in a recent study (Brandão et al., 2021), similar experiments were performed leading to antagonistic interpretations. Both studies acknowledge that Smc-Smc encounters are inevitable. In this thesis, I argue that occurrence of such meetings on the DNA is kept at low levels in wild type *B. subtilis* cells. Smc unloading is predicted to be very rare and stochastic and only a few Smc complexes were estimated to be

enough to sustain the longitudinal chromosome organisation in *B. subtilis* (Banigan et al., 2020), therefore there should be no need for bypassing events in the first place. By changing the number of loading sites and extending the distance between them, as well as increasing the abundance of available for loading Smc complexes, I increase the ratio of Smc complexes per loading site and observe perturbations in chromosome arm juxtaposition. The simplest explanation for loss of chromosome arm alignment as observed in 3C-seq contact maps is that the increased ratio forces encounters upon which Smc complexes would dissociate from the DNA and release the preformed loop. Smc blockage upon encounter is inconsistent with obtained 3C-seq maps and if the complexes were to freely bypass one another, the consequences of changing above mentioned parameters would not influence chromosomal disposition.

On the other hand, by using polymer simulations to recapitulate 3C-seq maps, Brandão et al., 2021 proposes that in wild type *B. subtilis* cells Smc-Smc collisions are readily resolved by traversal events. Such traversal of Smc complexes was reported *in vitro* in single molecule experiments for yeast condensin, on naked DNA (E. Kim et al., 2020). Nevertheless, a previous study investigating different variants of the LE showed that Smc traversal generates many pseudoknots and did not allow for chromosome juxtaposition observed in *B. subtilis*, nor could it maintain linear spatial ordering of the mitotic chromosome or recapitulate interphase HiC features (Banigan et al., 2020). Therefore, biological relevance of bypassing events needs to be carefully considered and require further experiments to validate it *in vivo*.

More importantly, yeast condensin was recently shown to be able to perform LE over a range of obstacles: nucleosomes, RNA polymerase, and dCas9 (Pradhan et al., 2021). Based on this finding, non-topological Smc interactions with the DNA were proposed (Pradhan et al., 2021). The nature of Smc interactions with the DNA in the light of this surprising observation needs urgent addressing as it raises a lot of questions regarding the mechanism of not only bypassing of any obstacle (including other Smc complexes) but also LE in general. Correct bridging of the DNA segments and directional movement after potential bypass reaction by the Smc becomes even more enigmatic.

Why do elongated chimeric Smc complexes not align the chromosome?

In Chapter 1, *B. subtilis* (*Bs*) hinge was replaced with a *S. pneumoniae* (*Sp*) 100-amino-acid-long coiled coil and hinge. *BsSmc* coiled coil was suggested to have a regulatory effect on protein activity, transmitting information between the hinge and head domains, controlling the availability of DNA binding surfaces within the Smc ring (Bürmann et al., 2017). Regardless of whether Smc associates with the DNA in a pseudo-topological or non-topological manner, it is possible that in the case of *SpBsSmc* this information flow is perturbed. *SpBsSmc* is not stimulated by addition of DNA in contrast to *BsSmc* (data not shown). Interestingly, hinge replacement only slightly perturbs chromosome disposition (the secondary diagonal becomes broader and fainter than in wild type). Strains carrying *SpBsSmc* complex reconstituting wild type *BsSmc* size however, completely lose the chromosome arm alignment and no arc around *parS334* is formed suggesting that the right amount of hinge proximal coiled coil might be important for proper loop extrusion allowing for chromosome juxtaposition in *B. subtilis*. Particular properties of *Sp* hinge and hinge-proximal coiled coil may come as a result of different chromosome folding mechanisms and distinct prerequisites for survival of *S. pneumoniae* cells. It is tempting to speculate that *SpSmc* is intrinsically more prone to falling off the DNA. Experiments assessing the ability of hinges and hinge-proximal coiled coils from other organisms to fold *B. subtilis* chromosome could help to explain this phenomenon. Does previously reported Zn-hook conferring to *B. subtilis* cell viability (Bürmann et al., 2017) maintain chromosomal arm alignment?

Viability of *B. subtilis* is not determined by maintaining chromosome arm juxtaposition.

Two main genome orientations were described for bacteria: longitudinal (*ori-ter*) and traverse (left-*ori*-right) (X. Wang & Rudner, 2014). Those genome folding patterns can fluctuate throughout the cell cycle and seem to be dictated by DNA replication. In *P. aeruginosa* and *B. subtilis* the longitudinal chromosome orientation is temporarily replaced by the traverse orientation prior to replication. Next, the two replicated chromosomal copies are segregated to their final polar destinations in the opposite halves of the cell (Vallet-Gely & Boccard, 2013; X. Wang et al., 2014). Non-replicating *B. subtilis* cells remain in left-*ori-ter* orientation (X. Wang & Rudner, 2014). Given that, a non-trivial question raises about the relation between proper folding, cell survival and

propagation. How permissive or strict is this system? How much variance can the cell accommodate?

In bacteria for which longitudinal chromosome organisation was reported, juxtaposition of the right and left arm depends on the presence of functional Smc-ScpAB complexes and its loading factor, ParB (Böhm et al., 2020; Le et al., 2013; Liroy et al., 2020; X. Wang et al., 2017). Sensitivity to absence of those factors and subsequent loss of chromosome fold differs among bacteria. Previously it was shown that deletion of *parB* has surprisingly mild consequences for actively dividing *B. subtilis*, resulting in only slightly elevated anucleate cell levels (Ireton et al., 1994). Deletion of *smc* is more detrimental and renders the cells sick even in slow growth conditions (Gruber et al., 2014). In both cases, $\Delta parB$ and Δsmc , chromosome juxtaposition is abolished (X. Wang et al., 2015). Here in Chapter 1, I show that cells carrying re-sized Smc complexes are incapable of maintaining expected chromosome fold despite being viable. This suggests that specific chromosome folding is not directly associated with cell fitness and survival, at least under tested experimental conditions. Taking the notion further, no specific chromosome organisation is needed for propagation, but perhaps maintaining it is important for yet to be discovered reasons, e.g., for processes requiring highly polarized chromosome disposition, like sporulation or DNA repair (see below).

Moreover, it is possible that only a limited amount of the chromosome, close to the origin of replication, must be segregated/separated actively. ParABS system (important for Smc-ScpAB recruitment and loading) is acting strictly in the vicinity of origin of replication and is known to contribute to origin segregation (P. S. Lee & Grossman, 2006). Possibly, disentangling this region is sufficient for successful cell cycle progression and cell division.

Recombinational repair as the pathway of choice in bacteria.

HR is a predominant pathway utilized by bacteria to deal with DNA damage as it allows for error-free repair, extremely important for fast dividing cells. The preference for HR is supported by the fact that deletion of genes encoding proteins involved in NHEJ, $\Delta ykoV \Delta ligD$, does not influence the strains viability on MMC supplemented plates. Therefore, suggesting that this pathway is not utilized in MMC-induced damage response when HR machinery is available in the cell. RecA is the main orchestrator of SOS-response and HR-dependent DNA repair. Cells lacking RecA grow slowly when untreated and are dead upon damage induction. In Chapter 2, in Figure 1B, a surprising phenotype was observed – $\Delta recA \Delta recN$ mutant grew significantly better on MMC supplemented plates than single $\Delta recA$ strain. This striking phenomenon of RecN toxicity in the absence of RecA however should be verified by repeating the experiment. In principle, nucleoid associated RecN-GFP foci were indeed observed in a fraction of cells in a RecA-independent manner in *B. subtilis* (McLean et al., 2021) – possibly this toxic effect is due to RecN establishing some sister chromatid cohesion (as reported previously for *E. coli*, (Vickridge et al., 2017)) that cannot be resolved. In the double mutant however, upon DSB induction, HR cannot occur, RecA dependent branch migration and HJ formation is impossible, and the cells are forced to employ alternative (error-prone) pathways to deal with the damage.

RecN-RecN dimers are a functional unit required for DNA repair.

The structural data for RecN is scarce and limited to protein fragments from *D. radiodurans*. Until now the crystallographic data was not backed up by respective experiments testing RecN architecture in living cells. In Chapter 2, I was able to verify the interactions between monomers *in vivo* using site-specific cysteine cross-linking. RecN monomers robustly dimerize at the coiled coils and interactions at this interface are crucial for dealing with DSBs. Single point mutations in the coiled coil (hydrophobic to negatively charged) prevent dimerization at the coiled coil region and render the cells incapable of growth on MMC supplemented plates, suggesting that those interactions are essential for the functional version of the protein and as such participate in DNA repair.

What is the role of RecN in DSB repair?

Despite several years of studying recombinational DNA repair, the exact role of RecN, a protein widely conserved among bacterial genomes, is unknown. Whether RecN plays a structural or enzymatic role is controversial. RecN was previously proposed to form elongated structures rather than closed dimeric rings (Pellegrino et al., 2012). The genome is readily segregated upon replication and if a break occurs, often the homologous template would be far (nm) away. Presence of a scaffolding protein, maintaining sister chromatids close together and supporting RecA in finding interaction partner is an attractive role for RecN, a protein from the SMC-like protein family. Nevertheless, here I show that multimeric RecN assemblies cannot be detected in cells even under conditions of DNA repair.

ATPase activity lays at the core of proteins from the SMC and SMC-like protein family. As expected, cells carrying ATPase domain mutants of *BsRecN* are sensitive to MMC treatment, suggesting that ATP turnover is required for RecN mediated DNA repair. Interestingly, here I confirm that the EQ mutant in the Walker B motif did not behave as previously reported in the literature (Hirano & Hirano, 2004; Lammens et al, 2004). Head-head engagement *in vivo* in *BsRecN* could only be detected when two mutations in the ATPase domain were present. Interestingly, the sensitivity to MMC in the double mutant (KA EQ) could be partially rescued by introducing a HaloTag, which presumably influences relative head-head positioning, highlighting the importance of transient interactions between monomers at this interface. The rare or transient nature of the head-head interaction further argues against RecN having a structural role in DNA repair. Moreover, in the light of the recent paper, confirming RecA and AddAB-dependent RecN foci formation *in B. subtilis* (McLean et al., 2021) and reports from *D. radiodurans* regarding RecN stimulating RecA-mediated strand exchange and D-loop formation (Uranga et al., 2017), RecN emerges rather as an enzymatic partner for facilitating HR and not driving it in the first place.

Correlation between the position of the cut-site and RecN presence.

Studies in *E. coli*, using I-SceI endonuclease for introduction of site-specific lesions, have shown that in $\Delta recN$ cells a single DSB has a modest effect on viability, however when there are two or more breaks RecN becomes essential (Meddows et al., 2005). Here I show that the viability of *B. subtilis* cells differs depending on whether one or

two cuts are induced as well as on where the cut-site was positioned. In wild type *B. subtilis* cells, single cut-site close to the origin of replication is tolerated reasonably well. Conversely, single cuts at positions further away from the origin had severe consequences. Deletion of RecN, leads to further deterioration of the phenotypes, especially those in the proximity to the origin of replication. Importantly, induction of two DSBs, leads to very poor survival regardless RecN's presence.

Several attempts at tracking DNA repair of multiple DSBs are reported in literature. Fluorescently labelled loci surrounding a directed cut site in *E. coli* were pairing in the middle of the cell before being reseggregated to their original positions (Wiktor et al., 2021). Conversely, data from *C. crescentus* indicate that homologous loci pair near where the undamaged locus resides (Badrinarayanan et al., 2015). It is conceivable that repair of a single cut is different from managing several breaks at the same time. RecN likely facilitates HR, probably becoming more important if many simultaneous breaks occur and need to find their respective homologues. Whether RecN facilitates homology search by participating in forming previously described 'repair centers' (Kidane et al., 2004) or supports RecA in local pairing with the template at the site of DNA damage remains to be elucidated. More studies combining spatial distribution at high resolution and break management are thus required. It would be interesting to perform high-throughput study like Transposon-insertion sequencing or by using CRISPR-Cas9 system to introduce single and/or multiple cut sites all along the chromosome and assess whether RecN-sensitive repair zones exist in *B. subtilis*.

How does 3D genome organisation influence DNA repair?

Little is known about the contribution of chromosome conformation to DNA repair processes. Studies show that the initial spatial proximity between the break and a homologous donor sequence is a key feature that determines the efficiency of HR (C.-S. Lee et al., 2016). In eukaryotes, local DNA organization is known to guide the DNA repair process (Arnould et al., 2021). DNA damage leads to local genome rearrangements, possibly helping to restrict the response to a given area and prevent misrepair across different TADs (Lang et al., 2017; Luo et al., 2008; Sanders et al.,

2020). Recent study reported TADs to be functional units of the DNA damage response (Arnould et al., 2021), with cohesin enriched within 2-5 kb around the DSB, independent of the repair pathway, HR or NHEJ.

Bacterial genomes are substantially smaller compared to their eukaryotic counterparts and often consist of a single chromosome. The homology search task is thus comparatively easy. However, if a DSB occurs in an area which is already segregated, HR repair must perform a genome-wide search for a homologous repair template (Renkawitz et al., 2014). RecN emerges as a tentative candidate participating in this search in concert with RecA.

It is tempting to speculate that intrinsic resistance to DSB in bacteria is dictated by chromosome conformation within the cell. Most of the reports about RecN come from studies performed in *E. coli* and *B. subtilis* – main representatives of G(-) and G(+) bacteria, respectively, with drastically different chromosomal architecture (see above). In Chapter 1 I showed that strains carrying elongated or shortened Smcs are viable but have a clear defect in chromosomal organisation. Whether that is influencing resistance to DSB formation or subsequent repair efficiency is an attractive possibility. A simple experiment testing the sensitivity to damage of *B. subtilis* mutants that are viable but with perturbed chromosome architecture e.g., $\Delta parB$ or elongated Smc strains could open a new area of very interesting research in SMC-mediated chromosome organisation biology in bacteria.

MATERIALS AND METHODS

Methods regarding experiments described in Chapter 1 are thoroughly described and enclosed in the annexed paper. Here I only describe methods relevant to the Chapter 2.

***B. subtilis* strain construction and growth**

Mutations were introduced into naturally competent *B. subtilis* 1A700 isolate using allelic replacement strategy as described in (M.-L. Diebold-Durand et al., 2019) and selected on ONA plates with appropriate antibiotic selection. Presence of desired mutations was verified by PCR and Sanger sequencing.

I-SceI cassette was cloned into non-essential *amyE* locus. To verify that the *amyE* locus was indeed disrupted, single isolates were patched on ONA plates supplemented with 10% starch and grown overnight at 37 °C. Next, the plates were exposed to iodine pellets for 40 minutes and the amylase activity of *B. subtilis* strains assessed.

Expression analysis of HaloTagged proteins

Overnight *B. subtilis* cell cultures were grown in LB containing 0.5% glucose at 30 °C, diluted the next day in fresh LB to OD₆₀₀ = 0.01 and cultured at 37°C in 100 mL LB to exponential phase (OD₆₀₀ = 0.022-0.030). Cells were harvested by centrifugation, pellets washed in cold PBS supplemented with 0.1% (v/v) glycerol ('PBSG') and split in a way that each pellet would contain a biomass equivalent to 1.25 OD₆₀₀ units. Next, cell pellets were resuspended in 40 µL PBSG containing 75 U/mL ReadyLyse Lysozyme, 750 U/mL Sm nuclease, 5 µM HaloTag TMR substrate and protease inhibitor cocktail ('PIC') and incubated at 37°C for 30 minutes to promote lysis. Next, 10 µL of 4X LDS-PAGE with DTT (200 mM final) buffer was added and samples were incubated for 5 minutes at 95 °C. Samples were resolved by SDS-PAGE and gels imaged on an Amersham Typhoon scanner with Cy3 DIGE filter setup.

MMC Challenge

Overnight *B. subtilis* cell cultures were grown in LB containing 0.5% glucose at 30 °C, diluted the next day in fresh LB to OD₆₀₀ = 0.01 and cultured to exponential phase at 37 °C. Cells were harvested by centrifugation and washed with fresh LB. Serial

dilutions were prepared and spotted onto ONA plates supplemented with MMC (0, 15, 25 or 50 ng/ml). Plates were incubated overnight at 37 °C.

For spotting experiments presented in Figure 4 and Figure 6 slightly different growth conditions were used. 5 µL of overnight cultures were diluted in 200 µL of fresh LB in 96-well plates and grown in a dedicated orbital plate shaker at 37 °C at 700 RPM for 3-4 hours. Previous experiments proved that after this time cells are in exponential phase, however as visible on plates, they grew to higher densities than when grown in flasks as described above. Serial dilutions and plating on MMC supplemented plates was performed as described in the previous paragraph.

Site-specific DSB induction

Overnight *B. subtilis* cell cultures were grown in LB containing 0.5% glucose at 30 °C, diluted the next day in fresh LB to OD₆₀₀ = 0.01 and cultured to exponential phase at 37 °C. Two treatments were performed: transient or constant induction of DSBs by I-SceI using theophylline. For transient DSB induction, exponentially growing culture was split in two flasks and theophylline was added to one of them at a final concentration of 2 mM for 40 minutes. Next, serial dilutions were prepared and spotted onto ONA plates. For constant induction, the cells at exponential growth phase were harvested by centrifugation and washed with fresh LB. Serial dilutions were prepared and spotted onto ONA plates supplemented with 2 mM theophylline. In both cases, plates were incubated at 30 °C overnight.

For spotting presented in Figure 12B, alternative protocol described in the previous section was used (culturing in 96-well plate). Serial dilutions and plating were performed as described in the previous paragraph.

***In vivo* cross-linking**

Overnight *B. subtilis* cell cultures were grown in LB containing 0.5% glucose at 30 °C, diluted the next day in fresh LB to OD₆₀₀ = 0.01 and cultured to exponential phase at 37 °C in 100ml of fresh LB. Next, cells were harvested by centrifugation and washed in cold PBS supplemented with 0.1% (v/v) glycerol ('PBSG') and split in a way that each pellet would contain a biomass equivalent to 1 OD₆₀₀ units. Next, cell pellets were resuspended in 200 µL of fresh PBSG and the cross-linking reaction was started by

the addition of 0.5 mM BMOE (Thermo Fisher) and incubated for 10 minutes on ice. The reaction was quenched by the addition of 14 mM 2-mercaptoethanol. Next, samples were centrifuged, and pellets resuspended in 30 μ L PBSG containing 75 U/mL ReadyLyse Lysozyme, 750 U/mL Sm nuclease, 5 μ M HaloTag TMR substrate and protease inhibitor cocktail ('PIC') and incubated at 37°C for 30 minutes to promote lysis. Finally, 10 μ L of 4X LDS-PAGE with DTT (200 mM final) buffer was added and samples were incubated for 5 minutes at 95 °C. Samples were resolved by SDS-PAGE and gels imaged on an Amersham Typhoon scanner with Cy3 DIGE filter setup.

For investigating influence of exposure to different MMC concentrations on efficiency of cross-linking, MMC (50, 100, 300 ng/ml) was added to exponentially growing cell cultures for varying amounts of time (20, 30 or 60 minutes). After exposure, the cells were pelleted by centrifugation and processed as described above.

For investigating influence of exposure to a single cut using I-SceI, the exponentially growing cells were exposed for 40 minutes to 2 mM theophylline. After exposure, the cells were pelleted by centrifugation and processed as described above.

TMR fluorescence bands were quantified using ImageJ. Bands corresponding to cross-linked species were defined manually, and their intensities were corrected for background signal. Values from two or three technical replicate experiments were exported to Microsoft Excel for calculation of average fractions and standard deviation.

REFERENCES

- Alonso, J. C., Stiege, A. C., & Lüder, G. (1993). Genetic recombination in *Bacillus subtilis* 168: effect of recN, recF, recH and addAB mutations on DNA repair and recombination. *Molecular and General Genetics MGG*, 239(1), 129–136. <https://doi.org/10.1007/BF00281611>
- Ames, B. N., Shigenaga, M. K., & Hagen, T. M. (1993). Oxidants, antioxidants, and the degenerative diseases of aging. *Proceedings of the National Academy of Sciences*, 90(17), 7915 LP – 7922. <https://doi.org/10.1073/pnas.90.17.7915>
- Amundsen, S. K., & Smith, G. R. (2003). Interchangeable Parts of the *Escherichia coli* Recombination Machinery. *Cell*, 112(6), 741–744. [https://doi.org/https://doi.org/10.1016/S0092-8674\(03\)00197-1](https://doi.org/https://doi.org/10.1016/S0092-8674(03)00197-1)
- Anchimiuk, A., Liou, V. S., Bock, F. P., Minnen, A., Bocard, F., & Gruber, S. (2021). A low Smc flux avoids collisions and facilitates chromosome organization in *B. subtilis*. *ELife*, 10, e65467. <https://doi.org/10.7554/eLife.65467>
- Arnould, C., Rocher, V., Finoux, A.-L., Clouaire, T., Li, K., Zhou, F., Caron, P., Mangeot, P. E., Ricci, E. P., Mourad, R., Haber, J. E., Noordermeer, D., & Legube, G. (2021). Loop extrusion as a mechanism for formation of DNA damage repair foci. *Nature*, 590(7847), 660–665. <https://doi.org/10.1038/s41586-021-03193-z>
- Au, N., Kuester-Schoeck, E., Mandava, V., Bothwell, L. E., Canny, S. P., Chachu, K., Colavito, S. A., Fuller, S. N., Groban, E. S., Hensley, L. A., O'Brien, T. C., Shah, A., Tierney, J. T., Tomm, L. L., O'Gara, T. M., Goranov, A. I., Grossman, A. D., & Lovett, C. M. (2005). Genetic composition of the *Bacillus subtilis* SOS system. *Journal of Bacteriology*, 187(22), 7655–7666. <https://doi.org/10.1128/JB.187.22.7655-7666.2005>
- Ayora, S., Carrasco, B., Cárdenas, P. P., César, C. E., Cañas, C., Yadav, T., Marchisone, C., & Alonso, J. C. (2011). Double-strand break repair in bacteria: a view from *Bacillus subtilis*. *FEMS Microbiology Reviews*, 35(6), 1055–1081. <https://doi.org/10.1111/j.1574-6976.2011.00272.x>
- Badrinarayanan, A., Le, T. B. K., & Laub, M. T. (2015). Rapid pairing and re-segregation of distant homologous loci enables double-strand break repair in bacteria. *The Journal of Cell Biology*, 210(3), 385–400. <https://doi.org/10.1083/jcb.201505019>
- Banigan, E. J., & Mirny, L. A. (2019). Limits of Chromosome Compaction by Loop-Extruding Motors. *Physical Review X*, 9(3), 31007. <https://doi.org/10.1103/PhysRevX.9.031007>
- Banigan, E. J., van den Berg, A. A., Brandão, H. B., Marko, J. F., & Mirny, L. A. (2020). Chromosome organization by one-sided and two-sided loop extrusion. *ELife*, 9, 1–46. <https://doi.org/10.7554/eLife.53558>
- Baumann, P., & West, S. C. (1999). Heteroduplex Formation by Human Rad51 Protein: Effects of DNA End-structure, hRP-A and hRad52. *Journal of Molecular Biology*, 291(2), 363–374. <https://doi.org/https://doi.org/10.1006/jmbi.1999.2954>
- Bermúdez-López, M., Ceschia, A., de Piccoli, G., Colomina, N., Pasero, P., Aragón, L., & Torres-Rosell, J. (2010). The Smc5/6 complex is required for dissolution of DNA-mediated sister chromatid linkages. *Nucleic Acids Research*, 38(19), 6502–6512. <https://doi.org/10.1093/nar/gkq546>
- Böhm, K., Giacomelli, G., Schmidt, A., Imhof, A., Koszul, R., Marbouty, M., & Bramkamp, M. (2020). Chromosome organization by a conserved condensin-ParB system in the actinobacterium *Corynebacterium glutamicum*. *Nature Communications*, 11(1), 1485. <https://doi.org/10.1038/s41467-020-15238-4>
- Brandão, H. B., Ren, Z., Karaboja, X., Mirny, L. A., & Wang, X. (2021). DNA-loop-extruding SMC complexes can traverse one another in vivo. *Nature Structural & Molecular Biology*. <https://doi.org/10.1038/s41594-021-00626-1>
- Bremer, H., & Dennis, P. P. (2008). Modulation of Chemical Composition and Other Parameters of the Cell at Different Exponential Growth Rates. *EcoSal Plus*, 3(1). <https://doi.org/10.1128/ecosal.5.2.3>
- Brewer, B. J. (1988). When polymerases collide: replication and the transcriptional organization of the *E. coli* chromosome. *Cell*, 53(5), 679–686. [https://doi.org/10.1016/0092-8674\(88\)90086-4](https://doi.org/10.1016/0092-8674(88)90086-4)
- Bürmann, F., Basfeld, A., Vazquez Nunez, R., Diebold-Durand, M.-L., Wilhelm, L., & Gruber, S. (2017). Tuned SMC Arms Drive Chromosomal Loading of Prokaryotic Condensin. *Molecular Cell*, 861–872. <https://doi.org/10.1016/j.molcel.2017.01.026>
- Bürmann, F., Funke, L. F. H., Chin, J. W., & Löwe, J. (2021). Cryo-EM structure of MukBEF reveals DNA loop entrapment at chromosomal unloading sites. *BioRxiv*, 2021.06.29.450292. <https://doi.org/10.1101/2021.06.29.450292>
- Bürmann, F., Lee, B. G., Than, T., Sinn, L., O'Reilly, F. J., Yatskevich, S., Rappsilber, J., Hu, B., Nasmyth, K., & Löwe, J. (2019). A folded conformation of MukBEF and cohesin. *Nature Structural and Molecular Biology*, 26(3), 227–236. <https://doi.org/10.1038/s41594-019-0196-z>
- Bürmann, F., Shin, H. C., Basquin, J., Soh, Y. M., Giménez-Oya, V., Kim, Y. G., Oh, B. H., & Gruber, S. (2013). An asymmetric SMC-kleisin bridge in prokaryotic condensin. *Nature Structural and Molecular Biology*, 20(3), 371–379. <https://doi.org/10.1038/nsmb.2488>
- Busslinger, G. A., Stocsits, R. R., van der Lelij, P., Axelsson, E., Tedeschi, A., Galjart, N., & Peters, J.-M. (2017). Cohesin is positioned in mammalian genomes by transcription, CTCF and Wapl. *Nature*, 544(7651), 503–507. <https://doi.org/10.1038/nature22063>
- Chiu, A., Revenkova, E., & Jessberger, R. (2004). DNA Interaction and Dimerization of Eukaryotic SMC Hinge Domains *. *Journal of Biological Chemistry*, 279(25), 26233–26242. <https://doi.org/10.1074/jbc.M402439200>
- Ciosk, R., Shirayama, M., Shevchenko, A., Tanaka, T., Toth, A., Shevchenko, A., & Nasmyth, K. (2000). Cohesin's binding to chromosomes depends on a separate complex consisting of Scc2 and Scc4 proteins. *Molecular Cell*, 5(2), 243–254. [https://doi.org/10.1016/s1097-2765\(00\)80420-7](https://doi.org/10.1016/s1097-2765(00)80420-7)

- Connelly, J. C., de Leau, E. S., & Leach, D. R. F. (2003). Nucleolytic processing of a protein-bound DNA end by the E. coli SbcCD (MR) complex. *DNA Repair*, 2(7), 795–807. [https://doi.org/10.1016/s1568-7864\(03\)00063-6](https://doi.org/10.1016/s1568-7864(03)00063-6)
- Connelly, J. C., Kirkham, L. A., & Leach, D. R. F. (1998). The SbcCD nuclease of Escherichia coli is a structural maintenance of chromosomes (SMC) family protein that cleaves hairpin DNA. *Proceedings of the National Academy of Sciences*, 95(14), 7969 LP – 7974. <https://doi.org/10.1073/pnas.95.14.7969>
- Connelly, J. C., & Leach, D. R. F. (1996). The sbcC and sbcD genes of Escherichia coli encode a nuclease involved in palindrome inviability and genetic recombination. *Genes to Cells*, 1(3), 285–291. <https://doi.org/https://doi.org/10.1046/j.1365-2443.1996.23024.x>
- Cremer, T., & Cremer, M. (2010). Chromosome territories. *Cold Spring Harbor Perspectives in Biology*, 2(3), a003889–a003889. <https://doi.org/10.1101/cshperspect.a003889>
- Cromie, G. A., & Leach, D. R. F. (2001). Recombinational repair of chromosomal DNA double-strand breaks generated by a restriction endonuclease. *Molecular Microbiology*, 41(4), 873–883. <https://doi.org/https://doi.org/10.1046/j.1365-2958.2001.02553.x>
- Cuylen, S., Metz, J., & Haering, C. H. (2011). Condensin structures chromosomal DNA through topological links. *Nature Structural and Molecular Biology*, 18(8), 894–901. <https://doi.org/10.1038/nsmb.2087>
- Davidson, I. F., Bauer, B., Goetz, D., Tang, W., Wutz, G., & Peters, J.-M. (2019). DNA loop extrusion by human cohesin. *Science*, 366(6471), 1338 LP – 1345. <https://doi.org/10.1126/science.aaz3418>
- de Wit, E., Vos, E. S. M., Holwerda, S. J. B., Valdes-Quezada, C., Verstegen, M. J. A. M., Teunissen, H., Splinter, E., Wijchers, P. J., Krijger, P. H. L., & de Laat, W. (2015). CTCF Binding Polarity Determines Chromatin Looping. *Molecular Cell*, 60(4), 676–684. <https://doi.org/https://doi.org/10.1016/j.molcel.2015.09.023>
- Deardorff, M. A., Kaur, M., Yaeger, D., Rampuria, A., Korolev, S., Pie, J., Gil-Rodríguez, C., Arnedo, M., Loeys, B., Kline, A. D., Wilson, M., Lillquist, K., Siu, V., Ramos, F. J., Musio, A., Jackson, L. S., Dorsett, D., & Krantz, I. D. (2007). Mutations in cohesin complex members SMC3 and SMC1A cause a mild variant of cornelia de Lange syndrome with predominant mental retardation. *American Journal of Human Genetics*, 80(3), 485–494. <https://doi.org/10.1086/511888>
- Dekker, J. (2002). Capturing Chromosome Conformation. *Science*, 295(5558), 1306–1311. <https://doi.org/10.1126/science.1067799>
- Dervyn, E., Noirot-Gros, M.-F., Mervelet, P., McGovern, S., Ehrlich, S. D., Polard, P., & Noirot, P. (2004). The bacterial condensin/cohesin-like protein complex acts in DNA repair and regulation of gene expression. *Molecular Microbiology*, 51(6), 1629–1640. <https://doi.org/https://doi.org/10.1111/j.1365-2958.2003.03951.x>
- Diebold-Durand, M.-L., Bürmann, F., & Gruber, S. (2019). High-Throughput Allelic Replacement Screening in Bacillus subtilis. *Methods in Molecular Biology (Clifton, N.J.)*, 2004, 49–61. https://doi.org/10.1007/978-1-4939-9520-2_5
- Diebold-Durand, M. L., Lee, H., Ruiz Avila, L. B., Noh, H., Shin, H. C., Im, H., Bock, F. P., Bürmann, F., Durand, A., Basfeld, A., Ham, S., Basquin, J., Oh, B. H., & Gruber, S. (2017). Structure of Full-Length SMC and Rearrangements Required for Chromosome Organization. *Molecular Cell*, 67(2), 334–347.e5. <https://doi.org/10.1016/j.molcel.2017.06.010>
- Dixon, J. R., Selvaraj, S., Yue, F., Kim, A., Li, Y., Shen, Y., Hu, M., Liu, J. S., & Ren, B. (2012). Topological domains in mammalian genomes identified by analysis of chromatin interactions. *Nature*, 485(7398), 376–380. <https://doi.org/10.1038/nature11082>
- Earnshaw, W. C., & Laemmli, U. K. (1983). Architecture of metaphase chromosomes and chromosome scaffolds. *The Journal of Cell Biology*, 96(1), 84–93. <https://doi.org/10.1083/jcb.96.1.84>
- Fennell-Fezzie, R., Gradia, S. D., Akey, D., & Berger, J. M. (2005). The MukF subunit of Escherichia coli condensin: architecture and functional relationship to kleisins. *The EMBO Journal*, 24(11), 1921–1930. <https://doi.org/https://doi.org/10.1038/sj.emboj.7600680>
- Finch, P. W., Chambers, P., & Emmerson, P. T. (1985). Identification of the Escherichia coli recN gene product as a major SOS protein. *Journal of Bacteriology*, 164(2), 653–658. <https://doi.org/10.1128/jb.164.2.653-658.1985>
- Flemming, W. (1882). *Zellsubstanz, Kern und Zelltheilung*. F.C.W. Vogel. <https://www.biodiversitylibrary.org/item/280108>
- Fraser, C. M., Gocayne, J. D., White, O., Adams, M. D., Clayton, R. A., Fleischmann, R. D., Bult, C. J., Kerlavage, A. R., Sutton, G., Kelley, J. M., Fritchman, J. L., Weidman, J. F., Small, K. V., Sandusky, M., Fuhrmann, J., Nguyen, D., Utterback, T. R., Saudek, D. M., Phillips, C. A., ... Venter, J. C. (1995). The Minimal Gene Complement of Escherichia coli. *Science*, 270(5235), 397 LP – 404. <https://doi.org/10.1126/science.270.5235.397>
- Funayama, T., Narumi, I., Kikuchi, M., Kitayama, S., Watanabe, H., & Yamamoto, K. (1999). Identification and disruption analysis of the recN gene in the extremely radioresistant bacterium Deinococcus radiodurans. *Mutation Research/DNA Repair*, 435(2), 151–161. [https://doi.org/https://doi.org/10.1016/S0921-8777\(99\)00044-0](https://doi.org/https://doi.org/10.1016/S0921-8777(99)00044-0)
- Ganji, M., Shaltiel, I. A., Bisht, S., Kim, E., Kalichava, A., Haering, C. H., & Dekker, C. (2018). Real-time imaging of DNA loop extrusion by condensin. *Science*, 360(6384), 102–105. <https://doi.org/10.1126/science.aar7831>
- Gibcus, J. H., Samejima, K., Goloborodko, A., Samejima, I., Naumova, N., Nuebler, J., Kanemaki, M. T., Xie, L., Paulson, J. R., Earnshaw, W. C., Mirny, L. A., & Dekker, J. (2018). A pathway for mitotic chromosome formation. *Science (New York, N.Y.)*, 359(6376). <https://doi.org/10.1126/science.aao6135>
- Gligoris, T. G., Scheinost, J. C., Bürmann, F., Petela, N., Chan, K.-L., Uluocak, P., Beckouët, F., Gruber, S., Nasmyth, K., & Löwe, J. (2014). Closing the cohesin ring: structure and function of its Smc3-kleisin interface. *Science (New York,*

- N.Y.), 346(6212), 963–967. <https://doi.org/10.1126/science.1256917>
- Golfier, S., Quail, T., Kimura, H., & Brugués, J. (2020). Cohesin and condensin extrude DNA loops in a cell cycle-dependent manner. *ELife*, 9, e53885. <https://doi.org/10.7554/eLife.53885>
- Graham, J. E., Sherratt, D. J., & Szczelkun, M. D. (2010). Sequence-specific assembly of FtsK hexamers establishes directional translocation on DNA. *Proceedings of the National Academy of Sciences*, 107(47), 20263 LP – 20268. <https://doi.org/10.1073/pnas.1007518107>
- Griese, J. J., & Hopfner, K.-P. (2011). Structure and DNA-binding activity of the *Pyrococcus furiosus* SMC protein hinge domain. *Proteins: Structure, Function, and Bioinformatics*, 79(2), 558–568. <https://doi.org/https://doi.org/10.1002/prot.22903>
- Griese, J. J., Witte, G., & Hopfner, K.-P. (2010). Structure and DNA binding activity of the mouse condensin hinge domain highlight common and diverse features of SMC proteins. *Nucleic Acids Research*, 38(10), 3454–3465. <https://doi.org/10.1093/nar/gkq038>
- Grove, J. I., Wood, S. R., Briggs, G. S., Oldham, N. J., & Lloyd, R. G. (2009). A soluble RecN homologue provides means for biochemical and genetic analysis of DNA double-strand break repair in *Escherichia coli*. *DNA Repair*, 8(12), 1434–1443. <https://doi.org/10.1016/j.dnarep.2009.09.015>
- Gruber, S., & Errington, J. (2009). Recruitment of Condensin to Replication Origin Regions by ParB/SpoOJ Promotes Chromosome Segregation in *B. subtilis*. *Cell*, 137(4), 685–696. <https://doi.org/10.1016/j.cell.2009.02.035>
- Gruber, S., Veening, J. W., Bach, J., Blettinger, M., Bramkamp, M., & Errington, J. (2014). Interlinked sister chromosomes arise in the absence of condensin during fast replication in *B. subtilis*. *Current Biology*, 24(3), 293–298. <https://doi.org/10.1016/j.cub.2013.12.049>
- Gupta, R. C., Folta-Stogniew, E., & Radding, C. M. (1999). Human Rad51 Protein Can Form Homologous Joints in the Absence of Net Strand Exchange *. *Journal of Biological Chemistry*, 274(3), 1248–1256. <https://doi.org/10.1074/jbc.274.3.1248>
- Haarhuis, J. H. I., van der Weide, R. H., Blomen, V. A., Yáñez-Cuna, J. O., Amendola, M., van Ruiten, M. S., Krijger, P. H. L., Teunissen, H., Medema, R. H., van Steensel, B., Brummelkamp, T. R., de Wit, E., & Rowland, B. D. (2017). The Cohesin Release Factor WAPL Restricts Chromatin Loop Extension. *Cell*, 169(4), 693–707.e14. <https://doi.org/10.1016/j.cell.2017.04.013>
- Haber, J. E. (1995). In vivo biochemistry: Physical monitoring of recombination induced by site-specific endonucleases. *BioEssays*, 17(7), 609–620. <https://doi.org/https://doi.org/10.1002/bies.950170707>
- Han, K., Li, Z., Peng, R., Zhu, L., Zhou, T., Wang, L., Li, S., Zhang, X., Hu, W., Wu, Z., Qin, N., & Li, Y. (2013). Extraordinary expansion of a *Sorangium cellulosum* genome from an alkaline milieu. *Scientific Reports*, 3, 2101. <https://doi.org/10.1038/srep02101>
- Hartwell, L. H., & Weinert, T. A. (1989). Checkpoints: controls that ensure the order of cell cycle events. *Science (New York, N.Y.)*, 246(4930), 629–634. <https://doi.org/10.1126/science.2683079>
- Hassler, M., Shaltiel, I. A., & Haering, C. H. (2018). Towards a Unified Model of SMC Complex Function. *Current Biology*, 28(21), R1266–R1281. <https://doi.org/10.1016/j.cub.2018.08.034>
- Heinz, S., Texari, L., Hayes, M. G. B., Urbanowski, M., Chang, M. W., Givarkes, N., Rialdi, A., White, K. M., Albrecht, R. A., Pache, L., Marazzi, I., García-Sastre, A., Shaw, M. L., & Benner, C. (2018). Transcription Elongation Can Affect Genome 3D Structure. *Cell*, 174(6), 1522–1536.e22. <https://doi.org/https://doi.org/10.1016/j.cell.2018.07.047>
- Hendrickson, E. A. (1997). Cell-Cycle Regulation of Mammalian DNA Double-Strand-Break Repair. *The American Journal of Human Genetics*, 61(4), 795–800. <https://doi.org/https://doi.org/10.1086/514895>
- Hirano, M., & Hirano, T. (2004). Positive and negative regulation of SMC-DNA interactions by ATP and accessory proteins. *The EMBO Journal*, 23(13), 2664–2673. <https://doi.org/10.1038/sj.emboj.7600264>
- Hirano, M., & Hirano, T. (2006). Opening closed arms: long-distance activation of SMC ATPase by hinge-DNA interactions. *Molecular Cell*, 21(2), 175–186. <https://doi.org/10.1016/j.molcel.2005.11.026>
- Hirano, T. (2002). The ABCs of SMC proteins: Two-armed ATPases for chromosome condensation, cohesion, and repair. *Genes and Development*, 16(4), 399–414. <https://doi.org/10.1101/gad.955102>
- Hirano, T. (2016). Condensin-Based Chromosome Organization from Bacteria to Vertebrates. In *Cell* (Vol. 164, Issue 5). <https://doi.org/10.1016/j.cell.2016.01.033>
- Hopfner, K.-P., Craig, L., Moncalian, G., Zinkel, R. A., Usui, T., Owen, B. A. L., Karcher, A., Henderson, B., Bodmer, J.-L., McMurray, C. T., Carney, J. P., Petrini, J. H. J., & Tainer, J. A. (2002). The Rad50 zinc-hook is a structure joining Mre11 complexes in DNA recombination and repair. *Nature*, 418(6897), 562–566. <https://doi.org/10.1038/nature00922>
- Hopfner, K. P., Karcher, A., Shin, D., Fairley, C., Tainer, J. A., & Carney, J. P. (2000). Mre11 and Rad50 from *Pyrococcus furiosus*: cloning and biochemical characterization reveal an evolutionarily conserved multiprotein machine. *Journal of Bacteriology*, 182(21), 6036–6041. <https://doi.org/10.1128/JB.182.21.6036-6041.2000>
- Ireton, K., Gunther, N. W. 4th, & Grossman, A. D. (1994). spoOJ is required for normal chromosome segregation as well as the initiation of sporulation in *Bacillus subtilis*. *Journal of Bacteriology*, 176(17), 5320–5329. <https://doi.org/10.1128/jb.176.17.5320-5329.1994>
- Jacquier, A., & Dujon, B. (1985). An intron-encoded protein is active in a gene conversion process that spreads an intron into a mitochondrial gene. *Cell*, 41(2), 383–394. [https://doi.org/10.1016/S0092-8674\(85\)80011-8](https://doi.org/10.1016/S0092-8674(85)80011-8)

- Jensen, R. B., & Shapiro, L. (1999). The *Caulobacter crescentus* *smc* gene is required for cell cycle progression and chromosome segregation. *Proceedings of the National Academy of Sciences of the United States of America*, *96*(19), 10661–10666. <https://doi.org/10.1073/pnas.96.19.10661>
- Karaboja, X., Ren, Z., Brandão, H. B., Paul, P., Rudner, D. Z., & Wang, X. (2021). XerD unloads bacterial SMC complexes at the replication terminus. *Molecular Cell*, *81*(4), 756–766.e8. <https://doi.org/https://doi.org/10.1016/j.molcel.2020.12.027>
- Karl-Peter, H., Annette, K., David, S., Cecilia, F., A., T. J., & P., C. J. (2000). Mre11 and Rad50 from *Pyrococcus furiosus*: Cloning and Biochemical Characterization Reveal an Evolutionarily Conserved Multiprotein Machine. *Journal of Bacteriology*, *182*(21), 6036–6041. <https://doi.org/10.1128/JB.182.21.6036-6041.2000>
- Keyamura, K., & Hishida, T. (2019). Topological DNA-binding of structural maintenance of chromosomes-like RecN promotes DNA double-strand break repair in *Escherichia coli*. *Communications Biology*, *2*, 413. <https://doi.org/10.1038/s42003-019-0655-4>
- Keyamura, K., Sakaguchi, C., Kubota, Y., Niki, H., & Hishida, T. (2013). RecA protein recruits structural maintenance of chromosomes (SMC)-like RecN protein to DNA double-strand breaks. *The Journal of Biological Chemistry*, *288*(41), 29229–29237. <https://doi.org/10.1074/jbc.M113.485474>
- Kidane, D., Sanchez, H., Alonso, J. C., & Graumann, P. L. (2004). Visualization of DNA double-strand break repair in live bacteria reveals dynamic recruitment of *Bacillus subtilis* RecF, RecO and RecN proteins to distinct sites on the nucleoids. *Molecular Microbiology*, *52*(6), 1627–1639. <https://doi.org/10.1111/j.1365-2958.2004.04102.x>
- Kim, E., Kerssemakers, J., Shaltiel, I. A., Haering, C. H., & Dekker, C. (2020). DNA-loop extruding condensin complexes can traverse one another. *Nature*, *579*(7799), 438–442. <https://doi.org/10.1038/s41586-020-2067-5>
- Kim, Y., Shi, Z., Zhang, H., Finkelstein, I. J., & Yu, H. (2019). Human cohesin compacts DNA by loop extrusion. *Science*, *366*(6471), 1345–1349. <https://doi.org/10.1126/science.aaz4475>
- Klimova, A. N., & Sandler, S. J. (2020). An Epistasis Analysis of *recA* and *recN* in *Escherichia coli* K-12. *Genetics*, *216*(2), 381–393. <https://doi.org/10.1534/genetics.120.303476>
- Krantz, I. D., McCallum, J., DeScipio, C., Kaur, M., Gillis, L. A., Yaeger, D., Jukofsky, L., Wasserman, N., Bottani, A., Morris, C. A., Nowaczyk, M. J. M., Toriello, H., Bamshad, M. J., Carey, J. C., Rappaport, E., Kawachi, S., Lander, A. D., Calof, A. L., Li, H.-H., ... Jackson, L. G. (2004). Cornelia de Lange syndrome is caused by mutations in NIPBL, the human homolog of *Drosophila melanogaster* Nipped-B. *Nature Genetics*, *36*(6), 631–635. <https://doi.org/10.1038/ng1364>
- Krishnamurthy, M., Tadesse, S., Rothmaier, K., & Graumann, P. L. (2010). A novel SMC-like protein, SbcE (YhaN), is involved in DNA double-strand break repair and competence in *Bacillus subtilis*. *Nucleic Acids Research*, *38*(2), 455–466. <https://doi.org/10.1093/nar/gkp909>
- Kschonsak, M., Merkel, F., Bisht, S., Metz, J., Rybin, V., Hassler, M., & Haering, C. H. (2017). Structural Basis for a Safety-Belt Mechanism That Anchors Condensin to Chromosomes. *Cell*, *171*(3), 588–600.e24. <https://doi.org/https://doi.org/10.1016/j.cell.2017.09.008>
- Kurze, A., Michie, K. A., Dixon, S. E., Mishra, A., Itoh, T., Khalid, S., Strmecki, L., Shirahige, K., Haering, C. H., Löwe, J., & Nasmyth, K. (2011). A positively charged channel within the Smc1/Smc3 hinge required for sister chromatid cohesion. *The EMBO Journal*, *30*(2), 364–378. <https://doi.org/10.1038/emboj.2010.315>
- Lammens, A., Schele, A., & Hopfner, K.-P. (2004). Structural biochemistry of ATP-driven dimerization and DNA-stimulated activation of SMC ATPases. *Current Biology: CB*, *14*(19), 1778–1782. <https://doi.org/10.1016/j.cub.2004.09.044>
- Lang, F., Li, X., Zheng, W., Li, Z., Lu, D., Chen, G., Gong, D., Yang, L., Fu, J., Shi, P., & Zhou, J. (2017). CTCF prevents genomic instability by promoting homologous recombination-directed DNA double-strand break repair. *Proceedings of the National Academy of Sciences*, *114*(41), 10912 LP – 10917. <https://doi.org/10.1073/pnas.1704076114>
- Le, T. B. K., Imakaev, M. V., Mirny, L. A., & Laub, M. T. (2013). High-Resolution Mapping of the Spatial Organization of a Bacterial Chromosome. *Science*, *342*(6159), 731–734. <https://doi.org/10.1126/science.1242059>
- Lee, B.-G., Merkel, F., Allegritti, M., Hassler, M., Cawood, C., Lecomte, L., O'Reilly, F. J., Sinn, L. R., Gutierrez-Escribano, P., Kschonsak, M., Bravo, S., Nakane, T., Rappsilber, J., Aragon, L., Beck, M., Löwe, J., & Haering, C. H. (2020). Cryo-EM structures of holo condensin reveal a subunit flip-flop mechanism. *Nature Structural & Molecular Biology*, *27*(8), 743–751. <https://doi.org/10.1038/s41594-020-0457-x>
- Lee, C.-S., Wang, R. W., Chang, H.-H., Capurso, D., Segal, M. R., & Haber, J. E. (2016). Chromosome position determines the success of double-strand break repair. *Proceedings of the National Academy of Sciences*, *113*(2), E146 LP-E154. <https://doi.org/10.1073/pnas.1523660113>
- Lee, P. S., & Grossman, A. D. (2006). The chromosome partitioning proteins Soj (ParA) and Spo0J (ParB) contribute to accurate chromosome partitioning, separation of replicated sister origins, and regulation of replication initiation in *Bacillus subtilis*. *Molecular Microbiology*, *60*(4), 853–869. <https://doi.org/https://doi.org/10.1111/j.1365-2958.2006.05140.x>
- Leiserson, M. D. M., Vandin, F., Wu, H.-T., Dobson, J. R., Eldridge, J. V., Thomas, J. L., Papoutsaki, A., Kim, Y., Niu, B., McLellan, M., Lawrence, M. S., Gonzalez-Perez, A., Tamborero, D., Cheng, Y., Ryslik, G. A., Lopez-Bigas, N., Getz, G., Ding, L., & Raphael, B. J. (2015). Pan-cancer network analysis identifies combinations of rare somatic mutations across pathways and protein complexes. *Nature Genetics*, *47*(2), 106–114. <https://doi.org/10.1038/ng.3168>
- Liang, F., Han, M., Romanienko, P. J., & Jasin, M. (1998). Homology-directed repair is a major double-strand break repair pathway in mammalian cells. *Proceedings of the National Academy of Sciences of the United States of America*,

- 95(9), 5172–5177. <https://doi.org/10.1073/pnas.95.9.5172>
- Lieberman-Aiden, E., van Berkum, N. L., Williams, L., Imakaev, M., Ragoczy, T., Telling, A., Amit, I., Lajoie, B. R., Sabo, P. J., Dorschner, M. O., Sandstrom, R., Bernstein, B., Bender, M. A., Groudine, M., Gnirke, A., Stamatoyannopoulos, J., Mirny, L. A., Lander, E. S., & Dekker, J. (2009). Comprehensive mapping of long-range interactions reveals folding principles of the human genome. *Science (New York, N.Y.)*, 326(5950), 289–293. <https://doi.org/10.1126/science.1181369>
- Lioy, V. S., Junier, I., Lagage, V., Vallet, I., & Boccard, F. (2020). Distinct Activities of Bacterial Condensins for Chromosome Management in *Pseudomonas aeruginosa*. *Cell Reports*, 33(5). <https://doi.org/10.1016/j.celrep.2020.108344>
- Livny, J., Yamaichi, Y., & Waldor, M. K. (2007). Distribution of centromere-like parS sites in bacteria: Insights from comparative genomics. *Journal of Bacteriology*, 189(23), 8693–8703. <https://doi.org/10.1128/JB.01239-07>
- Lloyd, R. G., Picksley, S. M., & Prescott, C. (1983). Inducible expression of a gene specific to the RecF pathway for recombination in *Escherichia coli* K12. *Molecular and General Genetics MGG*, 190(1), 162–167. <https://doi.org/10.1007/BF00330340>
- Luo, H., Li, Y., Mu, J.-J., Zhang, J., Tonaka, T., Hamamori, Y., Jung, S. Y., Wang, Y., & Qin, J. (2008). Regulation of Intra-S Phase Checkpoint by Ionizing Radiation (IR)-dependent and IR-independent Phosphorylation of SMC3. *Journal of Biological Chemistry*, 283(28), 19176–19183. <https://doi.org/10.1074/jbc.M802299200>
- Marbouty, M., Le Gall, A., Cattoni, D. I., Cournac, A., Koh, A., Fiche, J. B., Mozziconacci, J., Murray, H., Koszul, R., & Nollmann, M. (2015). Condensin- and Replication-Mediated Bacterial Chromosome Folding and Origin Condensation Revealed by Hi-C and Super-resolution Imaging. *Molecular Cell*, 59(4), 588–602. <https://doi.org/10.1016/j.molcel.2015.07.020>
- Marsden, M. P., & Laemmli, U. K. (1979). Metaphase chromosome structure: evidence for a radial loop model. *Cell*, 17(4), 849–858. [https://doi.org/10.1016/0092-8674\(79\)90325-8](https://doi.org/10.1016/0092-8674(79)90325-8)
- Martin, C.-A., Murray, J. E., Carroll, P., Leitch, A., Mackenzie, K. J., Halachev, M., Fetit, A. E., Keith, C., Bicknell, L. S., Fluteau, A., Gautier, P., Hall, E. A., Joss, S., Soares, G., Silva, J., Bober, M. B., Duker, A., Wise, C. A., Quigley, A. J., ... Jackson, A. P. (2016). Mutations in genes encoding condensin complex proteins cause microcephaly through decatenation failure at mitosis. *Genes & Development*, 30(19), 2158–2172. <https://doi.org/10.1101/gad.286351.116>
- Mascarenhas, J., Sanchez, H., Tadesse, S., Kidane, D., Krisnamurthy, M., Alonso, J. C., & Graumann, P. L. (2006). *Bacillus subtilis* SbcC protein plays an important role in DNA inter-strand cross-link repair. *BMC Molecular Biology*, 7, 20. <https://doi.org/10.1186/1471-2199-7-20>
- Matoba, K., Yamazoe, M., Mayanagi, K., Morikawa, K., & Hiraga, S. (2005). Comparison of MukB homodimer versus MukBEF complex molecular architectures by electron microscopy reveals a higher-order multimerization. *Biochemical and Biophysical Research Communications*, 333(3), 694–702. <https://doi.org/10.1016/j.bbrc.2005.05.163>
- McLean, E. K., Lenhart, J. S., & Simmons, L. A. (2021). RecA is required for the assembly of RecN into DNA repair complexes on the nucleoid. *Journal of Bacteriology*, JB0024021. <https://doi.org/10.1128/JB.00240-21>
- Meddows, T. R., Savory, A. P., Grove, J. I., Moore, T., & Lloyd, R. G. (2005). RecN protein and transcription factor DksA combine to promote faithful recombinational repair of DNA double-strand breaks. *Molecular Microbiology*, 57(1), 97–110. <https://doi.org/https://doi.org/10.1111/j.1365-2958.2005.04677.x>
- Meddows, T. R., Savory, A. P., & Lloyd, R. G. (2004). RecG helicase promotes DNA double-strand break repair. *Molecular Microbiology*, 52(1), 119–132. <https://doi.org/https://doi.org/10.1111/j.1365-2958.2003.03970.x>
- Mercier, R., Petit, M.-A., Schbath, S., Robin, S., El Karoui, M., Boccard, F., & Espéli, O. (2008). The MatP/matS Site-Specific System Organizes the Terminus Region of the *E. coli* Chromosome into a Macrodomain. *Cell*, 135(3), 475–485. <https://doi.org/https://doi.org/10.1016/j.cell.2008.08.031>
- Merrick, H., Zhang, Y., Grossman, A. D., & Wang, J. D. (2012). Replication–transcription conflicts in bacteria. *Nature Reviews Microbiology*, 10(7), 449–458. <https://doi.org/10.1038/nrmicro2800>
- Minnen, A., Bürmann, F., Wilhelm, L., Anchimiuk, A., Diebold-Durand, M. L., & Gruber, S. (2016). Control of SMC Coiled Coil Architecture by the ATPase Heads Facilitates Targeting to Chromosomal ParB/parS and Release onto Flanking DNA. *Cell Reports*, 14(8), 2003–2016. <https://doi.org/10.1016/j.celrep.2016.01.066>
- Moreno-Herrero, F., de Jager, M., Dekker, N. H., Kanaar, R., Wyman, C., & Dekker, C. (2005). Mesoscale conformational changes in the DNA-repair complex Rad50/Mre11/Nbs1 upon binding DNA. *Nature*, 437(7057), 440–443. <https://doi.org/10.1038/nature03927>
- Nagashima, K., Kubota, Y., Shibata, T., Sakaguchi, C., Shinagawa, H., & Hishida, T. (2006). Degradation of *Escherichia coli* RecN aggregates by ClpXP protease and its implications for DNA damage tolerance. *The Journal of Biological Chemistry*, 281(41), 30941–30946. <https://doi.org/10.1074/jbc.M606566200>
- Naumova, N., Imakaev, M., Fudenberg, G., Zhan, Y., Lajoie, B. R., Mirny, L. A., & Dekker, J. (2013). Organization of the mitotic chromosome. *Science*, 342(6161), 948–953. <https://doi.org/10.1126/science.1236083>
- Niki, H., Jaffé, A., Imamura, R., Ogura, T., & Hiraga, S. (1991). The new gene mukB codes for a 177 kd protein with coiled-coil domains involved in chromosome partitioning of *E. coli*. *The EMBO Journal*, 10(1), 183–193.
- Noll, D. M., Mason, T. M., & Miller, P. S. (2006). Formation and repair of interstrand cross-links in DNA. *Chemical Reviews*, 106(2), 277–301. <https://doi.org/10.1021/cr040478b>
- Nomura, M., & Morgan, E. A. (1977). Genetics of bacterial ribosomes. *Annual Review of Genetics*, 11, 297–347. <https://doi.org/10.1146/annurev.ge.11.120177.001501>

- Nora, E. P., Lajoie, B. R., Schulz, E. G., Giorgetti, L., Okamoto, I., Servant, N., Piolot, T., van Berkum, N. L., Meisig, J., Sedat, J., Gribnau, J., Barillot, E., Blüthgen, N., Dekker, J., & Heard, E. (2012). Spatial partitioning of the regulatory landscape of the X-inactivation centre. *Nature*, *485*(7398), 381–385. <https://doi.org/10.1038/nature11049>
- Odsbu, I., & Skarstad, K. (2014). DNA compaction in the early part of the SOS response is dependent on RecN and RecA. *Microbiology (Reading, England)*, *160*(Pt 5), 872–882. <https://doi.org/10.1099/mic.0.075051-0>
- Ogawa, T., Yu, X., Shinohara, A., & Egelman, E. H. (1993). Similarity of the yeast RAD51 filament to the bacterial RecA filament. *Science*, *259*(5103), 1896 LP – 1899. <https://doi.org/10.1126/science.8456314>
- Parelho, V., Hadjur, S., Spivakov, M., Leleu, M., Sauer, S., Gregson, H. C., Jarmuz, A., Canzonetta, C., Webster, Z., Nesterova, T., Cobb, B. S., Yokomori, K., Dillon, N., Aragon, L., Fisher, A. G., & Merkenschlager, M. (2008). Cohesins functionally associate with CTCF on mammalian chromosome arms. *Cell*, *132*(3), 422–433. <https://doi.org/10.1016/j.cell.2008.01.011>
- Pellegrino, S., Radzimanowski, J., de Sanctis, D., Boeri Erba, E., McSweeney, S., & Timmins, J. (2012). Structural and functional characterization of an SMC-like protein RecN: new insights into double-strand break repair. *Structure (London, England : 1993)*, *20*(12), 2076–2089. <https://doi.org/10.1016/j.str.2012.09.010>
- Pennington, J. M., & Rosenberg, S. M. (2007). Spontaneous DNA breakage in single living Escherichia coli cells. *Nature Genetics*, *39*(6), 797–802. <https://doi.org/10.1038/ng2051>
- Petrushenko, Z. M., Lai, C.-H., & Rybenkov, V. V. (2006). Antagonistic Interactions of Kleisins and DNA with Bacterial Condensin MukB *. *Journal of Biological Chemistry*, *281*(45), 34208–34217. <https://doi.org/10.1074/jbc.M606723200>
- Petrushenko, Z. M., She, W., & Rybenkov, V. V. (2011). A new family of bacterial condensins. *Molecular Microbiology*, *81*(4), 881–896. <https://doi.org/10.1111/j.1365-2958.2011.07763.x>
- Picksley, S. M., Atfield, P. V., & Lloyd, R. G. (1984). Repair of DNA double-strand breaks in Escherichia coli K12 requires a functional recN product. *Molecular and General Genetics MGG*, *195*(1), 267–274. <https://doi.org/10.1007/BF00332758>
- Plessis, A., Perrin, A., Haber, J. E., & Dujon, B. (1992). Site-specific recombination determined by I-SceI, a mitochondrial group I intron-encoded endonuclease expressed in the yeast nucleus. *Genetics*, *130*(3), 451–460. <https://pubmed.ncbi.nlm.nih.gov/1551570>
- Pradhan, B., Barth, R., Kim, E., Davidson, I. F., Bauer, B., van Laar, T., Yang, W., Ryu, J.-K., van der Torre, J., Peters, J.-M., & Dekker, C. (2021). SMC complexes can traverse physical roadblocks bigger than their ring size. *BioRxiv*, 2021.07.15.452501. <https://doi.org/10.1101/2021.07.15.452501>
- Rao, S. S. P., Huang, S.-C., Glenn St Hilaire, B., Engreitz, J. M., Perez, E. M., Kieffer-Kwon, K.-R., Sanborn, A. L., Johnstone, S. E., Bascom, G. D., Bochkov, I. D., Huang, X., Shamim, M. S., Shin, J., Turner, D., Ye, Z., Omer, A. D., Robinson, J. T., Schlick, T., Bernstein, B. E., ... Aiden, E. L. (2017). Cohesin Loss Eliminates All Loop Domains. *Cell*, *171*(2), 305–320.e24. <https://doi.org/https://doi.org/10.1016/j.cell.2017.09.026>
- Reichenbach, H. (1999). The ecology of the myxobacteria. *Environmental Microbiology*, *1*(1), 15–21. <https://doi.org/https://doi.org/10.1046/j.1462-2920.1999.00016.x>
- Renkawitz, J., Lademann, C. A., & Jentsch, S. (2014). Mechanisms and principles of homology search during recombination. *Nature Reviews Molecular Cell Biology*, *15*(6), 369–383. <https://doi.org/10.1038/nrm3805>
- Reyes, E. D., Patidar, P. L., Uranga, L. A., Bortoletto, A. S., & Lusetti, S. L. (2010). RecN is a cohesin-like protein that stimulates intermolecular DNA interactions in vitro. *The Journal of Biological Chemistry*, *285*(22), 16521–16529. <https://doi.org/10.1074/jbc.M110.119164>
- Rocha, E. P. C. (2008). The Organization of the Bacterial Genome. *Annual Review of Genetics*, *42*(1), 211–233. <https://doi.org/10.1146/annurev.genet.42.110807.091653>
- Rocha, E. P. C., Cornet, E., & Michel, B. (2005). Comparative and Evolutionary Analysis of the Bacterial Homologous Recombination Systems. *PLOS Genetics*, *1*(2), e15. <https://doi.org/10.1371/journal.pgen.0010015>
- Rojowska, A., Lammens, K., Seifert, F. U., Direnberger, C., Feldmann, H., & Hopfner, K.-P. (2014). Structure of the Rad50 DNA double-strand break repair protein in complex with DNA. *The EMBO Journal*, *33*(23), 2847–2859. <https://doi.org/10.15252/embj.201488889>
- Rösch, T. C., Altenburger, S., Oviedo-Bocanegra, L., Pediaditakis, M., Najjar, N. El, Fritz, G., & Graumann, P. L. (2018). Single molecule tracking reveals spatio-temporal dynamics of bacterial DNA repair centres. *Scientific Reports*, *8*(1), 16450. <https://doi.org/10.1038/s41598-018-34572-8>
- Rowley, M. J., Lyu, X., Rana, V., Ando-Kuri, M., Karns, R., Bosco, G., & Corces, V. G. (2019). Condensin II Counteracts Cohesin and RNA Polymerase II in the Establishment of 3D Chromatin Organization. *Cell Reports*, *26*(11), 2890–2903.e3. <https://doi.org/https://doi.org/10.1016/j.celrep.2019.01.116>
- Rubio, E. D., Reiss, D. J., Welcsh, P. L., Distech, C. M., Filippova, G. N., Baliga, N. S., Aebersold, R., Ranish, J. A., & Krumm, A. (2008). CTCF physically links cohesin to chromatin. *Proceedings of the National Academy of Sciences*, *105*(24), 8309 LP – 8314. <https://doi.org/10.1073/pnas.0801273105>
- Rybenkov, V. V. (2014). Maintenance of chromosome structure in Pseudomonas aeruginosa. *FEMS Microbiology Letters*, *356*(2), 154–165. <https://doi.org/10.1111/1574-6968.12478>
- Sanchez, H., & Alonso, J. C. (2005). Bacillus subtilis RecN binds and protects 3'-single-stranded DNA extensions in the presence of ATP. *Nucleic Acids Research*, *33*(7), 2343–2350. <https://doi.org/10.1093/nar/gki533>
- Sanders, J. T., Freeman, T. F., Xu, Y., Gollosi, R., Stallard, M. A., Hill, A. M., San Martin, R., Balajee, A. S., & McCord, R. P. (2020). Radiation-induced DNA damage and repair effects on 3D genome organization. *Nature Communications*,

- 11(1), 6178. <https://doi.org/10.1038/s41467-020-20047-w>
- Sargentini, N. J., & Smith, K. C. (1985). Growth-medium-dependent repair of DNA single-strand and double-strand breaks in X-irradiated *Escherichia coli*. *Radiation Research*, *104*(1), 109–115.
- Seifert, F. U., Lammens, K., Stoehr, G., Kessler, B., & Hopfner, K.-P. (2016). Structural mechanism of ATP-dependent DNA binding and DNA end bridging by eukaryotic Rad50. *The EMBO Journal*, *35*(7), 759–772. <https://doi.org/10.15252/embj.201592934>
- Sexton, T., Yaffe, E., Kenigsberg, E., Bantignies, F., Leblanc, B., Hoichman, M., Parrinello, H., Tanay, A., & Cavalli, G. (2012). Three-Dimensional Folding and Functional Organization Principles of the *Drosophila* Genome. *Cell*, *148*(3), 458–472. <https://doi.org/https://doi.org/10.1016/j.cell.2012.01.010>
- Sharma, S., Javadekar, S. M., Pandey, M., Srivastava, M., Kumari, R., & Raghavan, S. C. (2015). Homology and enzymatic requirements of microhomology-dependent alternative end joining. *Cell Death & Disease*, *6*(3), e1697. <https://doi.org/10.1038/cddis.2015.58>
- Sharples, G. J., & Leach, D. R. F. (1995). Structural and functional similarities between the SbcCD proteins of *Escherichia coli* and the RAD50 and MRE11 (RAD32) recombination and repair proteins of yeast. *Molecular Microbiology*, *17*(6), 1215–1217. https://doi.org/https://doi.org/10.1111/j.1365-2958.1995.mmi_17061215_1.x
- Shi, Z., Gao, H., Bai, X., & Yu, H. (2020). Cryo-EM structure of the human cohesin-NIPBL-DNA complex. *Science*, *368*(6498), 1454 LP – 1459. <https://doi.org/10.1126/science.abb0981>
- Shibata, A., Moiani, D., Arvai, A. S., Perry, J., Harding, S. M., Genois, M.-M., Maity, R., van Rossum-Fikkert, S., Kertokalio, A., Romoli, F., Ismail, A., Ismalaj, E., Petricci, E., Neale, M. J., Bristow, R. G., Masson, J.-Y., Wyman, C., Jeggo, P. A., & Tainer, J. A. (2014). DNA double-strand break repair pathway choice is directed by distinct MRE11 nuclease activities. *Molecular Cell*, *53*(1), 7–18. <https://doi.org/10.1016/j.molcel.2013.11.003>
- Shuman, S., & Glickman, M. S. (2007). Bacterial DNA repair by non-homologous end joining. *Nature Reviews. Microbiology*, *5*(11), 852–861. <https://doi.org/10.1038/nrmicro1768>
- Siegl, T., Petzke, L., Welle, E., & Luzhetskyy, A. (2010). I-SceI endonuclease: a new tool for DNA repair studies and genetic manipulations in *Streptomyces*. *Applied Microbiology and Biotechnology*, *87*(4), 1525–1532. <https://doi.org/10.1007/s00253-010-2643-y>
- Simmons, L. A., Goranov, A. I., Kobayashi, H., Davies, B. W., Yuan, D. S., Grossman, A. D., & Walker, G. C. (2009). Comparison of responses to double-strand breaks between *Escherichia coli* and *Bacillus subtilis* reveals different requirements for SOS induction. *Journal of Bacteriology*, *191*(4), 1152–1161. <https://doi.org/10.1128/JB.01292-08>
- Sjögren, C., & Nasmyth, K. (2001). Sister chromatid cohesion is required for postreplicative double-strand break repair in *Saccharomyces cerevisiae*. *Current Biology: CB*, *11*(12), 991–995. [https://doi.org/10.1016/s0960-9822\(01\)00271-8](https://doi.org/10.1016/s0960-9822(01)00271-8)
- Smith, P. C., Karpowich, N., Millen, L., Moody, J. E., Rosen, J., Thomas, P. J., & Hunt, J. F. (2002). ATP Binding to the Motor Domain from an ABC Transporter Drives Formation of a Nucleotide Sandwich Dimer. *Molecular Cell*, *10*(1), 139–149. [https://doi.org/https://doi.org/10.1016/S1097-2765\(02\)00576-2](https://doi.org/https://doi.org/10.1016/S1097-2765(02)00576-2)
- Sofueva, S., Yaffe, E., Chan, W.-C., Georgopoulou, D., Vietri Rudan, M., Mira-Bontenbal, H., Pollard, S. M., Schroth, G. P., Tanay, A., & Hadjur, S. (2013). Cohesin-mediated interactions organize chromosomal domain architecture. *The EMBO Journal*, *32*(24), 3119–3129. <https://doi.org/https://doi.org/10.1038/emboj.2013.237>
- Soh, Y. M., Bürmann, F., Shin, H. C., Oda, T., Jin, K. S., Toseland, C. P., Kim, C., Lee, H., Kim, S. J., Kong, M. S., Durand-Diebold, M. L., Kim, Y. G., Kim, H. M., Lee, N. K., Sato, M., Oh, B. H., & Gruber, S. (2015). Molecular basis for SMC rod formation and its dissolution upon DNA binding. *Molecular Cell*, *57*(2), 290–303. <https://doi.org/10.1016/j.molcel.2014.11.023>
- Stohl, E. A., & Seifert, H. S. (2006). *Neisseria gonorrhoeae* DNA recombination and repair enzymes protect against oxidative damage caused by hydrogen peroxide. *Journal of Bacteriology*, *188*(21), 7645–7651. <https://doi.org/10.1128/JB.00801-06>
- Ström, L., Lindroos, H. B., Shirahige, K., & Sjögren, C. (2004). Postreplicative recruitment of cohesin to double-strand breaks is required for DNA repair. *Molecular Cell*, *16*(6), 1003–1015. <https://doi.org/10.1016/j.molcel.2004.11.026>
- Sullivan, N. L., Marquis, K. A., & Rudner, D. Z. (2009). Recruitment of SMC by ParB-parS Organizes the Origin Region and Promotes Efficient Chromosome Segregation. *Cell*, *137*(4), 697–707. <https://doi.org/10.1016/j.cell.2009.04.044>
- Sweetman, W. A., Moxon, E. R., & Bayliss, C. D. (2005). Induction of the SOS regulon of *Haemophilus influenzae* does not affect phase variation rates at tetranucleotide or dinucleotide repeats. *Microbiology (Reading, England)*, *151*(Pt 8), 2751–2763. <https://doi.org/10.1099/mic.0.27996-0>
- Syed, A., & Tainer, J. A. (2018). The MRE11-RAD50-NBS1 Complex Conducts the Orchestration of Damage Signaling and Outcomes to Stress in DNA Replication and Repair. *Annual Review of Biochemistry*, *87*, 263–294. <https://doi.org/10.1146/annurev-biochem-062917-012415>
- Szabo, Q., Bantignies, F., & Cavalli, G. (2019). Principles of genome folding into topologically associating domains. *Science Advances*, *5*(4), eaaw1668. <https://doi.org/10.1126/sciadv.aaw1668>
- Taschner, M., Basquin, J., Steigenberger, B., Schäfer, I. B., Soh, Y.-M., Basquin, C., Lorentzen, E., Räsche, M., Scheltema, R. A., & Gruber, S. (2021). Nse5/6 inhibits the Smc5/6 ATPase and modulates DNA substrate binding. *The EMBO Journal*, *n/a*(n/a), e107807. <https://doi.org/https://doi.org/10.15252/embj.2021107807>
- Terakawa, T., Bisht, S., Eeftens, J. M., Dekker, C., Haering, C. H., & Greene, E. C. (2017). The condensin complex is a mechanochemical motor that translocates along DNA. *Science*, *358*(6363), 672 LP – 676.

- <https://doi.org/10.1126/science.aan6516>
- Tran, N. T., Laub, M. T., & Le, T. B. K. (2017). SMC Progressively Aligns Chromosomal Arms in *Caulobacter crescentus* but Is Antagonized by Convergent Transcription. *Cell Reports*, 20(9), 2057–2071. <https://doi.org/10.1016/j.celrep.2017.08.026>
- Trujillo, K. M., & Sung, P. (2001). DNA Structure-specific Nuclease Activities in the Rad50/Mre11 Complex. *Journal of Biological Chemistry*, 276(38), 35458–35464. <https://doi.org/10.1074/jbc.M105482200>
- Unal, E., Arbel-Eden, A., Sattler, U., Shroff, R., Lichten, M., Haber, J. E., & Koshland, D. (2004). DNA damage response pathway uses histone modification to assemble a double-strand break-specific cohesin domain. *Molecular Cell*, 16(6), 991–1002. <https://doi.org/10.1016/j.molcel.2004.11.027>
- Uranga, L. A., Reyes, E. D., Patidar, P. L., Redman, L. N., & Lusetti, S. L. (2017). The cohesin-like RecN protein stimulates RecA-mediated recombinational repair of DNA double-strand breaks. *Nature Communications*, 8(1), 15282. <https://doi.org/10.1038/ncomms15282>
- Vallet-Gely, I., & Boccia, F. (2013). Chromosomal Organization and Segregation in *Pseudomonas aeruginosa*. *PLoS Genetics*, 9(5), e1003492. <https://doi.org/10.1371/journal.pgen.1003492>
- Vazquez Nunez, R., Ruiz Avila, L. B., & Gruber, S. (2019). Transient DNA Occupancy of the SMC Interarm Space in Prokaryotic Condensin. *Molecular Cell*, 75(2), 209–223.e6. <https://doi.org/10.1016/j.molcel.2019.05.001>
- Vickridge, E., Planchenault, C., Cockram, C., Junceda, I. G., & Espéli, O. (2017). Management of *E. coli* sister chromatid cohesion in response to genotoxic stress. *Nature Communications*, 8(1), 14618. <https://doi.org/10.1038/ncomms14618>
- Wang, G., & Maier, R. J. (2008). Critical role of RecN in recombinational DNA repair and survival of *Helicobacter pylori*. *Infection and Immunity*, 76(1), 153–160. <https://doi.org/10.1128/IAI.00791-07>
- Wang, S., Su, J.-H., Beliveau, B. J., Bintu, B., Moffitt, J. R., Wu, C., & Zhuang, X. (2016). Spatial organization of chromatin domains and compartments in single chromosomes. *Science (New York, N.Y.)*, 353(6299), 598–602. <https://doi.org/10.1126/science.aaf8084>
- Wang, S. T., Setlow, B., Conlon, E. M., Lyon, J. L., Imamura, D., Sato, T., Setlow, P., Losick, R., & Eichenberger, P. (2006). The Forespore Line of Gene Expression in *Bacillus subtilis*. *Journal of Molecular Biology*, 358(1), 16–37. <https://doi.org/https://doi.org/10.1016/j.jmb.2006.01.059>
- Wang, X., Brandão, H. B., Le, T. B. K., Laub, M. T., & Rudner, D. Z. (2017). *Bacillus subtilis* SMC complexes juxtapose chromosome arms as they travel from origin to terminus. *Science*, 355(6324), 524–527. <https://doi.org/10.1126/science.aai8982>
- Wang, X., Le, T. B. K., Lajoie, B. R., Dekker, J., Laub, M. T., & Rudner, D. Z. (2015). Condensin promotes the juxtaposition of dna flanking its loading site in *Bacillus subtilis*. *Genes and Development*, 29(15), 1661–1675. <https://doi.org/10.1101/gad.265876.115>
- Wang, X., & Rudner, D. Z. (2014). Spatial organization of bacterial chromosomes. *Current Opinion in Microbiology*, 22, 66–72. <https://doi.org/10.1016/j.mib.2014.09.016>
- Wang, X., Tang, O. W., Riley, E. P., & Rudner, D. Z. (2014). The SMC condensin complex is required for origin segregation in *Bacillus subtilis*. *Current Biology*, 24(3), 287–292. <https://doi.org/10.1016/j.cub.2013.11.050>
- Weller, G. R., Kysela, B., Roy, R., Tonkin, L. M., Scanlan, E., Della, M., Devine, S. K., Day, J. P., Wilkinson, A., d'Adda di Fagagna, F., Devine, K. M., Bowater, R. P., Jeggo, P. A., Jackson, S. P., & Doherty, A. J. (2002). Identification of a DNA nonhomologous end-joining complex in bacteria. *Science (New York, N.Y.)*, 297(5587), 1686–1689. <https://doi.org/10.1126/science.1074584>
- Wendel, B. M., Cole, J. M., Courcelle, C. T., & Courcelle, J. (2018). SbcC-SbcD and Exol process convergent forks to complete chromosome replication. *Proceedings of the National Academy of Sciences*, 115(2), 349 LP – 354. <https://doi.org/10.1073/pnas.1715960114>
- Wendt, K. S., Yoshida, K., Itoh, T., Bando, M., Koch, B., Schirghuber, E., Tsutsumi, S., Nagae, G., Ishihara, K., Mishiro, T., Yahata, K., Imamoto, F., Aburatani, H., Nakao, M., Imamoto, N., Maeshima, K., Shirahige, K., & Peters, J.-M. (2008). Cohesin mediates transcriptional insulation by CCTC-binding factor. *Nature*, 451(7180), 796–801. <https://doi.org/10.1038/nature06634>
- Wiktor, J., Gynnå, A. H., Leroy, P., Larsson, J., Coceano, G., Testa, I., & Elf, J. (2021). Live cell imaging reveals that RecA finds homologous DNA by reduced dimensionality search. *BioRxiv*, 2020.02.13.946996. <https://doi.org/10.1101/2020.02.13.946996>
- Wilhelm, L., Bürmann, F., Minnen, A., Shin, H.-C., Toseland, C. P., Oh, B.-H., & Gruber, S. (2015). SMC condensin entraps chromosomal DNA by an ATP hydrolysis dependent loading mechanism in *Bacillus subtilis*. *ELife*, 4, e06659. <https://doi.org/10.7554/eLife.06659>
- Woo, J.-S., Lim, J.-H., Shin, H.-C., Suh, M.-K., Ku, B., Lee, K.-H., Joo, K., Robinson, H., Lee, J., Park, S.-Y., Ha, N.-C., & Oh, B.-H. (2009). Structural Studies of a Bacterial Condensin Complex Reveal ATP-Dependent Disruption of Intersubunit Interactions. *Cell*, 136(1), 85–96. <https://doi.org/10.1016/j.cell.2008.10.050>
- Yamazoe, M., Onogi, T., Sunako, Y., Niki, H., Yamanaka, K., Ichimura, T., & Hiraga, S. (1999). Complex formation of MukB, MukE and MukF proteins involved in chromosome partitioning in *Escherichia coli*. *The EMBO Journal*, 18(21), 5873–5884. <https://doi.org/https://doi.org/10.1093/emboj/18.21.5873>

Yatskevich, S., Rhodes, J., & Nasmyth, K. (2019). Organization of Chromosomal DNA by SMC Complexes. *Annual Review of Genetics*, 53(1). <https://doi.org/10.1146/annurev-genet-112618-043633>